Process Simulation of Lime Calcination in Mixed Feed Shaft Kilns

Dissertation
zur Erlangung des akademischen Grades

**Doktoringenieurin
(Dr.-Ing.)**

von **M.Sc. Magda Kotb Moursy El-Fakharany**
geb. am 6. Juli 1975 in Kafr Elsheikh, Ägypten

genehmigt durch die Fakultät für Verfahrens- und Systemtechnik
der Otto-von-Guericke-Universität Magdeburg

Gutachter:

Prof. Dr.-Ing. Eckehard Specht
Prof. Dr.-Ing. Reinhard Scholz
Dr.-Ing. Peer Hosenthien

Promotionskolloquium am: 09. Januar 2012

Schriftliche Erklärung

Ich erkläre hiermit, dass ich die vorliegende Arbeit ohne unzulässige Hilfe Dritter und ohne Benutzung anderer als der angegebenen Hilfsmittel angefertigt habe. Die aus fremden Quellen direkt oder indirekt übernommenen Gedanken sind als solche kenntlich gemacht.

Insbesondere habe ich nicht die Hilfe einer kommerziellen Promotionsberatung in Anspruch genommen. Dritte haben von mir weder unmittelbar noch mittelbar geldwerte Leistungen für Arbeiten erhalten, die im Zusammenhang mit dem Inhalt der vorgelegten Dissertation stehen.

Die Arbeit wurde bisher weder im Inland noch im Ausland in gleicher oder ähnlicher Form als Dissertation eingereicht und ist als Ganzes auch noch nicht veröffentlicht.

Magdeburg, den 09.01.2012

Magda El-Fakharany

Abstract

Mixed feed shaft kilns are widely used throughout the world in the industries using both lime and carbonation gas, such as soda ash, sugar and magnesia industries. This work aims to improve the mixed feed lime kiln operation through a better understanding of the process.

The work focuses on development of a mathematical model for a mixed feed lime kilns. The results from full scale measurements were used as input to the model of the kiln and also for validation of the model. The models of a single particle have been used to determine supply input information to the model. Meanwhile, an energy balance of the whole kiln process was done.

The experimental measurement of the vertical temperature profile of the kiln was done using thermocouples . The temperature profile from the preheating zone to the cooling zone was achieved during the measurement. The gas composition was measured with gas analyzer at the top of the kiln. The inputs and outputs of the kiln were also measured. The measurements showed that the kiln has some problems due to low quality of limestone and distribution of the solid materials affecting its performance.

Simulations of a single coke particle combustion have been conducted using unsteady state model that includes a detailed description of transport phenomenon coupled with chemical reactions. The model predicts the particle's temperature, burning rate, conversion degree and particle shrinkage, given ambient conditions and initial coke particle properties. The results of simulations have a good agreement with experimental data available in the literature.

The calcination behavior of a single limestone particle was simulated. The equations describing the behavior are assembled from the literature. The shrinking core model was employed for the mechanics and chemical reactions of the reacting particle of limestone. Then this model is introduced to the kiln model.

A basic model was developed using the mass and heat balances for the gas species and the solid phases. It includes chemical reaction enthalpies for the conversion of fuel and

limestone. Heat and mass transfer between phases are modeled as convection. The model predicts temperatures, conversion degree, mass flow rate, gas concentrations, profiles of gas and solid phases as a function of vertical position. Also, the pressure drop inside the kiln and gas velocity are predicted by the model.

The mathematical model uses the measured input data of the kiln. The experimental measurements of the kiln and output data formed the basis of the validation. The validation shows that, the model has captured the essential phenomena sufficiently detailed for predicting temperature in the kiln as a function of the vertical position.

The mathematical model of mixed feed lime kiln is used to illustrate the effects of different operating conditions on the kiln operation. The parameters studied include fuel ratio, air excess number, lime throughput, limestone size and reactivity, kind of fuel, coke size and reactivity. The applications show how the model can give insight for the kiln performance under different operating conditions.

Zusammenfassung

Schachtöfen, die mit einer Mischung aus Kalk und karbonisiertem Gas beschickt werden, werden für viele industrielle Prozesse, wie zum Beispiel zur Herstellung von Soda, Zucker und Magnesiumoxid, verwendet. Zielsetzung dieser Arbeit ist die Optimierung des Betriebes eines solchen Kalkschachtofens durch ein besseres Verständnis des Gesamtprozesses.

Hierfür wird ein mathematisches Modell entwickelt, wobei Betriebsmessungen als Eingabeparameter und zur Validierung des Modells dienen. Zur Bestimmung der notwendigen Eingabeparameter wurde ein Modell für den Einzelpartikel hergeleitet. Zudem wurde der gesamte Ofenprozess energetisch bilanziert.

Mit Thermoelementen wurde das vertikale Temperaturprofil des Ofens von der Vorwärmzone bis zur Kühlzone experimentell gemessen. Des Weiteren wurden die Eintritts- und Austrittsdaten an beiden Enden des Ofens ermittelt. Am oberen Ende wurde zusätzlich die Zusammensetzung des Abgases mittels eines Gasanalyse-Messgerätes aufgenommen. Aufgrund der verminderten Qualität des verwendeten Kalksteins, kann der Ofen nicht optimal gefahren werden. Anhand der ermittelten Messdaten wird dies ersichtlich.

Simulationen der Kohlepartikelverbrennung wurden mittels eines instationären Modells durchgeführt. Dieses beinhaltet eine detaillierte Beschreibung der Transportphänomene in Kopplung mit den chemischen Reaktionen. Mit dem Modell lassen sich bei vorgegebenen Umgebungsbedingungen und Kohlepartikel-eigenschaften die Partikeltemperatur, die Brennrate, der Umsatz, die Partikelschrumpfung und die spezifische Zusammensetzung des Partikels berechnen. Ein Vergleich der Simulationsergebnisse mit Literaturwerten ergibt eine gute Übereinstimmung.

Das Kalzinationsverhalten eines Kalksteinpartikels wurde simuliert. Die verwendeten Gleichungen zur Beschreibung des Verhaltens wurden aus der Literatur übernommen. Das Kernschrumpfungsmodell wurde zur Beschreibung der Mechanik sowie der chemischen Reaktionen des reagierenden Kalksteinpartikels angewendet und im Ofenmodell implementiert.

Ein Basismodell wurde auf Grundlage von Massen- und Energiebilanzen für die Gas- und Solidphase entwickelt. Es beinhaltet die chemischen Reaktionsenthalpien zur Beschreibung des Brennstoff- und Kalksteinumsatzes. Der Wärme- und Stoffübergang zwischen den einzelnen Phasen findet dabei durch Konvektion statt. Es werden die Temperatur-, Umsatzgrad-, Massenstrom- und Konzentrationsprofile der Gas- und Solidphase als Funktion der vertikalen Position berechnet. Zudem werden der Druckverlust im Innern des Ofens und die Gasgeschwindigkeit ermittelt.
Die Eintrittsdaten des Ofens werden für das mathematische Modell benötigt. Wohingegen die experimentell ermittelten und die Austrittsdaten zur Validierung des Modells benötigt werden. Eine Analyse der Validierung zeigt, dass mit Hilfe des Modells die essentiellen Phänomene hinreichend genau zur Bestimmung der axialen Temperaturprofile beschrieben werden.

Des Weiteren wird das mathematische Modell zur Darstellung des Einflusses bei variierenden Betriebsbedingungen genutzt. Die Parameterstudie enthält die Brennstoffmenge, die Luftzahl, die Kalksteinaufgabe, die Partikelgröße und Reaktivität des Kalksteins und der Kohle sowie die Art des Brennstoffes. Diese Anwendungen zeigen den Einfluss auf die Ofenleistung bei variierenden Betriebsbedingungen.

Acknowledgement

Table of Contents

Nomenclature

Nomenclature	Description
a	specific surface area, m^2/m^3
A	area, m^2
c_p	specific heat capacity, $kJ/kg.K$
C	concentration, $kmol/m^3$
d	diameter, m
$\bar{d}$	mean Sauter diameter, m
D	diffusion coefficient, m^2/s
E	activation energy, $kJ/kmol$
h_u	net calorific value of fuel, kJ/kg
h_{co}	reaction enthalpy of co, kJ/kg
h_v	enthalpy of water vaporization, kJ/kg
ΔH	enthalpy of reaction, kJ/kg
$\Delta \tilde{H}$	molar enthalpy of reaction, $kJ/kmole$
e	emissivity, -
l	length, m
L	air demand, kg_a/kg_f
k	reaction rate coefficient, m/s
$\dot{M}$	mass flow rate, kg/s
M	Molecular weight, $kg/kmol$
N	number of particles
$\dot{N}$	molar flow rate, $kmol/s$
P	pressure, Pa
ΔP	pressure drop, Pa
q	heat transfer,kW/m^3
Q	heat, kW
r	radius,m
r_c	fuel ratio
R	universal gas constant, $kJ/kmol.K$
T	temperature, K
u	overall transfer coefficient, $W/m^2.K$
U	superficial velocity, m/s
v	velocity, m/s
V	volume, m^3

Nomenclature	Description
x_i	mass fraction of component i
$\tilde{x}_i$	volume or molar fraction of component i
X	conversion degree
z	axial position, m

Greek symbols

ϵ	particle porosity
ε	bed void fraction
α	heat transfer coefficient, $W/m^2.K$
β	mass transfer coefficient, m/s
λ	thermal conductivity, $W/m.K$
λ	air excess number
μ	viscosity, $kg/m.s$
ρ	density, kg/m^3
$\tilde{\rho}$	molar density, $kmol/m^3$
σ	Stephan- Boltzmann constant, W/m^2K^4
τ	tortuosity factor
φ	sphericity of particles
$\Re$	rate of reaction, $kmol/m^3.s$

Superscript

a	air, ambient
av	average
b	bed
c	coke
CO	carbon monoxide
CO_2	carbon dioxide
eff	effective
f	fuel, core
g	gas
H_2O	water
i	initial
k	kiln
l	lime
ls	limestone
N_2	nitrogen
O_2	oxygen
p	particle
r	reaction
s	solid, surface
v	vapor
w	wall

Dimensionless numbers

Nu	Nusselt number, heat transfer
Pr	Prandtl number, heat capacity
Re	Reynolds number, velocity
Sc	Schmidt number, diffusivity
Sh	Sherwood number, mass transfer

Chapter 1

Introduction

1.1 Mixed feed shaft Kiln

The mixed feed shaft kiln is the most basic and oldest shaft kiln design, it has been used in many industries through the centuries. A schematic diagram representing a mixed feed shaft Kiln is given in figure 1.1. Many improvements of the kiln operation have been made in the past years. However, the developments were mainly done by trial and error. Therefore, this work was initiated to increase the knowledge about the mixed feed shaft kiln to improve the operation of the kiln.

1.1.1 Geometrical features

The mixed feed shaft Kiln has varying heights, diameters and construction details to suit the type of applications. A cylinder is the most common type of kiln used commercially. In general, the diameter to height ration in this kiln vary from 1: 2.5 to 1: 5. The sizing of the kiln depends on the application. Typically, the capacity, the height of the kiln varies from 3 to 22 m and the inside diameter varies from 1.5 to 4 m. The inside of the kiln is lined with two layers of refractory and insulating bricks for several reasons but the primary purposes are to withstand the operating temperature and to save energy. Four outlet doors of suitable sizes about 60 cm wide and 75 cm high were provided for the discharge of lime.

1.1.2 Process description

The mixed feed shaft kiln works on a very simple principal, it is charged continuously from the top with mixed feed of limestone and coke, while the air is injected from the bottom of the kiln. The solid charge travels down by gravity through the kiln against rising stream from burning products. It moves slowly down the kiln through three zones; preheating, calcination and cooling. The height of each zone to total height of kiln cannot be determined exactly because the height of the zones changes
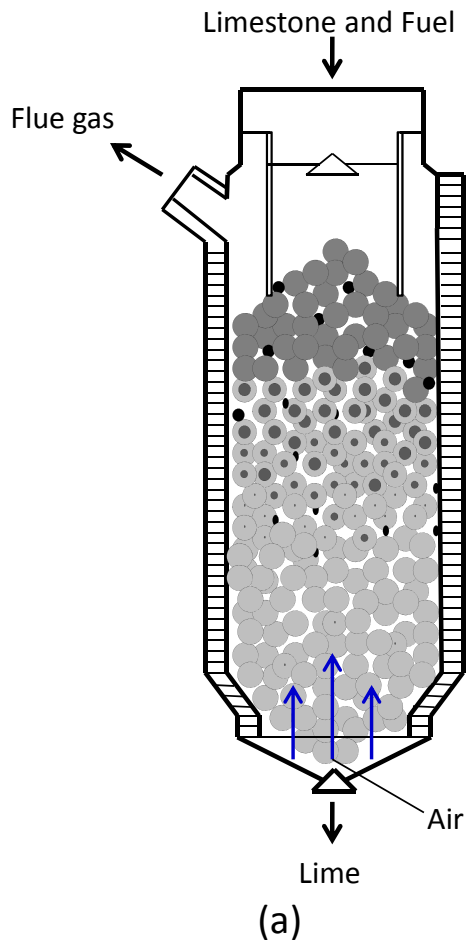
Figure 1.1: (a) Schematic overview of the mixed feed lime shaft kiln. (b) Lime kiln (soda ash plant).

with variations in operating parameters. In the upper part of the kiln (preheating zone), the rising hot gases from the burning zone come in contact with downward moving solid charge (limestone and coke) and heat it to the calcination temperature as it moves downward. The gases flow up and leave from the top of the kiln at a temperature of 100 to 200 °C. When the solid charge moves from preheating zone to the calcination zone, it is already heated to about 800 to 900 °C. In the calcination zone with the high temperatures, several complex processes take place: the coke burns and limestone decomposes into lime (CaO) and carbon dioxide (CO_2). Lime is cooled gradually in the lower part of the kiln by incoming air from below before it is discharged, see figure 1.1.

1.1.3 Applications of mixed feed shaft Kilns

Mixed feed lime kilns are widely employed in Europe and Asia. They have good thermal efficiency. They can use coke or anthracite as a fuel, so they are the most popular in the industries using both lime and gas, such as the soda ash, sugar and magnesia industries. In these industries, considering quantities of limestone to be burned and the necessary CO_2 concentration, the energy is generally provided by coke or anthracite. Use of gaseous fuel leads to too low a CO_2 concentration in the flue gas. In this section, we mainly focused on the application of the mixed feed lime kiln in soda ash plants and the production process in details.

1.1.3.1 Mixed feed shaft kiln in soda ash plant

The operating conditions for a lime kiln fitted to soda ash production are critically different from those used for lime production, because of the need to produce flue gas with the maximum concentration of carbon dioxide (CO_2) for its subsequent use in the process. This is done to the deteriment of produced lime purity, which will be less than that necessary in the lime industry. Therefore, the soda ash manufacturers placed a number of constraints on the type and design of lime kiln that can be used. These constraints can are as follows:

- CO_2 concentration in the flue gas as high as possible $> 40\,\%$.

- Maximum thermal efficiency of the calcination process.

- An ability to accept a wide particle size distribution of limestone to minimize the take at the quarrying step.

- High unit capacity considering tonnages to be treated.

Analyzing the standard available types of kiln such as vertical shaft, annular, Maerz and rotary kilns, fueled with coke, natural gas or fuel oil , one can conclude that the vertical shaft kiln, fed with coke, represents the best compromise satisfying the constraints mentioned above. Following are the advantages of mixed feed shaft kilns, fed with coke over the other kilns which air compatible with the requirements above:

- CO_2 concentration in a gas is between 36 and 42 %. The other kilns can only deliver a gas ranging between 25 and 32 % CO_2.

- Achieves the maximum thermal efficiency, it has the lowest heat usage of all kilns. The other solutions have an energy demand up to 52 % greater.

- The other types of kilns require limestone with a narrower particle size distribution. Other types of kilns, therefore, need a more highly graded product

producing larger quantities of rejected fines and less efficient use of natural resources.

- The design and operation of the vertical shaft kiln also gives the additional advantage of providing a reserve gas capacity of several hours without loss of kiln.

1.1.3.2 Sodium carbonate production (Solvay process)

The Solvay process (ammonia soda process) is the major industrial process for the production of sodium carbonate (Na_2CO_3), washing soda ($Na_2CO_3.10H_2O$) and sodium bicarbonate (Na_2HCO_3) [1, 2]. In addition, it offers an opportunity for reducing greenhouse gas emissions. In 1860s, Ernest Solvay (Belgium) developed the ammonia soda process to its modern form and the process became known as the Solvay process which is the basis for sodium carbonate production today [3]. The world production of sodium carbonate increased steadily and reached 42 million tons per year in 2005 [4] which is more than six kilograms per year for each person on earth, roughly two- thirds of the world production is by Solvay process. Production sites in the European Union are shown on a map in figure 1.2.
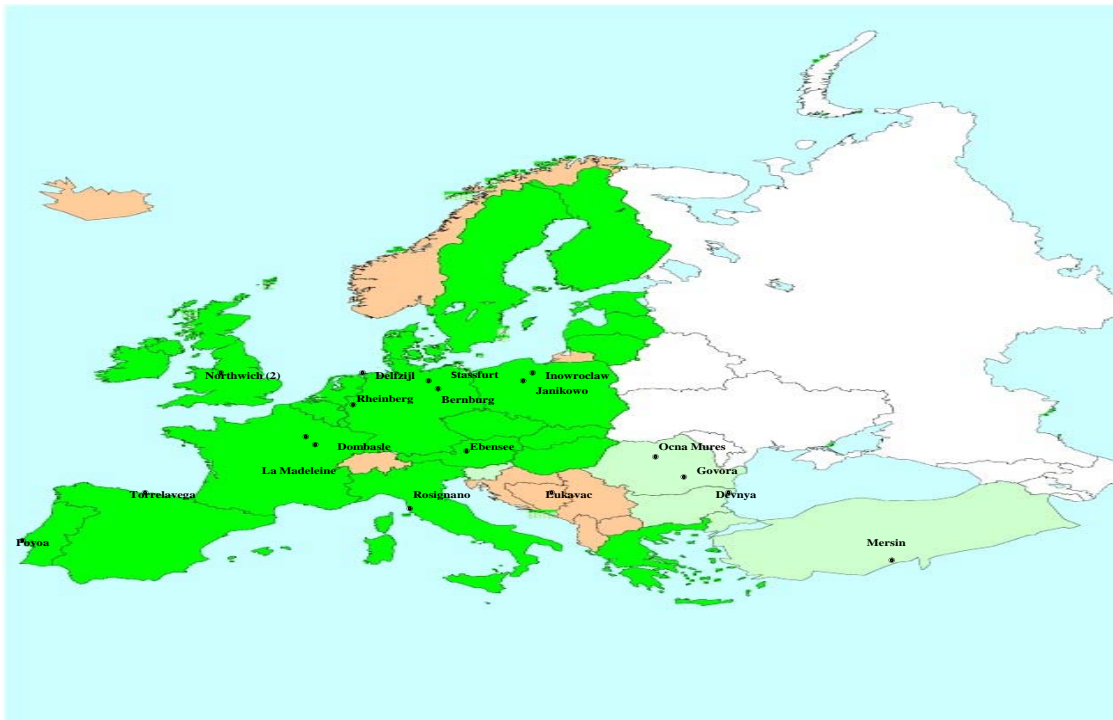
Figure 1.2: Overview of the location of soda ash plants (Solvay process)within the European Union (2002).
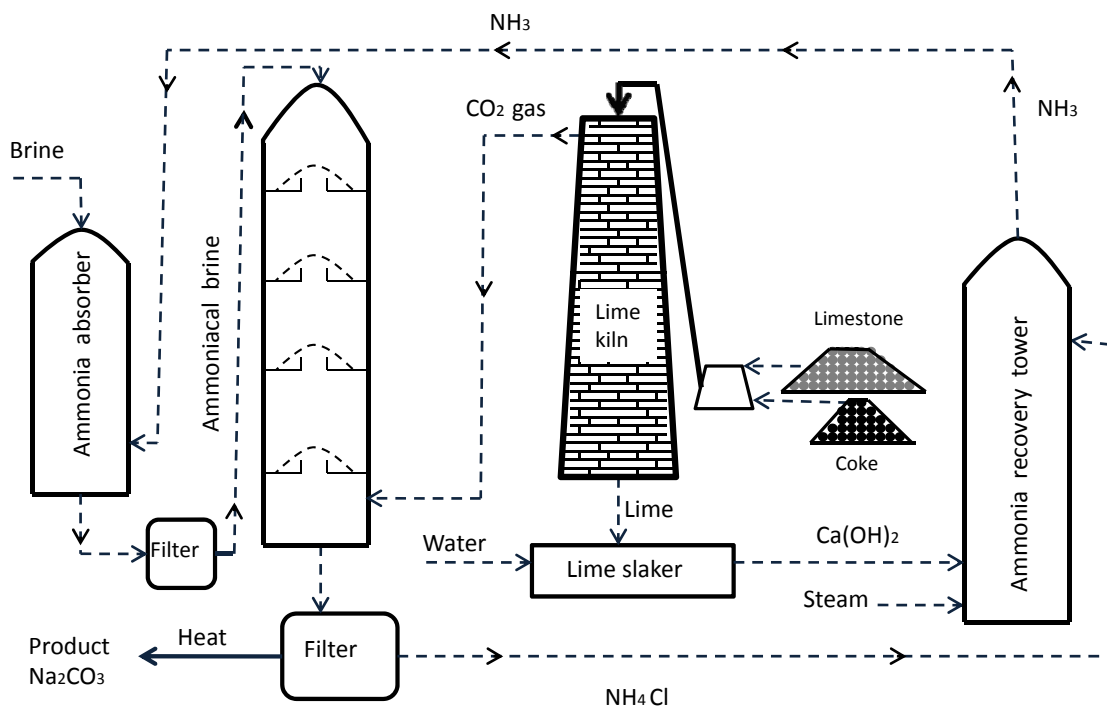
Figure 1.3: Flow diagram of soda ash plant.

The production process of sodium carbonate from Solvay process is illustrated in figure 1.3. In this process, the main raw materials are readily available and inexpensive; brine ($NaCl$) from (inland sources or the sea) and limestone ($CaCO_3$) from (mines). Ammonia, which is also used in the process is almost totally regenerated and recycled. At the beginning of the production line, the limestone and coke are weighed automatically and mixed together into buckets, which are transported to the top of mixed feed shaft kiln by a bucket elevator. In mixed feed shaft kiln the coke is burned and the heat released heats limestone to convert to quicklime (CaO) and carbon dioxide (CO_2).

$$C + O_2 \rightarrow CO_2 + Heat \tag{1.1}$$

$$CaCO_3 + Heat \rightarrow CaO + CO_2 \tag{1.2}$$

The gas is continuously withdrawn at the top of mixed feed shaft kiln and piped to a filter where the dust particles are removed. Then the clean gas is compressed to a suitable pressure by a gas compressor. At this point, the gas is ready to be used in the carbonation process.

In the carbonating tower, Ammoniacal brine enters from the top and meets the rising stream of carbon dioxide to form crystals of sodium bicarbonate and ammonium

chloride.

$$NaCl + NH_3 + CO_2 + H_2O \rightarrow NaHCO_3 + NH_4Cl \qquad (1.3)$$
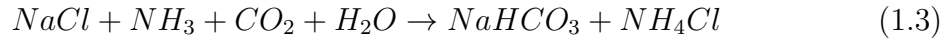
Sodium bicarbonate crystals are separated from the solution by filtration, then Sodium bicarbonate is heated to achieve calcination into a solid phase sodium carbonate which is the main product of the process and releases water and carbon dioxide as a gaseous phase where the gas is compressed and sent back to the carbonation tower:

$$2NaHCO_3 \rightarrow Na_2CO_3 + H_2O + CO_2 \qquad (1.4)$$
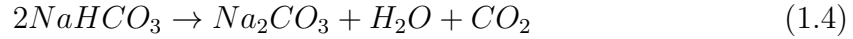
At the bottom of the mixed feed shaft kiln, quicklime is discharged continuously from the kiln and transported to the slaker by a conveyer belt. In the slaker, the quicklime is mixed with water to produce lime milk $Ca(OH)_2$ in an exothermic reaction.

$$CaO + H_2O \rightarrow Ca(OH)_2 + Heat \qquad (1.5)$$
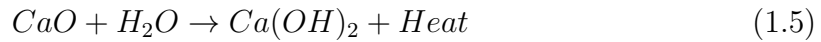
The milk of lime $Ca(OH)_2$ is pumped into the ammonia recovery tower and reacts with the ammonium chloride to regenerate ammonia.

$$Ca(OH)_2 + 2NH_4Cl \rightarrow CaCl_2 + 2NH_3 + 2H_2O \qquad (1.6)$$
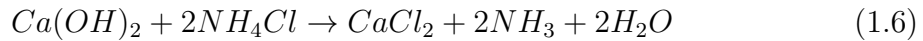
Because the Solvay process recycles its ammonia, and has calcium chloride as its only waste product, this makes it more economical than the other processes.

As shown above, the mixed feed shaft kiln is considered the heart of the soda ash plant. Therefore, it is important to optimize the kiln operation to produce high quality lime and gas because the quality of lime and carbonation gas largely determines the performance of the soda ash plant.

1.1.4 Raw materials for mixed feed lime shaft kiln

Limestone and coke or anthracite are the basic raw materials for the production of lime and carbonation gas.

1.1.4.1 Limestone

Limestone is a naturally occurring mineral that consists principally of calcium carbonate and some impurities. It exists in large quantities throughout the world in many forms and is classified in terms of its origin, chemical composition, structure, and geological formation [5]. Limestone should meet certain specifications with regard to its composition, size, and size distribution to be calcined well in the lime kiln. A high content of $CaCO_3$ in limestone is an important parameter to consider to avoid difficulties related to limestone decomposition and improves the efficiency of production. Typical composition of limestone suitable for use in the lime kiln is given in the following table.

Table 1.1: Typical composition of limestone for the lime kiln

components	%
$CaCO_3$	> 95
$MgCO_3$	< 2
SiO_2	< 2
Al_2O_3	< 0.4
$Na_2O + K_2O$	< 0.2
SO_4	< 0.2

Particle size distribution of limestone from quarries is generally between 40 and 200 mm. The more homogeneous they are, the better lime kiln will work. Before limestone is put into the kiln it should be clean of clay and mud because these materials block the complete exit of the gas from the kiln.

1.1.4.2 Coke

Coke or anthracite is mostly used as lime kiln fuel to produce flue gas with the high concentration of carbon dioxide required for the process. The following table indicates the composition of suitable coke to use in the lime kiln:

Table 1.2: Suitable coke composition for use in the lime kiln

components	%
C	> 80
N	< 1
O	< 5
S	< 0.5
H_2O	< 6
Ash	< 12
Net calorific value	$> 26.6 kJ/kg_{fuel}$

The particle size distribution of the coke has to be appropriate in order to get a homogeneous distribution within the kiln. In general, uniform coke particle size of 30 to 60 mm is suitable for use.

1.1.5 Mixed feed lime shaft kiln problems

The production of quality lime and carbonation gas, is important to optimize the Solvay process. Although, mixed feed lime kilns have evolved over the centuries there has been little investigation of the fundamentals which affect their performance. For

the effective operation of a kiln, a supply of suitable coke and limestone is needed. The major problems that can occur in mixed feed shaft Kiln operations are discussed as follows:

1. **Low efficiency of kiln**
   The usual causes of kiln's low efficiency are as follows:

   (a) **Low quality of limestone**: Limestone is a natural resource, the structure and composition of which varies from layer to layer within the same quarry. Consequently, this causes varying limestone quality. see figure 1.4. Limestone consists mainly of calcium carbonate $CaCO_3$ and some impu-

Figure 1.4: Photograph of limestone quarry.

rities ($MgCO_3$, SiO_2, Al_2O_3, Fe_2O_3, Na_2O, K_2O, SO_4 etc.). Low quality limestone refers to its low $CaCO_3$ content and high impurities. It is generally difficult to estimate spatial distributions of impurities of limestone so it can not be avoided or removed [5,6]. Therefore, the temperature in the calcination zone of the kiln should be kept at about 1100 °C. At high temperature above 1300 °C, the impurities present in the limestone form clinkers (hard and cement type material) which can block the kiln and also damage the refractory brick lining of the kiln. In addition, reducing the concentration of CO_2 in flue gas. Figure 1.5 shows a photograph of a crystalline slag.

   (b) **Non-uniform limestone size**: Limestone sizes play an important role in calcination of limestone in the kiln. Large particles are more difficult to calcine uniformly and require a longer burning time. If the time is short, the lime is not completely burned, the efficiency of the kiln is reduced. Small particles increase the resistance to the flow of gas so quality of preparation of limestone is one of the factors determining the efficiency of kiln operation. Gamej et al. [8] investigated the various methods of limestone preparation and showed that one of the efficient methods to produce high quality lime is removal of fines from the raw materials charged to the kiln.
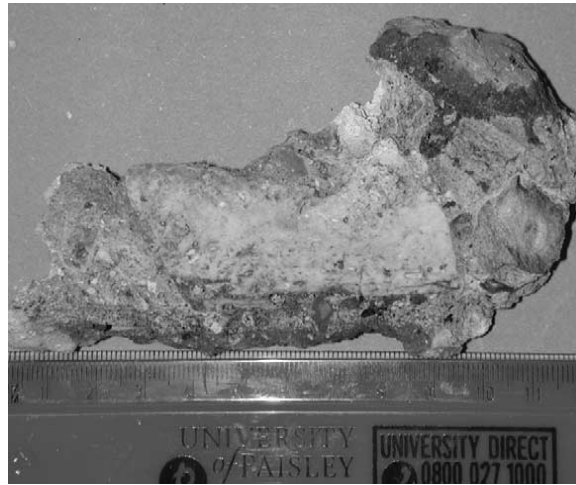
Figure 1.5: Photograph of a crystalline slag fragment roughly 70 mm in diameter [7].

2. **Much unburned lime**: Unburned lime due to imperfect conversion reactions inside the kiln, are drawn with the lime to the slaker. It can be separated at the slaker and used again by mixing with new limestone and fed to the kiln. With a lot of unburned lime, the quality of lime is reduced. The parameters that cause unburned lime are:

   - insufficient air for combustion cause incomplete combustion and consequently, the kiln temperature is lower than normal, producing under-calcined lime and also insufficient coke use.

   - large particles of limestone do not have sufficient residence time in the kiln to fully calcine and consequently, they contain more residual carbonate.

   - incomplete mixing of limestone and coke causes under-burning of lime in some parts of the kiln and also over-burning of lime in other parts of the kiln.

   Figure 1.6 shows cross section of unburned lime particles from a lime kiln. It can be seen from the figure that the particles have a dark unreacted grey core surrounded by a white calcined shell.

Figure 1.6: Cross section of unburned lime particles [9].

3. **Influence of fuel type and size on kiln performance**: Traditionally, coke has been used in mixed feed kiln. Coke is produced by heating high ranking coals with an absence of oxygen for a period of time at temperatures up to 1200 °C to remove the volatile. Different types of ovens have been used for manufacturing the coke. The properties of coke and its size differ by the coal properties and the oven design as well as the carbonizing conditions used. The quality of coke influences the kiln operation. Recent developments in the coke market, increasing prices and availability, have made it interesting to consider anthracite as an alternative. Therefore, many mixed feed kilns should be able to switch to anthracite. But use of anthracite needs trials to ensure that there are no unexpected problems with its use. So, the selection of fuel is dependent on the difference in price between coke and anthracite, where the price has the main influence on the decision of which kind of fuel to use, because cost of fuel would be one of the largest, if not the largest, cost of kiln operation.

   With non-uniform coke particle sizes, the height of the zones of the kiln change where small particles of coke burn fast, causing the preheating and calcination zones to move. Therefore, the flue gas exits from the kiln with a high temperature and energy is lost. Large particles continue burning after they pass the calcination zone, causing the calcination and cooling zone to move. Therefore, the lime discharged from the kiln is hot.

4. **High CO content in flue gas**: Mixed feed kiln generally uses coke or anthracite in operation. Where coke is used, the coke reacts with carbon dioxide to form carbon monoxide. At high temperatures and without enough oxygen for combustion ($C + CO_2 \rightarrow 2CO$) the coke should have low reactivity with respect to the reduction of carbon dioxide, where the reaction causes the reduction in yield of CO_2. Which is important for the ammonia soda process and formation of carbon monoxide (CO) which is hazardous. Where anthracite is used, it produces a lot of volatile which contains CO. The volatiles are released from anthracite in the preheating zone. The oxygen required for combustion is not available so, the CO exits as flue gas.

5. **Coke and limestone distribution**: The distribution of limestone and coke into the kiln is critical to good kiln operation. The buckets of mixed limestone and coke are transported by an elevator to the top of the kiln. Here, most kilns have rotating discharging distribution or rotating vibratory discharging distribution to distribute the charge into the kiln [10]. However, the distribution of coke and limestone is random. Distribution depends on the type of mixing between limestone and coke which is either uniform mixing or incomplete mixing. [11] used physical models to study the distribution of limestone and coke in the lime kilns. The actual plant observations and identified aspects of equipment and operation which are most likely to cause poor solid distribution

are simulated. They showed that distribution problems can be recognized and corrected distribution problems before they impair performance of kiln. Also physical models can be used to delineate distribution problems in beds of solids.

1.2 Motivation

The mixed feed shaft kiln is widely used in industries using both lime and carbonation gas. Although it was used in through industries since the centuries, there have been only a few research works on the kiln. Therefore, the processes occurring inside the kiln are scarcely understood and only little improvements have been achieved during the past years on the kiln. The objective of this work is to improve the operation of mixed feed lime kiln through improved understanding of the process. To achieve this goal certain things were accomplished. (1) Experimental measurements have been performed to obtain depth of knowledge about the process of kiln, which can also be used in the development of the mathematical model. (2) A mathematical model was developed for simulating the performance of the kiln. The simulation of the kiln helps to understand the complex interaction of the significant phenomena taking place in the kiln. These interactions include: the rates of the combustion and gasification reactions of coke, the heat and mass transfer to and from the coke, the calcination mechanisms of limestone and heat and mass transfer of limestone. The models of single particles of coke and limestone are used for describing the behavior of single reacting particles. Then these models of single particles are introduced in a more general one dimensional model describing the kiln, where the different properties depend upon the location within the kiln. The model of the kiln should result in a tool that can give insight into how different phenomena in the process constrain the kiln performance under different operating conditions.

1.3 Literature review

A large variety of lime shaft kiln designs have been used over the centuries and around the world. The main types of lime shaft kilns are: the single shaft counter flow heating kiln and the multiple shaft parallel flow heating kiln. Today, under conditions of an increase in price the energy and under conditions of an extremely stressed ecological situation in industrially developed regions, it is important to develop lime shaft kilns, create new kilns and improve existing kilns. They have been developed to obtain high productivity, lime quality and thermal efficiency in two ways: (1) experience and experiment, and (2) simulation of the kilns using mathematical models.

The single shaft counter flow kilns have quite efficient heat transfer in preheating and cooling zones. In calcination zone, where the rate and quality of decarbonization is completely determined by the heat and mass transfer processes, which depend on

factors such as the physicochemical and granulocytic parameters of the raw material, the fuel employed, its distribution, and also the distribution of the gases and their oxygen concentration over the sectors of the kiln is important. In this zone, the reaction of lump limestone proceeds towards the core of particle of un-reacted limestone, leaves behind it a layer of lime. With increasing the lime shell, the heat resistance of the lump calcined shell limits the heat transfer from the surface of the lump to the reacting core. At the same time the fuel burn and the temperature of the gases formed during fuel combustion is excessively high and consequently, the temperature of the material surface can rise over 1600 °C. Excessively high temperatures in combustion zone cause damage to the kiln lining, formation of clinker, and over-burnt lime which causes a nonuniform lime quality. Senegacnik et al. [12] investigated the effect of air excess ratio and flue gas recirculation on kiln operation to prevent temperatures in the combustion zone from exceeding the permissible levels. They showed that with increasing air excess ratios, the temperature in combustion zone is reduced but the heat loss with the exhaust gas at the kiln outlet increases. With flue gas recirculation, air excess ratio can be at optimal values and the temperatures in combustion zone remain within the permissible range and also stack loss is reduced. To avoid burnout of the lime, the combustion gas temperature of natural gas must be reduced to 1300 - 1350 °C, with the increase in air excess coefficient to 1.5 -1.7 [13].

In charging the shaft, the volume of space at the kiln wall is always greater than in the central part. In view of this, the resistance of aerodynamic of a shaft filled with material is always higher in the central part than in the periphery. This leads to non-uniform gas distribution through the kiln cross section, and consequently to excessive fuel consumption and reduction in lime quality. Therefore the firing system of lime shaft kilns has been the subject of many studies. Accinelli [14] designed a Central Burner Kiln (CBK) technology for achieving the heat distribution over the kiln cross-section and using low cost fuels. The burner beams achieved uniform heat distribution over the kiln cross-section. They span the entire kiln cross-section and distribute the hot combustion air which is supplied from the cooling zone and fuel at selected positions in the internal kiln. Due to uniform heat distribution in the kiln, overheating in the calcining zone is avoided and damage to the refractory materials of the kiln, due to zones of overburnt material, is eliminated [15]. Reshetnyak et al. [16] developed a new roasting technology aimed at increasing the quality of lime and reducing the fuel consumption. In this technology, the fuel is introduced by means of gas distributors at two levels: at the upper level, a large portion of the fuel (about of 60 %) is fed with higher combustion temperatures (1250 -1300 °C) and at the lower level, a small portion of fuel is fed with combustion temperatures of 1200 -1250 °C. The uniformity of gas distribution over the kiln cross section is achieved. When the size of limestone particles in lime shaft kiln is about 50 -150 mm, the effective penetration depth of the burner gases in the bed from the periphery is no more than 0.7

-0.9 m. Therefore, for more uniform fuel distribution, they use not only peripheral burners but also floor and roof mounted central burners, girder mounted burners and peak burners to ensure that the gas penetrates into the internal zones of the bed [13]. The uniformity of gas distribution in shaft kiln is due to the optimization of the tuyere supply of air blasting and materials with the use of distributive facilities [17]. The uniformity of gas distribution depends on the supply method of driving air and its parameters (pressure, temperature and consumption). In the TREIVO system, the driving air for the injectors is supplied at a pressure of about 0.9 bar and preheated with natural gas to 900 to 950 °C [18, 19].

A wide range of fuels (solid fuel, natural gas and oil) are consumed in lime kilns during the calcining process. Due to sharp increases in the price of fuels, the selection of fuel for firing lime shaft kilns is determined mainly by cost and availability of the fuel where fuel costs represent about 40 to 50 % of the production cost of lime. Lime producers are progressively paying more attention to the possibility of using alternative fuels for lime production. The use of alternative fuels save the use of fossil fuels and reduces waste being sent to landfills, therefore it is environmentally friendly. Although the alternative fuels have significant financial benefit for the lime industry, the use of them in the European lime industry is only beginning. Piringer [20] examined the use of flue gases with low calorific value which are produced in some industrial sectors, the steel industry, pig iron and biomass gasification for a parallel flow regenerative (PFR) lime kilns. He showed that flue gases with a calorific value of $7.5 MJ/m^3$ have been used in PFR lime kilns. Even flue gases with a calorific value of $4.3\ MJ/m^3$ can be used. Depending on the calorific value of flue gases, gases can be used for lime production alone or mixed with another gas of higher calorific value. The firing system of TWIN-D kilns which were fueled with 100 % pulverized petroleum coke or 100 % natural gas, or a combination of the two fuels in a predetermined ratio is developed to use a lean gas which is generated as a by product during the production of steel by the COREX process. The quality of quicklime produced was consistent and in accordance with the client specification [21]. The firing parallel flow regenerative kilns with secondary fuels were available and were applied successfully two years ago at lime plants [22]. The use of coal dust firing for large diameter mixed firing kilns was examined by Piringer and Werner [23]. For supplying the required burning heat, the side burners were combined with a central burner. The lime qualities meet the requirements and the capacity of kilns can be increased. Kalkwerk Mueller, Ahuette, has operated with pulverized solid fuel instead of gas fuel. For modifying, the firing system used the blowers to introduce fuel centrally and peripherally into the hot limestone charge with feed control valves and pipe manifold distributors [24]. Two way pressure systems have made an important contribution to the further development of kiln systems for lime burning. The fuel (pulverized coal, fuel oil or gas) is introduced into the limestone bed by specially designed burner systems [25].

Modeling of lime shaft kilns is relatively complex because of the complex phenomena which take place inside the kiln: countercurrent mode of operation, chemical reactions, heat and mass transfer; all of which occur simultaneously. With the difficulties in experimental measurements inside the lime kilns, the processes of kilns are still not understood and there are many problems which have to be solved. Therefore, mathematical descriptions of the processes considered requires joint consideration of all above phenomena using equations of mechanics of heterogeneous systems. A large number of mathematical models have been developed to characterize lime shaft kiln operations. These models are of the following types: heat and mass balance models, reaction kinetic models, simulation models etc. Most models were developed on steady state one dimensional approaches and took into consideration major chemical reactions, heat and mass transfer and gave the distribution of process variables along kiln height. Bes [26] modeled the normal shaft kiln in a steady state using the system of differential equations. Various factors were taken into account like details of heat and mass transfer and chemical reactions in which gas, and solid phases, using different types of fuel for calcination, were considered. Hai Do and Specht [27] developed a numerical models for normal lime shaft kiln, which takes into account the heat and mass transfer to calculate dynamically the complete temperature and concentration profiles of the gas and solid. Marias and Bruyres [28] developed a mathematical model to describe the main physical and chemical processes occurring in normal lime kiln which use biomass as a fuel for limestone calcination by specific burners. The model was built on balanced equations and completed with phenomenological relations for the estimation of heat and mass transfer inside the kiln and for the estimation of the kinetics of the reaction. Their model is able to predict the design of a new industrial kiln. Gordon et al. [29] developed a numerical model for shaft furnaces to optimize design and operating parameters of shaft furnaces. Through mathematical simulations of heat and mass transfer and material and gas flow, it is possible to determine the dimensions of the thermal zone, the fuel distribution over kiln levels, and the temperature of the gas and the bed over the kiln height, as well as the temperature, flow rate, and structural parameters required for limestone calcination in specific systems. Analysis of an annular shaft kiln was performed by Senegacnik et al. [30,31]. Senegacnik et al. [30] presented the theoretical model of heat transfer and the variation of calcination in a limestone sphere. They reported that to reduce the amount of unburnt lime in large pieces or increasing the capacity of an existing annular shaft kiln, it makes sense to increase the heat transfer coefficient from kiln gases to the stones up to the value of 60 $W/(m^2K)$ during the initial part of calcination. Senegacnik et al. [31] focused on experimental measurements of the vertical temperature profile and kiln gas composition of an annular shaft kiln for lime burning. Modeling the calcination process in the kiln was performed on the basis of the measured temperature profile.

A three-dimensional model of a lime shaft kiln has also been developed by Zhiguo, Bluhm-Drenhaus et al. [32, 33]. Bluhm-Drenhaus et al. [33] developed a three dimensional model to describe the heat and mass transfer related to the chemical conversion of solid material. They modeled the transport of mass, momentum and energy in the gas phase by computational fluid dynamics (CFD) and the conversion reactions in the solid material by discrete element method (DEM). Zhiguo [32] simulated the 3-D flow in the industrial-scale shaft kilns using a commercial CFD code FLUENT 6.2 to investigate temperature distribution and radial gas mixing of burner zone of normal lime shaft kiln. Various factors were taken into consideration like lance depth, burner diameter, preheating of combustion air, burner arrangement. He showed that, the increase of the lance depth may be helpful to protect the refractory wall being overheated but has only a slight effect on the overall radial temperature distribution. Mixing between the combustion gas and the cooling air can be improved by reducing the burner diameter or by preheating the combustion air.

Although the mixed feed shaft kiln is the most basic and oldest shaft kiln design and used in many industries over the centuries, , only a few number of research articles were published in the field of mixed feed lime kiln operation. No published information is available on experimental investigations of mixed feed lime kiln. Modeling of mixed feed shaft kilns is more complex than other lime kilns because it has the complex phenomena which take place inside the other lime kilns and complex heterogeneous chemical and physical kinetics of coke. Therefore, a few publications are available on mathematical modeling and simulation of mixed feed lime kiln. The design of mixed feed shaft kilns is apparently based more on thumb rules, deduced from the operational behavior of kilns [34]. They developed a rational approach to correlate the effect of some significant influencing parameters, with a view to computing the process engineering design of the kilns for average conditions of operation, in the first instance. Virma [35] presented mixed feed shaft kiln model that described the steady state operation of the kiln in one dimension using a deterministic approach. Submodels have been evolved for describing the behavior of the burning fuel and of the calcining limestone particles. Yi et al. [36] have presented a mathematical physical model for the reaction and heat transfer process in lime kiln and on line monitoring model for the decomposition rate of limestone. The model was built upon the thermal balance and material balance. [37, 38] have presented 1-D mathematical model for a combined process of limestone calcination and coke burning in a kiln with allowance for kinetics of physical and chemical transformations. They developed the model on the basis of the laws of conservation of mass and energy using the system of differential equations. The details of the calcination of limestone is not explained in detail but the behavior of the fuel has been described in a more detailed manner. Compared to the model developed by [35], our model is different because it includes

the kinetics of the combustion and decomposition reactions. On the other hand, compared to the model developed by [37, 38], our model is slightly different because our model does not account for internal reactions and the fuel particles. Our model also includes the details for limestone calcination that the model by [37, 38] does not account for.

1.4 Thesis outline

- Chapter 2 is dedicated to address the energy balance of mixed feed lime kiln. The complete heat balance of coke fired kiln is discussed in detail. The set of equations for the calculations are given. The influence of operating parameters on the energy consumption and output of kiln is discussed. The concentration of carbon dioxide in flue gas of the kiln is also addressed.

- Chapter 3 describes the experimental work of mixed feed lime kiln which has been carried out to obtain information about the conditions inside operating kiln. This information is used for development of mixed feed lime kilns, since it provides better understanding of the kiln. Several experimental measurements have been performed on operating kiln. They involve temperature profiles inside the kiln, temperature and compositions of flue gas, wall temperature and input to and output from the operating kiln.

- Chapter 4 presents the modeling of single coke particle combustion in an atmosphere of O_2. The mathematical formulation is discussed in detail. The model includes heterogeneous chemical processes in the solid phase. It is able to qualitatively and quantitatively describe the unsteady-state behavior of the coke combustion.

- Chapter 5 presents the modeling of a single limestone particle decomposition. The mechanism of limestone decomposition and the properties of limestone are discussed in detail. The equations describing the behavior of a single particle is derived.

- Chapter 6 presents the mathematical model of mixed feed lime kiln. The model is developed on the basis of mass and energy balance in one dimensional approaches and takes into consideration, chemical reactions, heat and mass transfer. It gives the distribution of process variables (temperatures of gas and solid phases, gas composition mass flow, conversion degrees and pressure drop) along the kiln height as functions of input data. The model has been validated against the measurements results and the input/output data. The validation showed that the model describes the essential phenomena in kiln accurately.

- Chapter 7 describes the application of a mixed feed lime kiln Model. The different operating conditions were tested to investigate the impact on the kiln operation. The application shows that the model can give insight into how different phenomena in the process constrain the kiln operation under different operating conditions.

- Chapter 8 concludes the thesis by summarizing the results of this work as well as the possible improvements for future work.

Chapter 2

Mass and Energy Balances

Mass and energy balances are very important in an industry. Their calculations are usually carried out when developing new reactor processes or when improving old ones. They are used in the examination of the various stages of a process, over the whole process and even extending over the total production system to ensure that process variables do not exceed the design or permitted limits. Energy balances can be very complicated, but with increasing availability of computers, the complex energy balances can be set up and manipulated quite readily and therefore used in everyday process management to establish the thermal efficiency of the process so that necessary action can be taken to optimize fuel use and conserve energy. In this chapter, the energy and CO_2 balances of mixed feed lime shaft kiln will be presented.

2.1 Description of the kiln operation

A mixed feed lime kiln is basically a packed bed reactor and works on a counter flow principle where the hot gases move upward in the kiln and the solid charge moves downward. The solid materials (limestone and coke) are continuously charged from the top of the kiln and move slowly downwards through three zones: preheating, calcination and cooling. In the preheating zone, the solid charge is preheated by upward moving hot gases from the combustion zone. When the temperature of solid charge rises to about 600 °C the coke starts to burn while the limestone is still heated until it reaches calcination temperature in the range of 820 and 900 °C. In the calcination zone, limestone is decomposed to form quicklime and carbon dioxide and the coke burns. In the cooling zone, after the lime leaves the calcination zone, it is cooled by air from the bottom of the kiln where, the main part of the sensible heat of lime is transferred to the airflow while the coke is still burned where the combustion zone is longer than the calcination zone. From previous descriptions, it is known that the length of the three zones for limestone is different than the length of three zones for coke as it is shown in figure 2.1. So, the energy balance calculations of mixed feed lime kiln is very complicated with the dividing of the kiln into three zones.
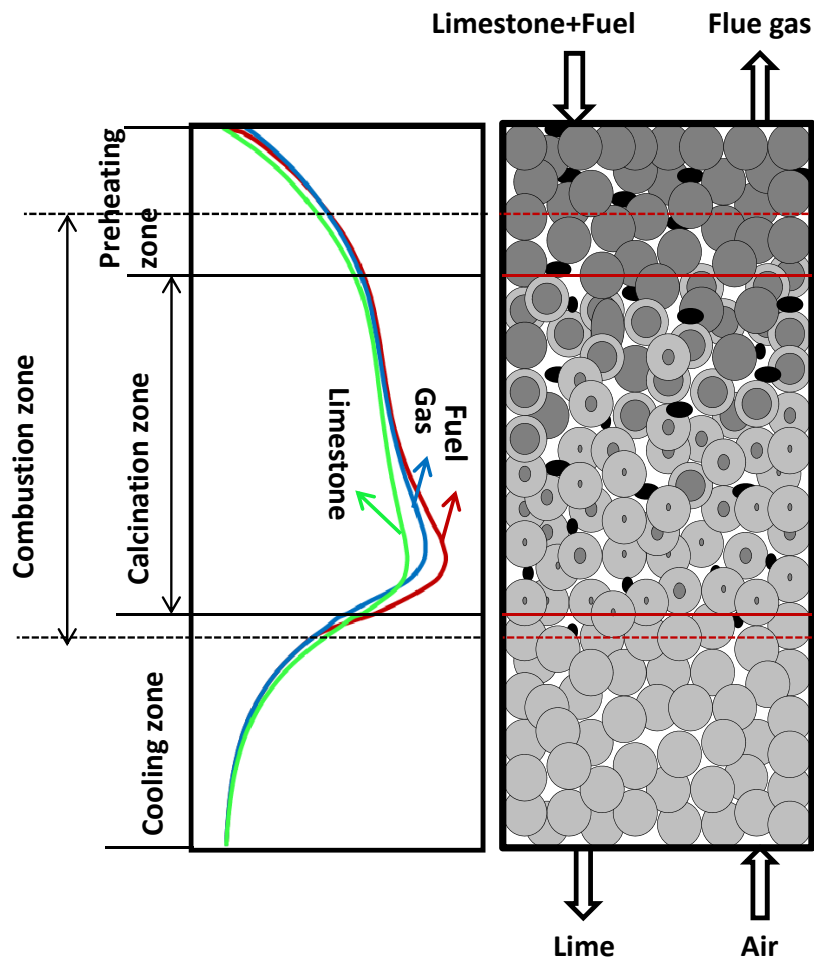
Figure 2.1: Temperature profile and flow direction of solid and gas.

2.2 Energy balance

2.2.1 Basic principles

Energy balance over the whole mixed-feed shaft kiln can be represented diagrammatically as a box, as shown in figure 2.2. The energy going into the kiln and the energy coming out are shown. Energy takes many forms, the most common important energy form is heat energy. In heat balances, the enthalpies are always referred to the reference temperature (0 °C).
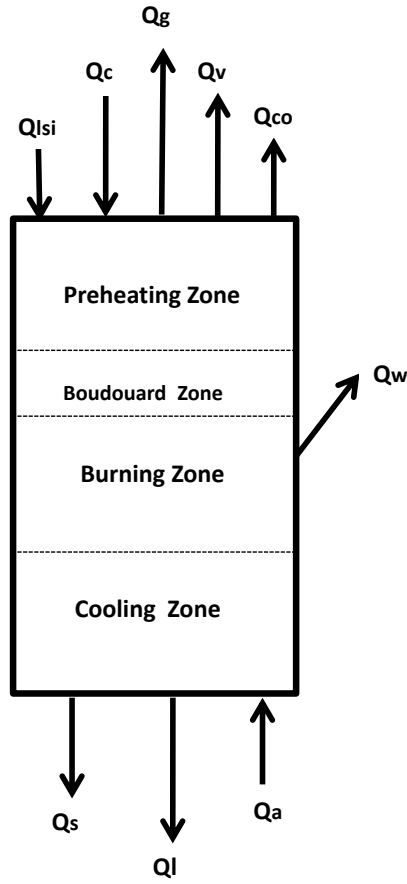
Figure 2.2: Heat input and output of Mixed feed shaft kiln.

2.2.1.1 Heat input

The heat input includes the chemical heat of fuel $\dot{Q}_c$, which equals the mass of fuel multiplied by its net calorific value, the sensible heat of the inlet air $\dot{Q}_a$, which is calculated relative to ambient temperature T_a, and the sensible heat of inlet limestone $\dot{Q}_{lsi}$, which is calculated relative to room temperature. Equations 2.1 to 2.3 covers the formulas which are used to determine the heat input to the kiln.

$$\dot{Q}_c = \dot{M}_f h_u \tag{2.1}$$

$$\dot{Q}_{lsi} = \dot{M}_{ls} cp_{ls} T_{lsi} \tag{2.2}$$

$$\dot{Q}_a = \dot{M}_a cp_a T_a \tag{2.3}$$

Where $\dot{M}$ is the mass flow rate, kg/s, h_u is the calorific value of fuel, kJ/kg, cp is the specific heat, $kJ/(kg.K)$, T is the temperature, °C. The subscripts f, ls and a

represent fuel, limestone and air, respectively.

2.2.1.2 Heat output

The heat output includes the heat of calcination, $\dot{Q}_l$, which is the useful energy, the vaporization heat of water, which is included in limestone and fuel, $\dot{Q}_v$, the sensible heat of exhaust gases $\dot{Q}_g$, the heat loss by CO, $\dot{Q}_{co}$, the heat loss by wall, $\dot{Q}_w$ and sensible heat of output solid (lime, unburned lime and ash from the fuel), $\dot{Q}_s$. Equations 2.4 to 2.9 covers the formulas which are used to determine the heat output from the kiln.

$$\dot{Q}_l = \dot{M}_l \Delta h_l X_l \tag{2.4}$$

$$\dot{Q}_v = \dot{M}_{ls} x_{H_2O} h_v + \dot{M}_f x_{H_2O} h_v \tag{2.5}$$

$$\dot{Q}_g = \dot{M}_g cp_g T_g \tag{2.6}$$

$$\dot{Q}_{co} = \dot{M}_g \tilde{x}_{co} h_{co} \tag{2.7}$$

$$\dot{Q}_w = u A_w \left(T_w - T_a \right) \tag{2.8}$$

$$\dot{Q}_s = \dot{M}_l cp_l T_{le} X_l + \left(1 - X_l \right) \dot{M}_{ls} cp_{ls} T_{le} + \dot{M}_f x_{ash} cp_{ash} T_{ash} \tag{2.9}$$

Where Δh_l is the reaction enthalpy of lime, kJ/mol, X_l is conversion degree of limestone, $1 - X_l$ gives the residual CO_2 content, x is the mass fraction, $\tilde{x}$ is the volume fraction, u is overall heat transfer coefficient, $W/(m^2.K)$, A_w is the surface area of the kiln wall, m^2. The subscripts l, v, g, co, w, a, le and ash represent lime, vapor, gases, carbon monoxide, wall, ambient, exit lime and ash, respectively.

The last term in equation 2.9 $\dot{M}_f x_{ash} cp_{ash} T_{ash}$ is the amount of ash from fuel which exits as a solid from the kiln, this amount is small and can be neglected.

2.3 Energy balance calculations

Energy balance calculations require knowledge of thermodynamic data such as specific heats, heats of combustion, enthalpies of phase change and densities and the conditions of the state such as input and output temperatures. Also it requires knowledge of mass flow rate of input and output materials. Therefore, we assume some data is able to calculate the energy balance of the kiln.

The mass flow rate of air is a function of air demand L which depends on kind of fuel and air excess number λ which depends on the operating conditions:

$$\dot{M}_a = \lambda L \dot{M}_f \tag{2.10}$$

The mass flow of exhaust gases consists of the mass of air flow, mass of fuel flow and mass of the CO_2 flow which is produced by decomposition of limestone.

$$\dot{M}_g = \dot{M}_a + \dot{M}_f + \dot{M}_{ls} y_{co_2} X_l = \left(1 + \lambda L \right) \dot{M}_f + \dot{M}_{ls} y_{co_2} X_l \tag{2.11}$$

Where y_{co2} is the mass fraction of CO_2 in the limestone, it varies for different limestone and is typically in the range of 0.4 to 0.44 kg_{CO_2}/kg_{ls}.
$\dot{M}_{ls}$ is the mass flow of limestone, which is given:

$$\dot{M}_{ls} = \dot{M}_l \frac{1}{1 - y_{co_2}} = \frac{\dot{M}_{co_2}}{y_{co_2}} \qquad (2.12)$$

Where $\dot{M}_l$ is mass flow rate of lime and $\dot{M}_{co_2}$ is mass flow rate of co_2

2.3.1 Primary assumptions

With the set of equations 2.1 to 2.9 the energy balance for the kiln can be calculated. Also, the assumptions in table 2.1 are postulated in order to calculate the energy balance of the kiln. The calculations were carried out with the mean values of specific heat capacities.

Table 2.1: Summary of assumptions to energy balance calculations

the kind of fuel	coke
calorific value of fuel h_u	$29000\,kJ/kg$
air demand L	$12\,kg_a/kg_f$
the inlet temperature of coke, limestone and air	20 °C
exhaust gas temperature	100 °C [5]
lime discharge temperature	50 °C [5]
mass fraction of CO_2 in limestone	$0.40 - 0.44$
specific heat capacity of exhaust gases	$1.022 kJ/kg.K$
specific heat capacity of limestone	$830 kJ/kg.K$
specific heat capacity of lime	$770 kJ/kg.K$
heat loss by wall	170 kJ/kg_{lime}
the reaction enthalpy of lime $\Delta\tilde{h}_l$	$178\,kJ/mol$
enthalpy of vaporization h_v	$2500\,kJ/kg$
the reaction enthalpy of CO $\tilde{h}_{CO}$	$283 kJ/mol$

2.3.2 Energy consumption

Due to rising energy costs, the energy consumption for decompositions of limestone has been the subject of many studies. Here, the energy consumption of mixed feed lime kiln and the parameters effect it will be studied. Based on the principle of

conservation of energy, the energy going into the kiln must balance with the energy coming out, when the kiln operates steadily. From equations 2.1 to 2.12 the energy consumption per kg of output is obtained:

$$
\frac{\dot{M}_f}{\dot{M}_{output}} h_u = \frac{\left(\dfrac{y_{co_2}}{1 - y_{co_2}}\right)(\Delta h_{co_2} X_l + cp_g T_g + x_{co} h_{co}) + cp_l T_{le} X_l + \dfrac{\dot{Q}_w}{\dot{m}_l}}{1 - \dfrac{(1 + \lambda L)(cp_g T_g + x_{co} h_{co}) - \lambda L cp_a T_a + x_{ash} cp_{ash} T_{ash}}{h_u}}
$$

$$
+ \frac{\left(\dfrac{1}{1 - y_{co_2}}\right)(x_{H_2O} h_v - cp_{ls} T_{lsi} + (1 - X_l) cp_{ls} T_{le})}{1 - \dfrac{(1 + \lambda L)(cp_g T_g + x_{co} h_{co}) - \lambda L cp_a T_a + x_{ash} cp_{ash} T_{ash}}{h_u}} \tag{2.13}
$$

From equation 2.13 and previous assumptions, the energy consumption of mixed feed lime kiln can be calculated. Figure 2.3 shows the energy consumption per output of kiln for different conversion degrees of limestone that are dependent on the air excess number. For mixed feed lime kiln, air excess number should be in a range of theoretical to 20 % over the theoretical. Therefore, here, the energy consumption is calculated for air excess number in the range of 1 to 1.2. The energy consumption increases linearly with air excess number and also increases with increasing conversion degree of limestone. The energy consumption for complete calcination of limestone is the highest and decreases by approximately 0.155 MJ/kg_{output} with 5 % of conversion degree.
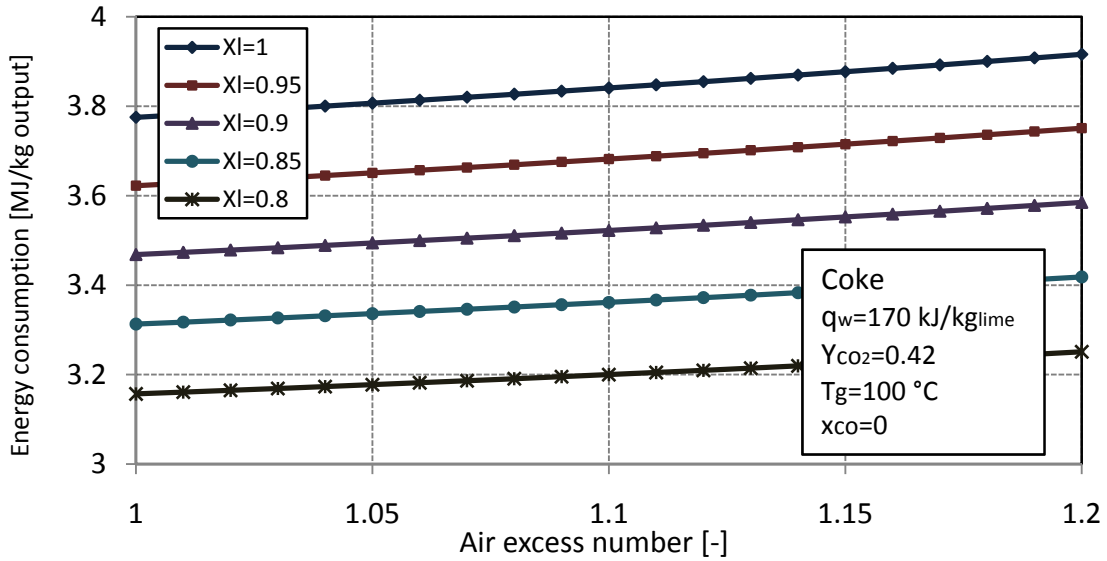

Figure 2.3: Energy consumption for different conversion degrees of limestone with air excess number.

The energy consumption per pure lime at different conversion degrees of limestone with air excess number is shown in Figure 2.4. For the same conditions, the energy consumption per lime is different than the energy consumption per output where the amount of lime increases with increasing conversion degree of limestone so, the energy consumption per pure lime for complete calcination of limestone is the lowest and increases with the decreasing of the conversion degree.
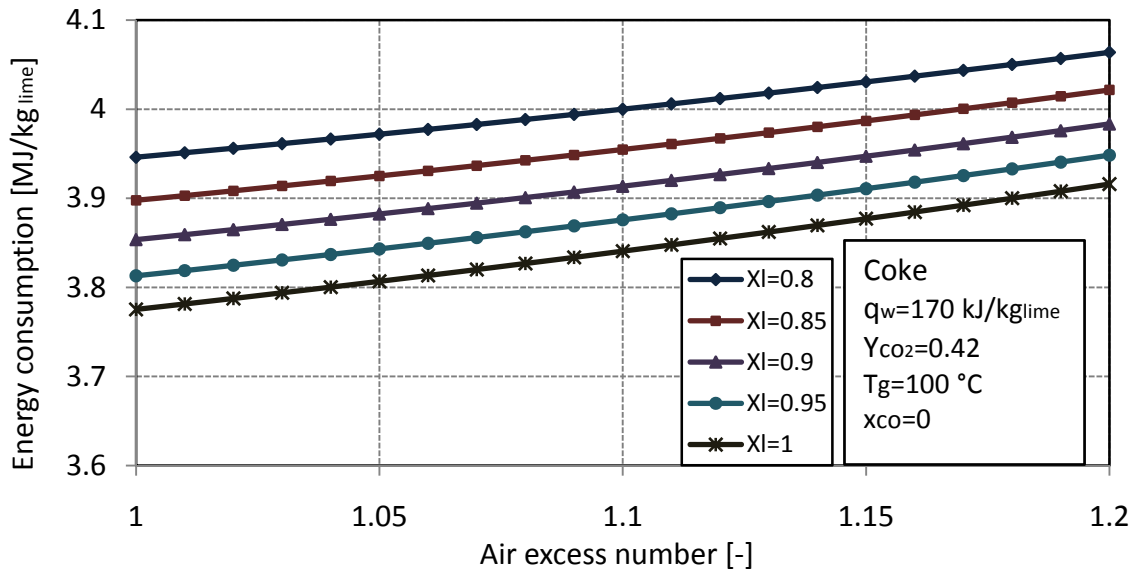
Figure 2.4: Energy consumption per lime with air excess number at different conversion degrees of limestone.

Figure 2.5 shows the energy consumption for different CO content in flue gas in dependence on air excess number for complete calcination of limestone. The content of CO in flue gas 0-2 % is usually typical for normal operation of mixed feed lime kiln where CO in flue gases is produced from incomplete combustion of fuel by insufficient air or, worse mixing between fuel and air. So, the high concentration of CO in flue gas is usually a sign that the kiln is not performing properly. The energy consumption increases with an increase of the content of CO in flue gases because the energy loss increases with the presence of CO in flue gases.

Figure 2.6 shows the energy consumption with mass fraction of CO_2 in limestone at different conversion degrees of limestone for theoretical excess air number. Energy consumption increases both with CO_2 mass fraction and conversion degree of limestone. It can be seen from Figure 2.6 that the mass fraction of CO_2 of limestone slowly influences the energy consumption.

Figure 2.5: Energy consumption for different x_{co} with air excess number.

Figure 2.6: Energy consumption for different conversion degree of limestone with CO_2 mass fraction in limestone.

2.3.3 Fuel ratio

The fuel ratio r_c is ratio of the amount of fuel to the amount of limestone $kg_f/kg_{limestone}$ charged to the kiln. From equations 2.1 to 2.12 the fuel ratio for mixed feed lime kiln is obtained:

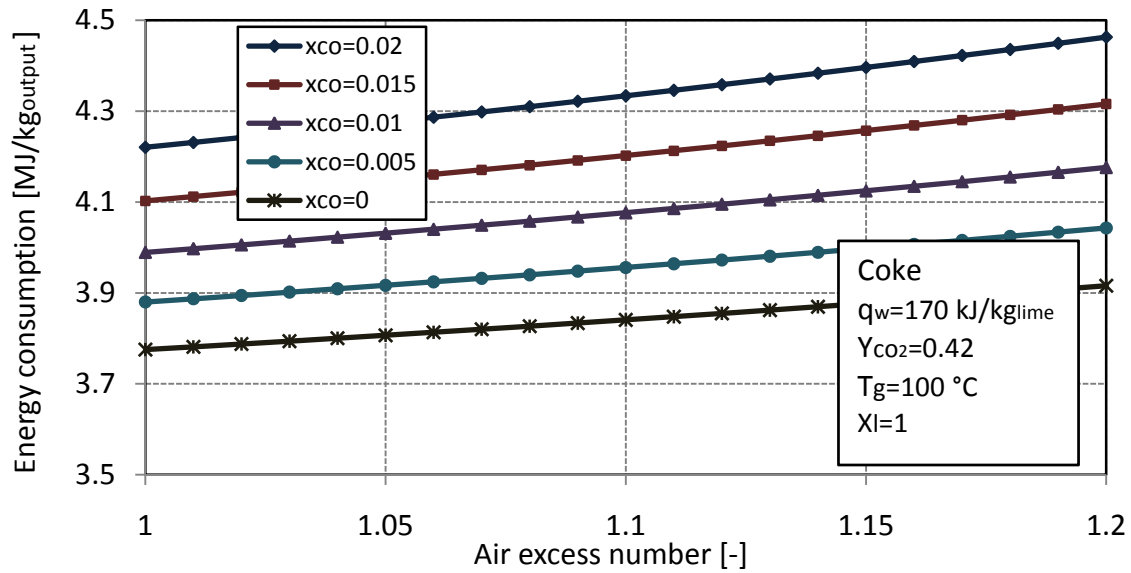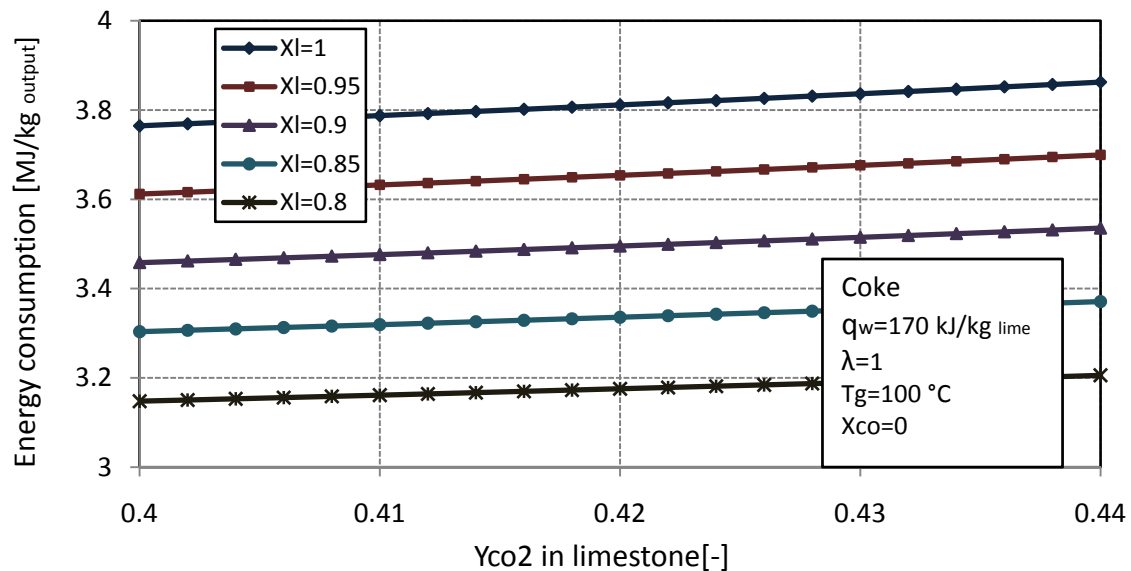$$r_c = \frac{(1-y_{co_2})\,\Delta h_l X_l + y_{co_2} X_l\,(cp_g T_g + x_{co} h_{co}) + x_{H_2O} h_v - cp_{ls} T_{lsi} + (1-X_l)\,cp_{ls} T_{le}}{h_u + \lambda L cp_a T_a - (1+\lambda L)\,(cp_g T_g + x_{co} h_{co}) - x_{ash} cp_{ash} T_{ash}}$$

$$+ \frac{(1-y_{co_2})\,cp_l T_{le} X_l + \dfrac{\dot{Q}_w}{\dot{m}_{ls}}}{h_u + \lambda L cp_a T_a - (1+\lambda L)\,(cp_g T_g + x_{co} h_{co}) - x_{ash} cp_{ash} T_{ash}} \tag{2.14}$$

Suitable fuel ratio for the kiln is important to produce high quality of lime and high concentration of CO_2 in flue gas and helps to maximize thermal efficiency and avoid excessive operating costs. So we study the fuel ratio for the kiln to determine the suitable value. Figure 2.7 shows the fuel ratio with conversion degree of limestone at different values of air excess number. With the increase of air excess number, the fuel ratio increases linearly with increasing of conversion degree of limestone. According to the assumption, the best value of fuel ratio is a bout $7\,\%$, for complete limestone calcination.

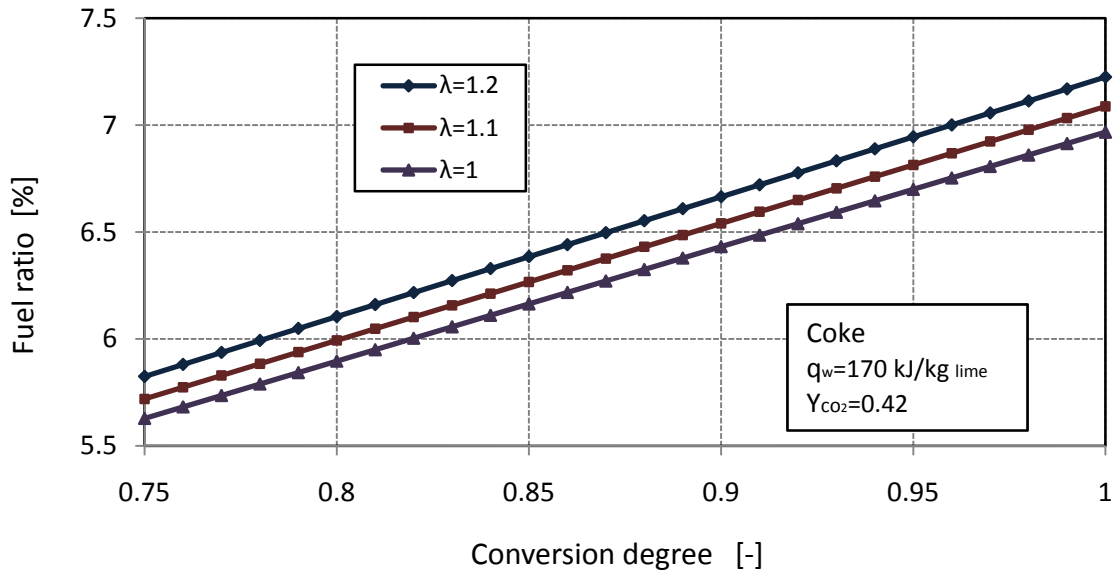Mixed feed lime kilns generally use coke or anthracite or both as fuel in operation.

Figure 2.7: Fuel ratio for different air excess number with conversion degrees of limestone.

The content of CO in flue gas is produced by the Bouduard reaction; incomplete fuel burning and volatile of fuel. Due to high amount of fuel in feed mixture, incomplete combustion of fuel causes CO in flue gas. At a high temperature and insufficient

oxygen, the carbon dioxide reacts with fuel to produce CO. Suitable fuel ratio would result in at lower concentration of CO in flue gas. Figure 2.8 shows the fuel ratio in dependence on the air excess number and volume fraction of CO in flue gas at complete calcination of limestone. For the previous assumption of exit temperatures and heat loss by the wall, the CO content in flue gas increases with fuel ratio. It can seen from Figure 2.8, that the lowest value of CO in flue gas is at the fuel ratio of 7 %. Figures 2.7 and 2.8 indicated that, the fuel ratio 7 % is the best value for high quality of lime and low concentration of CO in flue gas.
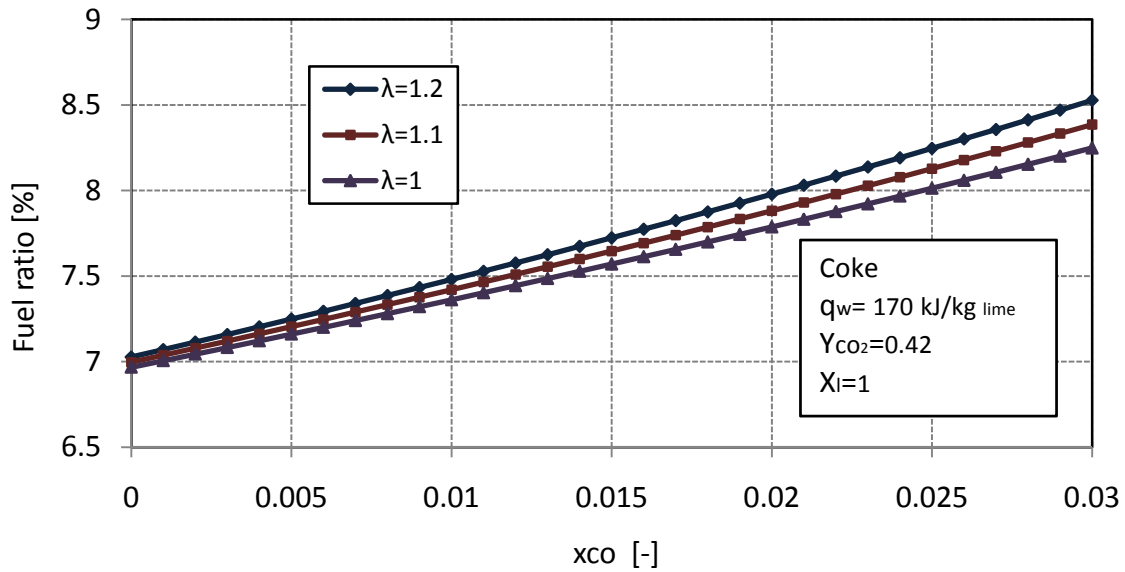
Figure 2.8: Fuel ratio for different air excess number with volume fraction of co in flue gas.

2.3.4 Flue gas temperature

The flue gas is continuously withdrawn at the top of mixed feed lime kiln and used in the other processes. In the kiln, the sensible heat of gases leaving the calcination zone is transferred to the solid charge in the preheating zone. Since the heat capacity of the gases is higher than the heat capacity of the solid materials, it is not possible to utilize the flue gas heat content completely. Therefore, flue gas from the preheating zone has a temperature of about 100-250 °C for normal operation. Figure2.9 shows the flue gas temperature for different conversion degrees of limestone with air excess number at 6 % fuel ratio. It increases more rapidly with air excess number and decreases when increasing the conversion degree of limestone. From figure 2.9, it can seen that the flue gas temperature is lowest at complete calcination, because of increasing the amount of gases through the production of CO_2 from calcination.
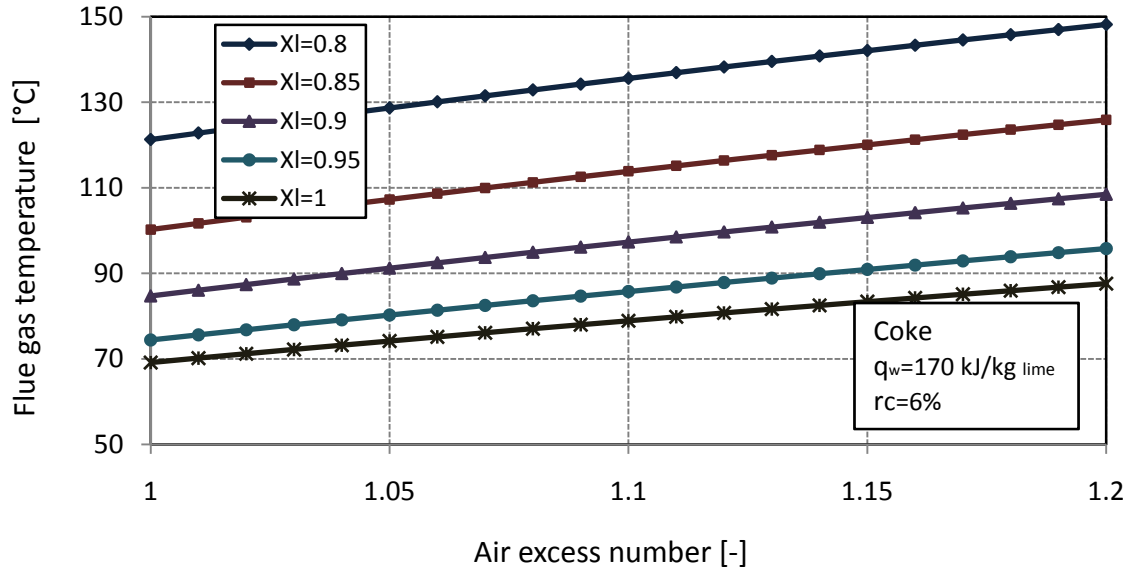
Figure 2.9: Flue gas temperature for different conversion degrees of limestone with air excess number.

2.3.5 Air amount

Air is injected from the bottom of the kiln for combustion of the fuel and also cooling of the lime in the cooling zone. The suitable amount of air is one an important factor in optimizing the kiln's operation. Without enough air, the combustion of fuel is not completed and will produce CO in flue gas. Figure 2.10 shows the air to outlet lime mass flow ratios with air excess number for different conversion degree of limestone. The ratio of air to lime increases when increasing both the conversion degree of limestone and air excess number. For complete calcination, the highest air to outlet ratio was needed, as it was expected, because of the air calculation based on fuel amount and also the mass flow of discharged lime is a minimum.

2.4 Carbon dioxide concentration

In the ammonia soda process, a high concentration of carbon dioxide (CO_2) in flue gas from mixed feed kilns is an important co-product because it is required for the process. The carbon dioxide in the flue gas is produced from the reactions of fuel combustion and the calcination of limestone, so it is necessary to study the parameters which effect the CO_2 concentration. The concentration of carbon dioxide in the flue gas can be calculated from the mass balance:

$$\dot{m}_{gf}x_{co_2f} + \dot{m}_{co_2l} = (\dot{m}_{gf} + \dot{m}_{co_2l})x_{co_2fg} \qquad (2.15)$$
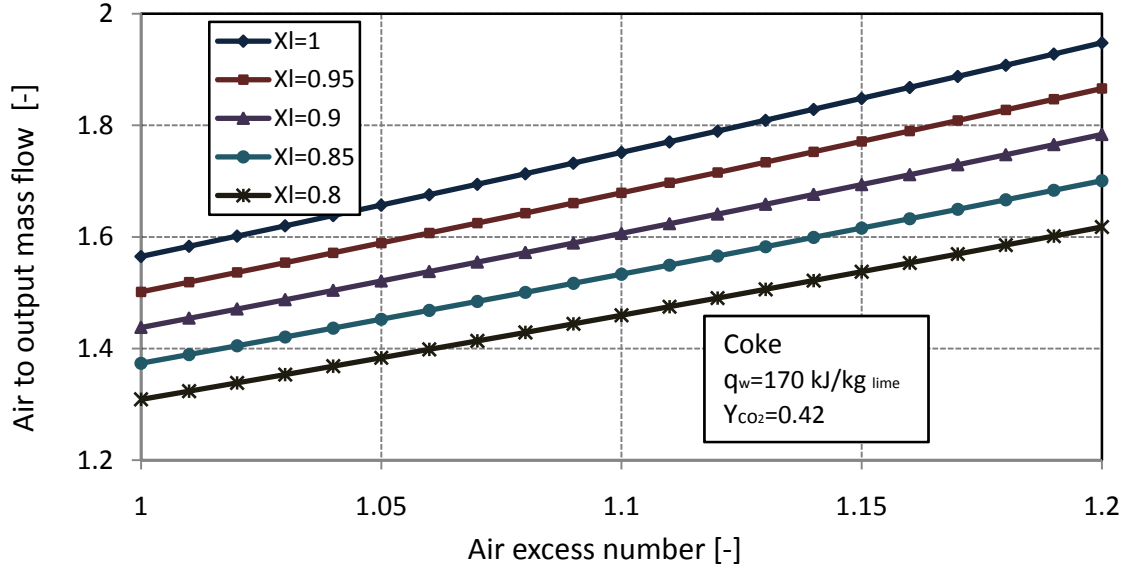
Figure 2.10: Air to outflow mass flow ratio for different conversion degrees of limestone with air excess number.

Where the $\dot{m}_{gf}x_{co_2f}$ and $\dot{m}_{co_2l}$ are the mass flows of CO_2 from the fuel combustion and from the calcination of limestone respectively. The mass flow of CO_2 from the calcination of limestone $\dot{m}_{co_2l}$ can be replaced by the limestone mass flow or lime mass flow.

$$\dot{m}_{co_2l} = \dot{m}_{ls}y_{co_2}X_l = \dot{m}_lX_l\frac{y_{co_2}}{1 - y_{co_2}} \tag{2.16}$$

From equations 2.15, 2.16 and 2.11 the concentration of CO_2 in flue gas can be written as:

$$x_{co_2fg} = \frac{(1 + \lambda L)\, r_c x_{co_2f}(\lambda) + y_{co_2}X_l}{(1 + \lambda L)\, r_c + y_{co_2}X_l} \tag{2.17}$$

From equation 2.17 it can be seen that the concentration of the CO_2 in flue gas of the mixed-feed lime kiln depends on the fuel ratio r_c, the conversion degrees of limestone X_l, the air excess number λ and x_{co_2f} which is generated by the combustion of the fuel.

The concentration of carbon dioxide x_{co_2f} in combustion gas has to be calculated from the molar balance for C, H_2, O_2 and N_2.

The following ensues for molar quantities fed in.

$$\upsilon_c = x_c\frac{1}{\tilde{M}_c}\frac{1}{\tilde{\rho}} \tag{2.18}$$

$$\upsilon_{H_2} = (\frac{1}{2}x_H\frac{1}{\tilde{M}_H} + x_w\frac{1}{\tilde{M}_{H_2O}} + x_{H_2OL}\frac{\lambda L}{\tilde{M}_{H_2O}})\frac{1}{\tilde{\rho}} \tag{2.19}$$

$$v_{O_2} = (\frac{1}{2}x_O\frac{1}{\tilde{M}_O} + x_{O_2L}\frac{\lambda L}{\tilde{M}_{O_2}} + \frac{1}{2}x_{H_2OL}\frac{\lambda L}{\tilde{M}_{H_2O}})\frac{1}{\tilde{\rho}} \tag{2.20}$$

$$v_{N_2} = (\frac{1}{2}x_N\frac{1}{\tilde{M}_N} + x_{N_2L}\frac{\lambda L}{\tilde{M}_{N_2}})\frac{1}{\tilde{\rho}} \tag{2.21}$$

Here, x_i is the content by mass of C, H, O, N, liquid water in the fuel, x_{iL} is the mass concentration of i in air and $\tilde{\rho} = \dfrac{P}{RT}$ is molar density.

The volume concentration of CO_2 in combustion gas $\tilde{x}_{CO_{2f}}$ follows:

$$\tilde{x}_{CO_{2f}} = \frac{v_c}{v} \tag{2.22}$$

where

$$v = v_c + v_{H_2} + v_{O_2}^* + v_{N_2} \tag{2.23}$$

Here v_c, v_{H_2}, v_{N_2} are the input mole flows according to previous equations. and $v_{O_2}^*$ is input of the non-reacted oxygen as follows:

$$v_{O_2}^* = (\lambda - 1)\, Lx_{O_2L}\frac{1}{\tilde{M}_{O_2}\tilde{\rho}} \tag{2.24}$$

The volume fractions have to be transferred into mass fractions using density.

$$x_{CO_{2f}} = \tilde{x}_{CO_{2f}}\frac{\rho_{CO_2}}{\rho_g} \tag{2.25}$$

From equation 2.14, equation 2.25 and equation 2.17, the concentration of carbon dioxide CO_2 in flue gas from mixed feed lime kiln can be calculated.

Figure2.11 shows the relation between carbon dioxide volumetric concentration in flue gas and air excess number at different values of conversion degree of limestone. The concentration of CO_2 in flue gas decreases with increasing air excess number while increasing with the increase of conversion degree of limestone. The higher value of carbon dioxide concentration is with complete decomposition of limestone and at theoretical air excess number.

Figure 2.12 shows the volumetric concentration of carbon dioxide in flue gas for different values of conversion degrees of limestone with an air excess number at 1 % content of CO in flue gas. By Comparing the results in figure 2.11 and figure 2.12, one can see that the concentration of CO_2 in flue gas decreases with content of CO in flue gas because the carbon from the fuel changes into CO_2 and some carbon changes into CO.

The volumetric concentration of carbon dioxide in flue gas for different values of conversion degrees of limestone with mass fractions of carbon dioxide in limestone at a theoretical air excess number is shown in figure 2.13. The concentration of CO_2 in flue gas increases with the increase of both conversion degree of limestone and mass fraction of CO_2 in limestone. At complete calcination and a mass fraction of carbon dioxide in limestone of 0.44, the concentration of CO_2 in flue gas is the highest.
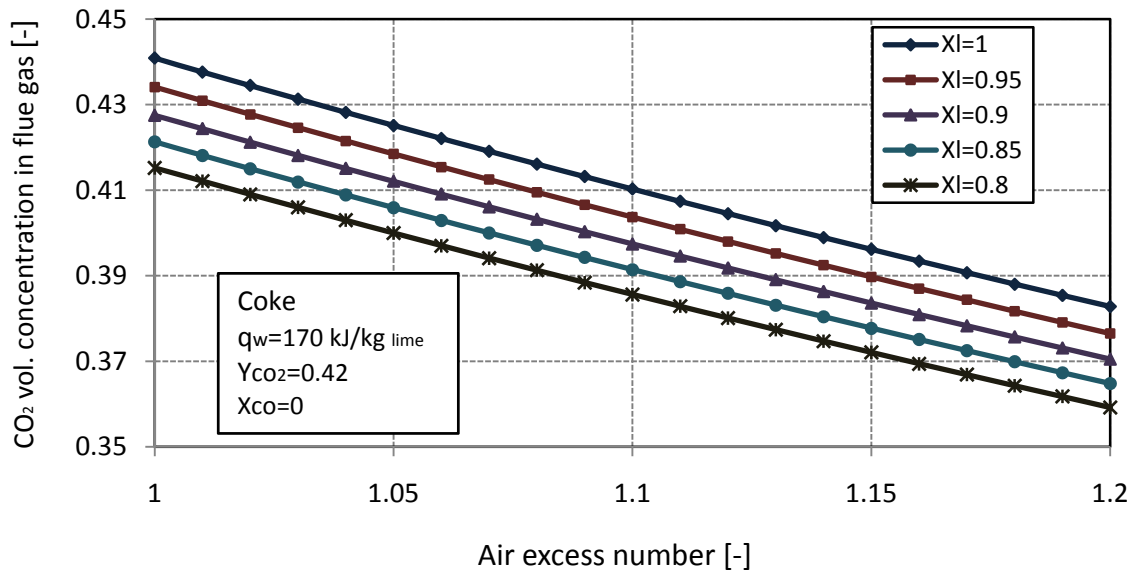
Figure 2.11: Volumetric concentration of CO_2 in flue gas with air excess number at different conversion degrees of limestone.
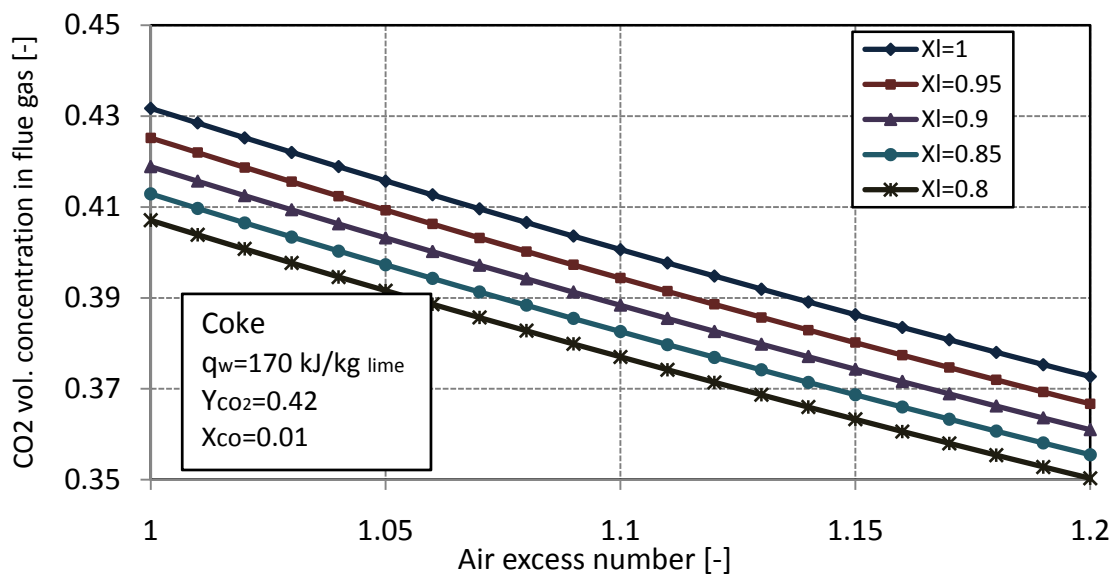
Figure 2.12: Volumetric concentration of CO_2 in flue gas with air excess number.
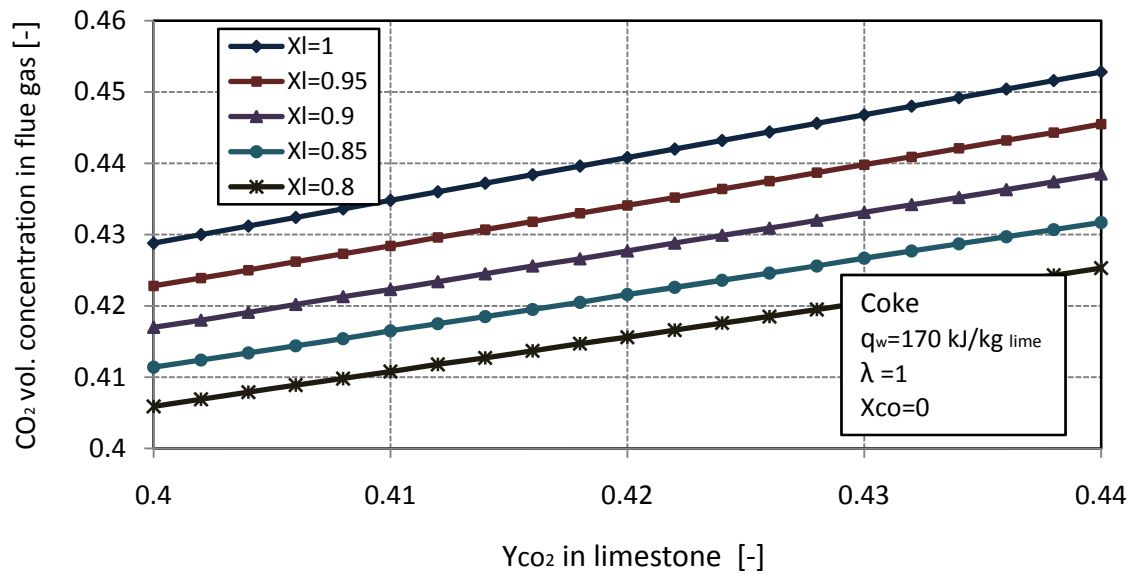
Figure 2.13: Volumetric concentration of CO_2 in flue gas with CO_2 mass fraction in limestone at different conversion degrees of limestone.

2.5 Concluding remark

The energy balance of the whole mixed feed lime kiln is analyzed. The energy consumption of the kiln is determined by the balance of the input and output heats, which are dependent on the input and output data to/from the kiln. The fuel ratio to the kiln and the concentration of carbon dioxide in flue gas of the kiln are also calculated. The results showed that the best value of fuel ratio to the kiln is about 7 % for high quality of lime and low concentration of CO in flue gas. The maximum concentration of carbon dioxide in flue gas is at complete calcination of limestone with theoretical excess air.

Chapter 3

Experimental Work

3.1 Introduction

In order to investigate the internal conditions of a full scale operating kiln, the experimental measurements were carried out on the operating mixed feed lime kiln. The experimental measurements inside the mixed feed lime kilns are very expensive and very complicated because the kilns are not designed for measurement purposes but for production and the retention time of lime in the kiln is in range of 24 to 48 hours. Therefore, interest has increased in the study of lime kiln problems by modeling due to the advancements in computer technology because we could not find detailed experimental data of kiln operation in available literatures. These are the first experimental measurements carried out on mixed feed lime kiln although, this kind of kiln is the oldest shaft kiln design. In the following sections, experiments are described that aim at measuring the internal state of the kiln (temperature profile and gas composition). Also, the measurements of the inputs and outputs of the kiln are described.

3.1.1 Description of the kiln

The experimental measurements are carried out on operating mixed feed lime kiln which were located at a soda ash plant. The kiln is one of several kilns which is used to produce the lime and carbonation gas required for the ammonia soda process at this plant, see figure 3.1. The kiln is a tall round shaft with a hight to diameter ratio of about 5. It can use coke or anthracite or a mix from both as a fuel. The air excess number is in a range of 1 to 1.2 depending on operation conditions. To withstand the operating temperature, the inside of the kiln is lined with two layers of refractory bricks.

Figure 3.1: Mixed feed lime kilns.

3.2 Experimental measurements

3.2.1 Measurement of the temperature profile

Measurement of the vertical temperature profile along the height of a mixed feed lime kiln with capacity of 150 ton/day was done using thermometers. The thermometers were inserted vertically in the stone layer at the top of kiln where they moved together with the solid charge towards the bottom of the kiln as shown in figure 3.2. The temperature profiles of the kiln were measured with 30 m long NiCr-Ni thermocouples with a diameter of 6 mm and Inconel coating and permissible temperature rang of 1300 °C. The measurements of temperature profiles for two positions of the kiln (one from the south east side (1) and another from the north west side (2)) were done, see figure 3.2. During the experiment, the thermometers traveled with the charge and the temperature was registered electronically every 30 s and the positions of the thermometers were also registered every 15 min.

3.2.2 Measurement of the gas concentrations

Gas concentrations of O_2, CO and CO_2 of mixed feed lime kiln were measured using gas analyzer. The probe gas analyzer was introduced vertically from the top of the kiln, see figure 3.2. During the experiment, the contents of O_2, CO and CO_2 in flue gas and temperature of flue gas were registered.
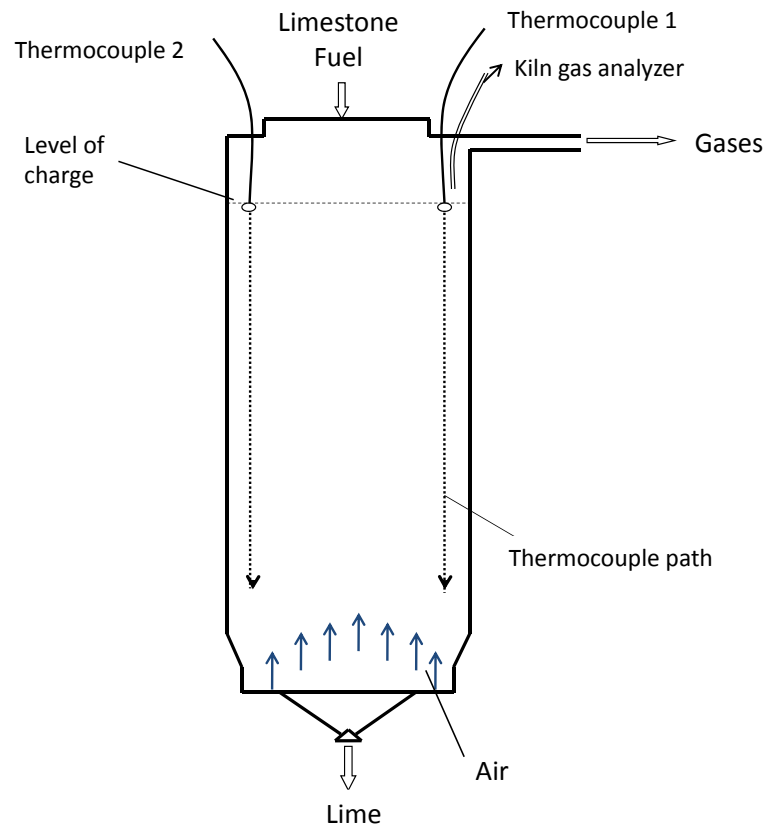
Figure 3.2: Measurement of temperature profile and kiln gas composition.

3.2.3 Measurement of the wall temperature

The wall temperature is required for calculating heat losses from the kiln through the walls. The measurement of wall temperature was done during the experiments of the kiln. It was measured by the use of Laser Sight Thermometer (non-contact thermometer). It was measured from two sides of kiln (north west side (2) and south east side (1)) where the direction of wind effected it.

3.2.4 Measurement of input/output data

During the experiment, the input and output data of the kiln were recorded. The input parameters include the amount, temperature and properties of solid fuel and limestone fed to the kiln and the amount of injected air for the combustion of fuel and cooling the lime. The amount of false air that dilutes the flue gas was also measured. The output data was the amount and temperature of lime and it's properties and the amount and temperature of flue gas and it's compositions. The main purpose of the measurement of input/output data was been to analyze the impact a change in input

has on the output and indication of problems in kiln operation. Also, input/output measurements give valuable information for mathematical models.

3.3 Results of measurements

3.3.1 Temperature profile

The measured temperature profiles as a function of time are shown in figure 3.3. As can be seen from the figure, the two sides of the kiln have different temperature profiles where the south east side (T_1) has the maximum temperature at the top of kiln of about 800 °C and started to reduce with time while the another side, northwest side (T_2), started with a low temperature of about 400 °C and increased slowly to about 860 °C and stopped for about 5 hours. After that, the temperature increased strongly to the maximum temperature of about 1100 °C and started to decreased. It is surprising that the temperature on one side is not similar to another side of the same kiln. Some factors can be suggested to explain these observations: (1) random distribution of fuel and limestone were charged to the kiln (2) the size of limestone particles were small and increased the resistance to the flow gas (3) the low quality of limestone containing more impurities which created clinker(hard and cement type materials). In addition, the measured temperature is a mix of the temperatures of limestone, fuel and gas, which makes the interpretation of the measured temperature difficult.

During the experiment, the photos for two sides of the kiln (south-east side (1) and north-west side (2)) were taken by infrared camera to show if the thermocouple which was put in the south-east side (1) was defective. The photos showed the same results as the thermometers for the two sides of the kiln, see figure 3.4. So the problem is not in the thermocouple but is actually in the kiln operation where, the limestone that is fed to the kiln is of low quality. As can be seen from figure 3.3, the time required for one experiment is over 30 hr and the thermocouple is inserted at the top of the kiln and moved with solid charge to the bottom so, it is so difficult to pull the thermocouple back out and when it comes out it is usually damaged. Therefore, it is costly and difficult to do another experiment.

The mixed feed lime kiln cross section is constant so, the speed of the limestone layer in the vertical direction is almost constant. The inserted thermometers moved with the moving limestone layer so, it can be assumed that the speed of the moving layer of limestone and thermometer traveling through the kiln is the same speed. Figure 3.5 shows the thermometer's position from the top level of the charge in the kiln to the bottom during the experiments. As can be seen from the figure, the thermocouple's measurements of both sides is quite uniform, although the temperature profiles of the two sides are different. It can be concluded from the obtained results, that the length of the preheating zone is about 6 m, where the speed of thermometers have some
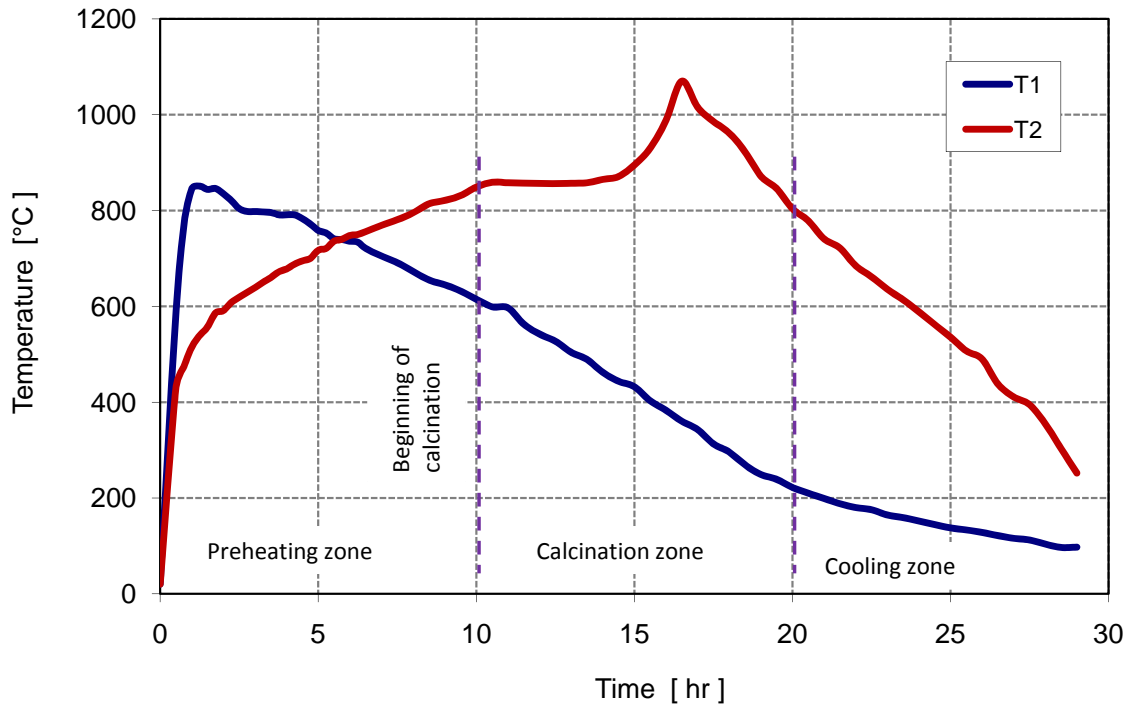
Figure 3.3: Measured temperature profile.

fluctuations and small difference between them due to traveling of the thermometers with hard particles.

The values of the measured temperature against the time were recalculated for the thermometer position. The calculation with respect to position of thermometer was performed using the results obtained from the measured thermometer position which is shown in figure 3.5. The temperature profiles a long the kiln from the top of the charge level to the bottom of the kiln are shown in figure 3.6. The discussion of the results will be on the temperature profile of the north-west side (T_2) where it is close to the actual performance of the kiln. Also, it is assumed for the measured temperature values, that these are the temperatures of limestone in the kiln. From the temperature profile, the thermometer could have measured all the zones of the kiln; preheating, calcination and cooling. Temperature increases to 860 °C at the depth of about 6.5 m where the preheating zone is located. In the region between 6.5 m and 9 m the temperature gradient is typically constant where the heat transported to the limestone was consumed only by reacting. The temperature in the core of limestone is nearly uniform, after it increases rapid to a maximum value of 1100 °C and then dropped to 800 °C at depth of about 3 m where the calcination zone ends. This is followed by continuous dropping of temperatures where the thermometer measured in the cooling zone. In this case, each zone occupies about one third of the kiln's
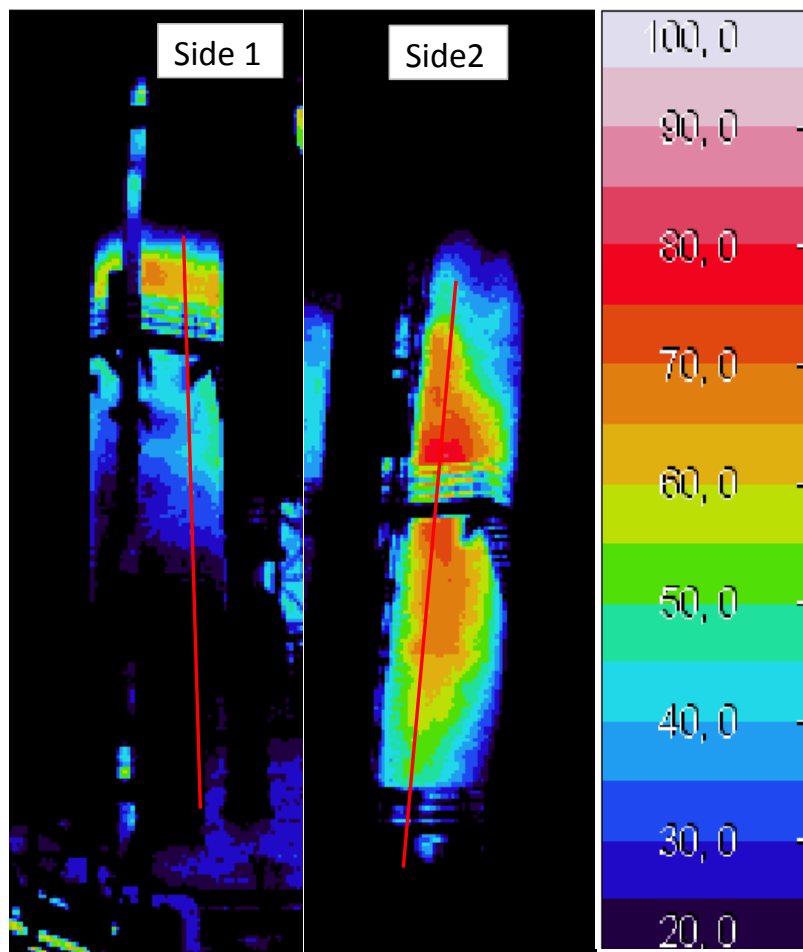
Figure 3.4: Infrared image of the kiln temperature.

height.

3.3.2 Initial calcination temperature

The initial calcination temperature is the the temperature where the process of limestone decomposition begins. It depends on the properties of limestone and the type of fuel. It follows from literature that the initial calcination temperature is between 830 to 860 °C for different kinds of fuel [39]. The initial calcination point is determined on the basis of the measured temperature profile from figure 3.6. As can be seen from figure 3.6, the temperature at the length of about 6.5 m stays constant. Assuming that the heat is used only for calcination, the chemical reaction will continue for as long as the temperature is sufficiently high. Based on the temperature profile, it can be estimated that the calcination begins at 860 °C , which also matches the data from literature.
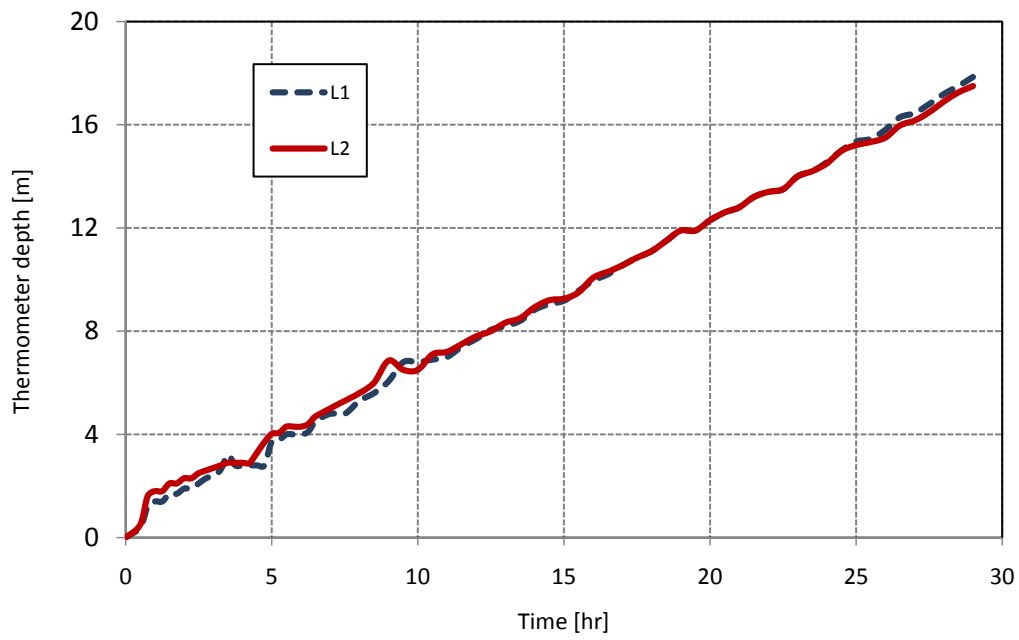
Figure 3.5: Thermometer depth.
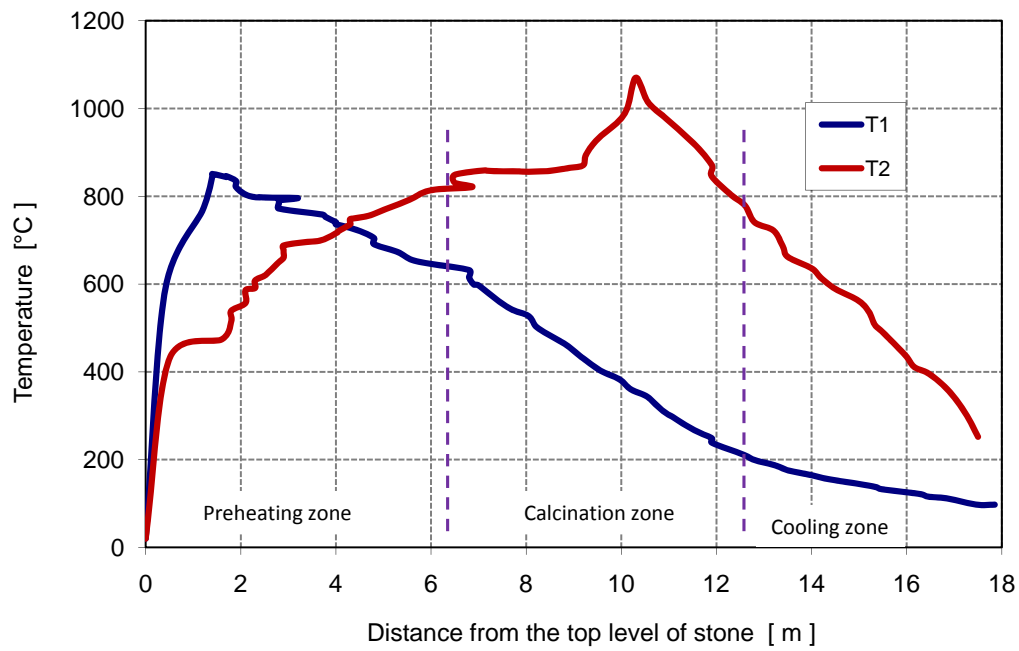
Figure 3.6: Measured temperature profile.

3.3.3 Gas concentrations

In a soda ash plant, the coke and anthracite are used as a fuel for the lime kiln to produce the high concentration of CO_2 in flue gas required for the process but these fuels also produced CO. Figure 3.7 shows the results of O_2, CO and CO_2 concentration of flue gas measured at the top of the kiln against time. The concentration of CO_2 is at about 30 to 40 %, but mostly at about 35 %, This value is lower than the amount required in soda process. These two factors can be explained with the following reasons: (1) the content of $CaCO_3$ in limestone is about 87.40 %, see section input/output data, (2) the conversion degree of limestone is about 80 %. The concentration of O_2 in flue gas is about 2 % because the air excess number is over the theoretical amount by 10 to 20 %. The concentration of CO in flue gas is about 0.8 %. CO in flue gas is produced from gasification of fuel (Boudourd reaction) or from volatiles but the flue gas also contains a certain a mount of oxygen. This is due to the waste mixing with air and fuel. Figure 3.7 also shows the variation of flue gas temperature with time. The flue gas temperature at the top of the kiln (at outlet) is between 80 and 150 °C. The variation in flue gas temperature is due to the temperature measured at the top of the kiln, so the flow profile and heat loss effects the measurement and also the false air measurement. The flue gas temperature from mixed feed lime kilns is lower than the other lime kilns because the fuel combusts with the onset of surface calcination, so that there is little waste with flue gas.
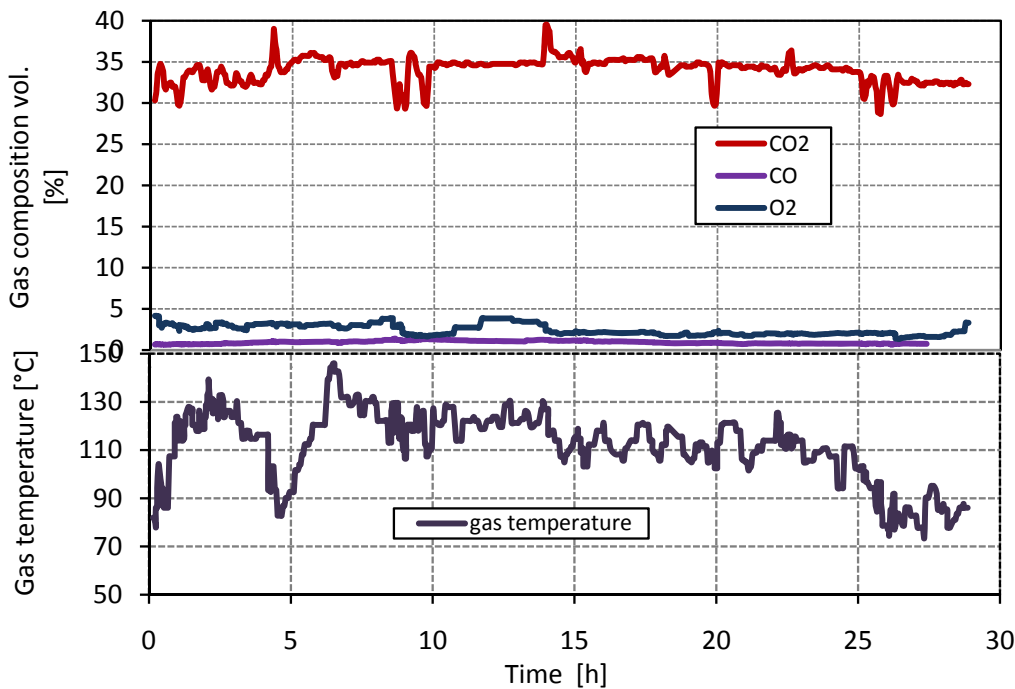
Figure 3.7: Composition of kiln gases.

3.3.4 Wall temperature

Figure 3.8 shows the results of wall temperature measurements at two sides of the kiln (south-east side (1) and north-west side (2)) plotted against vertical position. The wall temperature measurement is affected by the speed and direction of wind. It can be seen from the figure that the measured wall temperature has a similar trend to that of the temperature profile inside the kiln where the wall temperature of side (1) is high near the top of the kiln and reduced with the length of the kiln while the wall temperature of side (2) is low at the top of the kiln and increases until the middle of the kiln, and after that decreases. The wall temperature for both sides is decreased slowly after 14 m until the bottom of the kiln because the type of refractory materials are different than the above zones of the kiln.
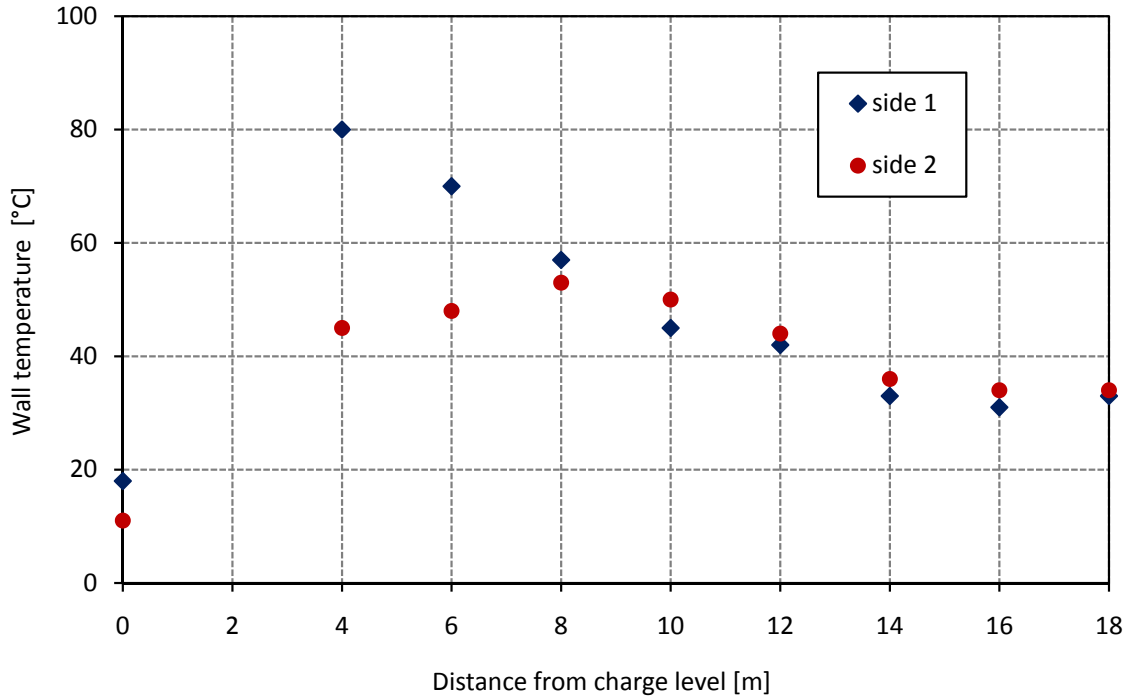
Figure 3.8: Measured wall temperature.

3.3.5 Input and output data

The results of input/output data of the kiln are summarized in table 3.1. The results provide valuable information for the development of a mathematical model of the kiln.

3.3.6   Heat balance of the kiln

From the input and output data of the kiln listed in table 3.1 and with the set of equations 2.1 to 2.12 in chapter 2, the heat balance of the kiln can be calculated. The results of heat balance of the kiln are summarized in table 3.2. From the results, it can be noted that the heat for calcination is about 78 %. In the case of a mixed feed lime kiln this useful heat is low. The heat lost by the walls of the kiln is about 10 %, because the refractory materials of the kiln are defective and need maintenance.

3.3.7   Efficiency of the kiln

Mixed feed lime kilns are seeking to produce high quality lime and carbonation gas from its stone while keeping the production costs to a minimum. The efficiency of a kiln is stated as the amount of calcination heat to the total heat of the fired fuel.The efficiency of the kiln is about 78 %. Although, the mixed feed lime kiln is known for high efficiency, the efficiency of the kiln is low because the limestone is of low quality, the amount of excess air used is (1.14 %) and the losses through the walls are about 10 %. The efficiency of the kiln could be increased by decreasing the amount of air and regenerating the refractory bricks.

3.4   Concluding remark

The experimental measurements in this work aimed to obtain information about the internal state of a full scale operating mixed feed lime kiln. The vertical temperature profile inside the kiln from the preheating zone to the cooling zone and the concentration of kiln gases have been measured. The location of beginning calcination has also been determined. Measurements of input and output streams from the kiln provided an energy balance that could be used for parameter estimation in the model of the kiln. The results of measurements show that the temperature profiles for two positions of the kiln are very different. One profile is near the normal performance and another is very far. Each zone occupies about one- third of the kiln height and is similar to the information presented in [40]. The initial calcination temperature is about 860 °C. The measurement results of gas concentration indicate a non-uniform distribution of gas and solid because the flue gas includes CO and O_2 together. The concentration of CO_2 in flue gas varied between 30 and 40 %. Finally, It is difficult to determine what the exact conditions were during the measurements so, the interpretation of measurement results should be viewed with caution. The input and output data will be used in the modeling of the kiln which is described in the sixth chapter and the measurements provide a good basis for validating the kiln model.

Table 3.1: Summary of input and output data of kiln No.6 for one operation

	limestone	coke	air	lime	gases
temperature	20 °C	20 °C	30 °C	34.80 °C	90°C
mass	$19.73t/(d.m^2)$	$1.11t/(d.m^2)$	$0.768 m^3_N/kg_{ivme}$	$12.9t/(d.m^2)$	$4.385\ m^3_N/h$
composition	$ma. - \%$	$ma. - \%$		$ma. - \%$	$vol. - \%$
	$CaCO_3 = 87.40$	$C = 83.08$		$CaCO_3 = 21.61$	$CO_2 = 36.80$
	$MgCO_3 = 1.72$	$H = 3.22$		$MgCO_3 = 0$	$CO = 0.88$
	$inerts = 9.82$	$N = 2.31$		$inerts = 14.69$	$SO_2 = 0.04$
	$H_2O = 1.07$	$O = 1.25$		$CaO = 62.47$	$N_2 = 59.99$
		$S = 0.64$		$MgO = 1.23$	$O_2 = 2.3$
		$ash = 5.43$			
		$H_2O = 4.07$			
		NCV= $30.950kJ/kg_f$			

Table 3.2: Heat balance of the kiln No.6

heat inputs	kJ/kg_{lime}	%
heat from fuel combustion	2648	97.8
sensible heat of limestone	28	1
sensible heat of (combustion and cooling) air	29.9	1
Total	2707	100
heat outputs	kJ/kg_{lime}	%
heat for calcination	2111	78
heat for vaporization	44	1.6
heat of flue gases	141	5
heat loss by CO	110.8	4
heat of dust	0.15	0
sensible heat in solid	5	0.19
general heat loss	293	10
Total	2707	100

Chapter 4

Modeling Coke Combustion

4.1   Introduction

Coke has importance in many industrial combustion processes, such as lime kilns for lime and carbonation gas production, blast furnaces for iron and steel production, and cupola furnaces for iron and rock wool production. The combustion behavior of coke particles in a kiln is usually an uncertain behavior which has strong influences on the process and creates difficulties of optimization design and regulation of the processes. Therefore, one of the main objectives in coke combustion research is the development of numerical models to solve the problems related to the combustion behavior of coke. Coke combustion is a highly complex process, involving the combination of different processes; chemical kinetics, heat and mass transfer which proceed at different rates and and mutually interdependent of one-another, see figure 4.1. So, understanding the combustion characteristics of a single coke particle in a kiln is the basis for improving the performance of the kiln for more efficient operating and less emissions. In order to describe the combustion of a single coke particle in a kiln, it is essential that the mechanism which governs the combustion is well understood. To establish the combustion mechanism, it is necessary to ascertain two important facts (1) what are the products of combustion on the particle surface. (2) which of the gases can diffuse to the surface, oxygen or carbon dioxide or both. Many workers have attempted to identify the nature of products formed at the particle surface. Two basic models will be considered, see figure 4.2. The double film model was proposed by Burke and Schuman in 1931. It assumed that the carbon reacts at the surface with carbon dioxide to form CO. The chemical reactions are represented in figure 4.2. The produced CO diffuses outwards into the air stream where it reacts with O_2 and is burned in a thin flame in the front of the boundary layer. The reaction between CO and O_2 is fast enough so that no oxygen will reach the surface of the coke particle. In the continuous film model, the O_2 from air diffuses to the surface of the particle and reacts with carbon to form CO_2 and CO. The CO_2 produced diffuses back to the surface of particle and reacts with carbon to form CO. CO is thus formed at

the surface and diffuses outwards and reacts with incoming oxygen to form CO_2 . Several researchers have argued that oxygen diffuses to the particle surface or carbon dioxide. Most of them decided that if the temperature is greater than about 1100 K, the diffusion coefficient of O_2 is slightly larger than that of CO_2 and O_2 diffuses the the particle surface. If the temperature of the particle is above 1373 K, the carbon dioxide is diffused to the surface of the particle and O_2 will not reach the surface. Depending on the size and temperature of the particle, the validity of the models is determined. Therefore, we have chosen to use the continuous film model in order to describe the combustion of the coke particle because of the change of temperature and size of the particle through the combustion.
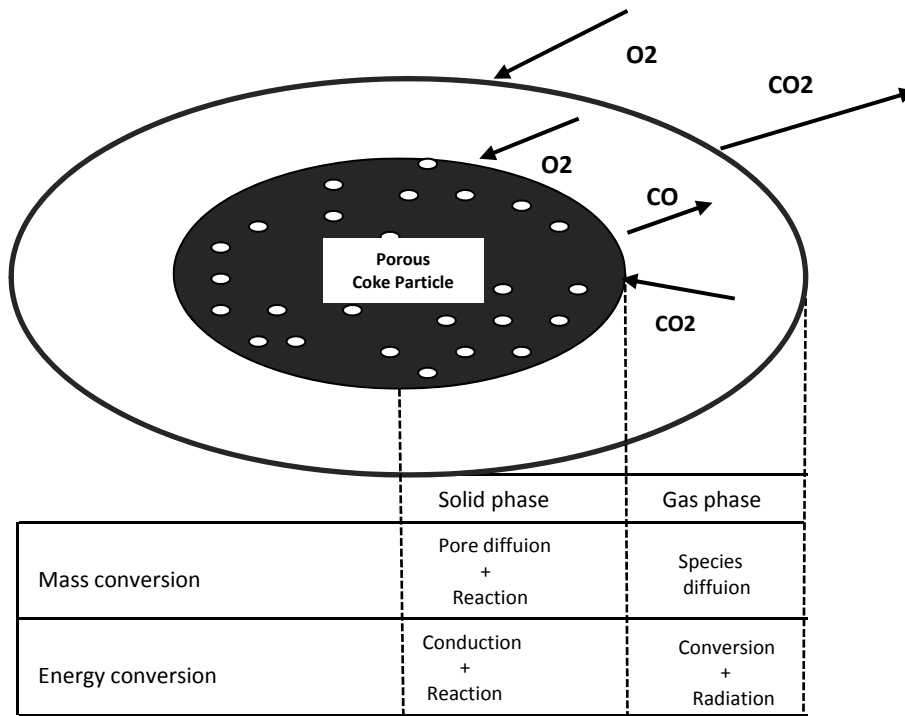
Figure 4.1: Basic scheme for description of combustion process of a single coke particle

A single coke particle can be considered a porous structure with pores of different size and shapes. The presence of pores allows for penetration of reactant species into the particle and, therefore, for much greater surface area for reactions. The internal surface area exceeds the external surface area of a particle by a factor greater than 10000 for a 1 mm particle [41]. These pores are responsible for internal diffusion resistance to the reactant when it diffuses inside the boundary of the particle. The diffusion of gas through the pores inside the char and the chemical reaction on the pore walls is referred to as intrinsic reactivity. For low intrinsic reactivity the oxygen

$$C + CO_2 \Rightarrow 2CO$$

$$CO + \frac{1}{2}O_2 \Rightarrow CO_2$$

Double Film Model

$$C + \frac{1}{2}O_2 \Rightarrow CO$$

$$C + O_2 \Rightarrow CO_2$$

$$CO + \frac{1}{2}O_2 \Rightarrow CO_2$$

$$C + CO_2 \Rightarrow 2CO$$

Continuous Film Model

Figure 4.2: Schematic concentration profiles in combustion models for burning of coke particle.

is able to travel into the interior of the char particle. the char diameter stays constant during combustion and the particle density continually decreases as particle mass is evenly removed throughout the particle on the pore surface. On the other hand if the reaction rate is very fast, all the oxygen is consumed as it reaches the particle surface. The density of the particle remain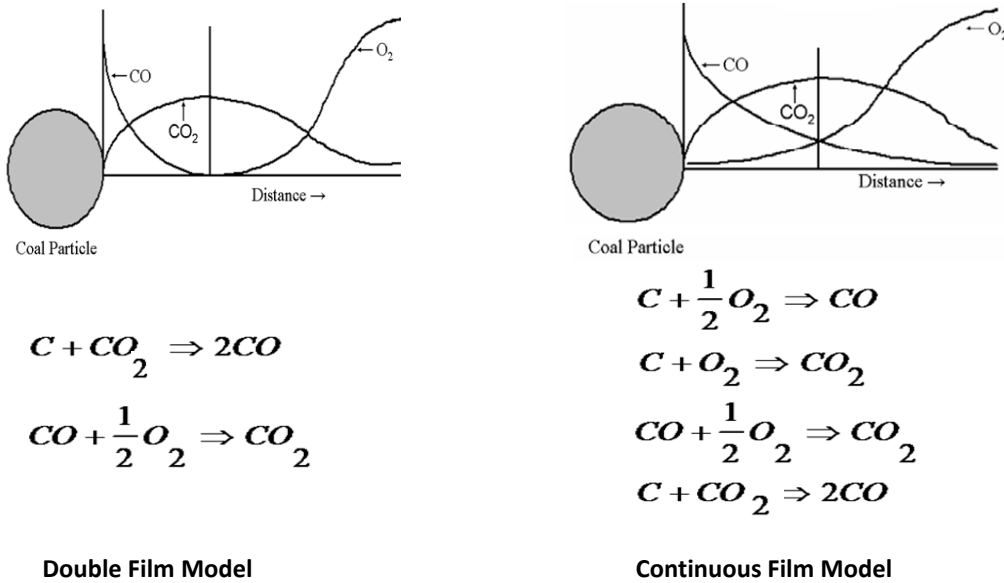s constant during the burnout and the particle size decreases as mass is removed solely from the particle surface. For large particles, particle diameter continuously shrinks because of many heterogeneous reactions; carbon with oxygen and carbon with carbon dioxide. During the combustion, the reactant first diffuses to macro-pores at the particle surface and then to micro-pores connected to these macro pores causing changes in the pore distribution and porosity inside the particle. These structural changes affect the reactivity of the process, see figure 4.3.

In general, coke particles contain a certain amount of ash. At the beginning of combustion, the carbon is depleted first at the surface, since the reaction rate is faster than diffusion, thus forming an ash layer. The thickness of the ash layer increases as combustion proceeds and the external diffusion resistance of ash shell increases. There are different models in the literature. Some models ignored the ash formation [42, 43, 44]. [45, 46, 47] developed models for a single char particle taking into account the formation of ash. [48] studied the influence of the ash layer on the burning char particle temperature. In our model, we do not take into account the formation of ash on the particle surface during combustion, where the coke particle loses its ash
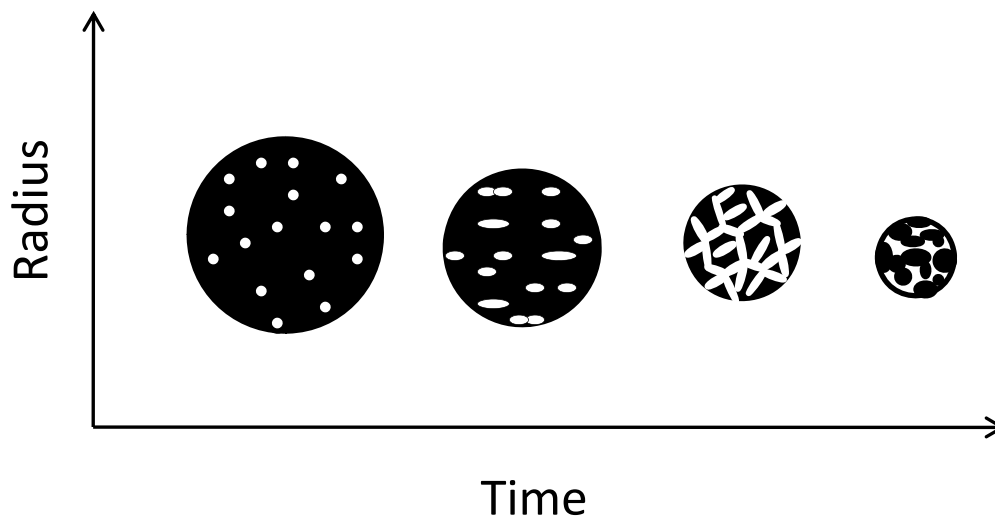
Figure 4.3: Schematic diagram of the particle shrinkage and porosity with time

layer because of attrition during combustion in the kiln.

4.2 Mathematical model

The mathematical model developed to describe the combustion of a single coke particle contains a number of assumptions. The model has been built on the basis of mass and heat balances. It solves for heat and mass transfer coupled with chemical reactions in a shrinking coke sphere. Since coke particle consists of a number of pores, the effective values of physical parameters are taken into account to consider the effect of internal diffusion.

The model is based on the following assumptions:

1. a coke particle is spherically symmetric.

2. ash falls off from the surface of the particle during combustion.

3. initially, the particle is assumed to be at room temperature.

4. the particle is a gray body radiator.

5. no fragmentation of the coke particle occurs during combustion.

4.2.1 Mass and heat balance

The governing equation for the conservation of species mass is as follows:

$$\frac{\partial C_i}{\partial t} - \frac{1}{r^2}\frac{\partial}{\partial r}(r^2 D_{eff,i}\frac{\partial C_i}{\partial r}) = \sum \nu_{j,i}\Re_j \tag{4.1}$$

Where the second term at the left is the diffusion term:
r is the radial distance inside the coke particle.
C_i is the concentration of i species (O_2, CO_2).
D_eff is the effective diffusion coefficient of species i. It can be written as the inverse of bulk diffusion, D_i, and Knudsen diffusion, $D_{K,i}$, of species i and given by

$$\frac{1}{D_{eff,i}} = \frac{1}{\dfrac{D_i\epsilon}{\tau}} + \frac{1}{D_{K,i}} \tag{4.2}$$

Where:
ϵ is the porosity of the coke particle.
τ is the tortuosity factor. It is used to account for the tortuous path through which gases diffuses, and for the unknown degrees of anisotropy and inhomogeneity of the pore structure. The tortuosity factor of 3 is taken for randomly oriented, uniform pores according to Satterfield et al. (quoted by [49]).
Knudsen diffusion, $D_{K,i}$ is defined as:

$$D_{K,i} = \frac{2r_\epsilon}{3}\sqrt{\frac{8RT_p}{\pi M_i}} \tag{4.3}$$

where r_ϵ is the pore raduis

The term at the right of equation 4.1 is the source term, which takes into account the changes due to the chemical reactions.
$\nu_{j,i}$ is the stoichiometric coefficient for the component i
$\Re_j$ is the rate of chemical reaction j and will be describe in the chemical reactions section.

The heat conservation equation can be written as:

$$c_{p,c}\frac{\partial T}{\partial t} - \frac{1}{r^2}\frac{\partial}{\partial r}(r^2 \lambda_{eff}\frac{\partial T}{\partial r}) = \sum \Delta H_j\Re_j \tag{4.4}$$

Where the second term at the left is heat transfer through the porous coke particle:
λ_{eff} is the effective heat conductivity, the value of λ_{eff} is calculated on the basis of both thermal conductivity of solid particle λ_c and gas λ_g. It can be calculated by the following equation.

$$\lambda_{eff} = \epsilon\lambda_g + (1 - \epsilon)\lambda_c \tag{4.5}$$

The thermal conductivity of coke λ_c can be determine as a function of temperature and porosity of coke according to [50].

$$\lambda_c = (0.973 + 6.34 * 10^{-3}(T_p - 273))(1 - \epsilon^{2/3}) \tag{4.6}$$

The term at the right of equation 4.4 is the source term, which involves temperature changes in the particle due to the heat of chemical reactions, ΔH_j.

4.2.2 Chemical reactions

The combustion process of a coke particle can be described by the following heterogeneous reactions:

$$C + \frac{1}{2}O_2 \rightarrow CO \qquad (1)$$

$$C + O_2 \rightarrow CO_2 \qquad (2)$$

$$C + CO_2 \rightarrow 2CO \qquad (3)$$
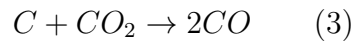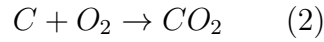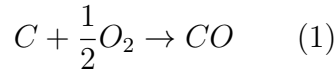
and one homogeneous reaction:

$$CO + \frac{1}{2}O_2 \rightarrow CO_2 \qquad (4)$$
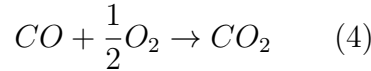
The particle of coke is preheated enough so that the content of moisture inside the particle becomes negligible. The burning of CO is catalyzed by the presence of water vapor, therefore, it is nearly impossible to oxidize CO in the absence of moisture. In this model, the homogeneous reaction is ignored.

The heterogeneous reaction rates are assumed to be first order reactions. Besides the oxygen concentration and carbon dioxide concentration, depend on the surface area available for reaction. The reaction rate $\Re_j$ is given by the following expression.

$$\Re_j = k_i a_c C_i \tag{4.7}$$

Where k_i is the reaction rate constants and is given by the Arrhenius type relation:

$$k_i = B_i exp(\frac{-E_i}{RT_p}) \tag{4.8}$$

The value of pre-exponential factor B_i and activation energy E_i for reactions which are used in the model are listed in table 4.1 according to Essenhigh et al.(quoted by [51]).

a_c is specific surface area of porous coke particle. During combustion, a_c is changing with the change of coke conversion degree X_c, as defined by the relation.

$$a_c = a_{ci}(1 - X_c)\sqrt{1 - \psi ln(1 - X_c)} \tag{4.9}$$

Table 4.1: Chemical kinetics constants (quoted by [51])

reaction	B (m/s)	E (kJ/kmol)
1	$1.813 * 10^3$	$1.089 * 10^5$
2	$1.225 * 10^3$	$0.998 * 10^5$
3	$7.351 * 10^3$	$1.38 * 10^5$

where a_{ci} is the initial value of the specific surface area of porous coke particle and ψ is the structure parameter.

The conversion degree X_c of particle is calculated by

$$X_c = 1 - \frac{m_c}{m_{c_i}} = 1 - (\frac{r}{r_i})^b \tag{4.10}$$

where the shape factor b=1, 2 or 3 for a plate, cylinder or sphere respectively.

4.2.3 Boundary and initial conditions

The model is solved using a number of initial and boundary condition. that are described as follows.

at t= 0.

$$m_p = m_{pi}$$

$$d_p = d_{pi}$$

$$T_p = T_{pi}$$

at particle center $(r = 0)$

$$\frac{\partial C_i}{\partial r} = 0 \qquad \text{(1a)}$$

$$\frac{\partial T}{\partial r} = 0 \qquad \text{(2a)}$$

at particle surface $(r = r_p)$

$$\frac{\partial C_i}{\partial r} = -\frac{\beta_i}{D_{eff,i}}(C_{s,i} - C_{a,i}) \qquad \text{(1b)}$$

$$\frac{\partial T}{\partial r} = -\frac{\alpha}{\lambda_{eff}}(T_s - T_a) - \frac{\sigma e}{\lambda_{eff}}(T_s^4 - T_a^4) \qquad \text{(2b)}$$

Where e is the emissivity and σ is the Stephan- Boltzmann constant $(5.67.10^-8 W/m^2 K^4)$. T_a is the ambient temperature, is set as the boundary temperature in this model. The first term on right of (2b) represents the heat transfer by convection between the particle and surrounding gas. The heat transfer coefficient, α is calculated by

$$\alpha = \frac{Nu\lambda_g}{d_p} \tag{4.11}$$

where Nu is Nusselt number, is estimated using the following equation.

$$Nu = 2 + 1.1Re^{1/2}Pr^{1/3} \tag{4.12}$$

4.3 Results and discussion

The equations 4.1 and 4.8 are complex coupled differential equations, where the process parameters, effective diffusivity, reaction rate coefficients and effective thermal conductivity are strongly influenced by the temperature of the particle. Therefore, PDF solver of matlab- 7 is used to solve the model where the model contains a number of algebraic equations with coupled differential equations under initial and boundary conditions. In the results presented in this section, the kinetic parameters shown in table 4.1 were employed, and the values of base parameters which were used in the model are listed in table 4.2. The model predictions, including the particle temperature, the mass fraction of the particle, the particle shrinkage, the conversion of the particle and the concentration of gas components inside the particle will be presented here.

Table 4.2: Parameters used in the simulations

T_{pi}	293 K
T_a	293 K
d_{pi}	0.03 m
m_{pi}	15 g
cp_p	850 kJ/kg K
ϵ_0	0.5
ψ	3
a_{ci}	$10^8 m^2/m^3$

Figure 4.4 shows the variation of temperature and mass fraction of the particle with burning time. As shown in figure 4.4, at the beginning, the coke particle is preheated by surrounding gases to reach the ignition temperature, the ignition of the particle starts in the range of 650 °C, but this is not visible on the temperature profile because the heat of combustion is so low. This temperature has been determined from the profile of mass fraction of the particle where it stays constant during heat up and starts to decrease with burning. The coke particle is preheated so the decrease of mass is due to combustion. The particle temperature increases continuously to reach the maximum temperature and then stays constant. Because the particle is large ($d_{pi} = 0.03m$), the reaction surface area is large and the oxygen diffusion rate to

the particle surface of the gases is large. Because of this, more coke is combusted but the heat transfer coefficient is small with a large particle so the temperature of the particle increases to a maximum value. During the combustion of the particle, the mass fraction of the particle decreases continuously with time until burnout. Figure 4.4 shows also the comparison of the model's predictions to the data available in the literature for the particle temperature in 21% O_2 composition in the gas stream [52]. The model simulation's results seem to have a good agreement with the experimental data.
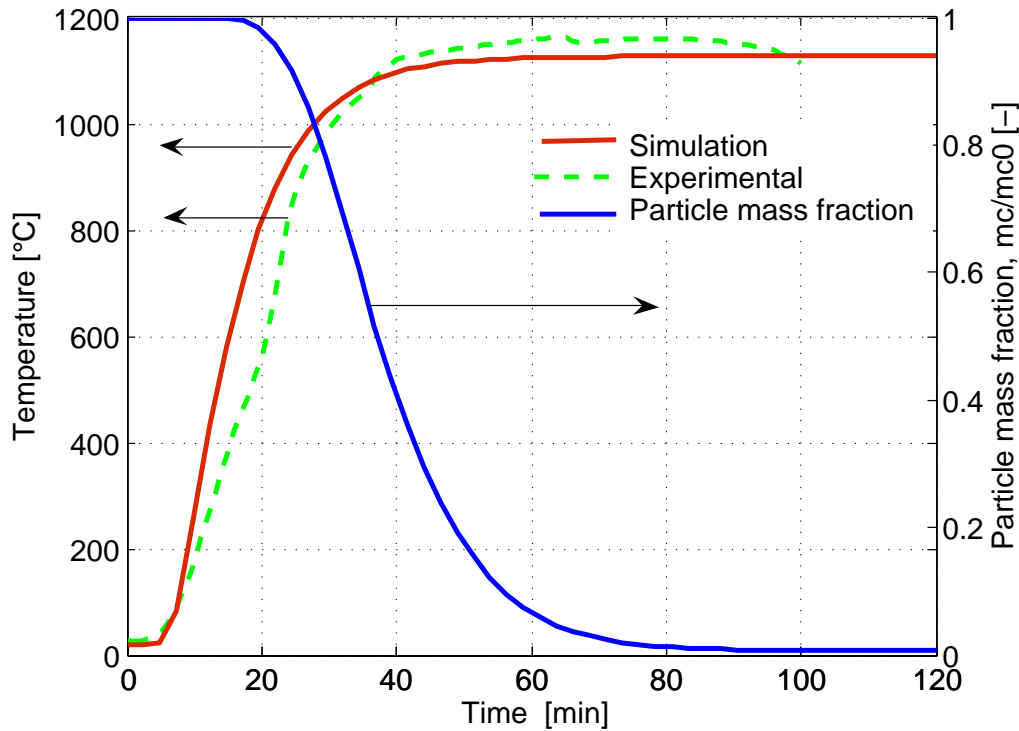
Figure 4.4: Profiles of particle temperature and particle mass fraction during combustion

Figure 4.5 shows the conversion degree of large particle during combustion and also the predicate profile of particle shrinkage with time. Here, the model has been used to describe the particle shrinkage where the experimental measurement of the particle shrinkage with time is one of the major problems associated with single particle combustion. It can be seen from the figure that the change of conversion and shrinkage of particle starts from the beginning of the particle combustion and achieves complete conversion and shrinkage at burnout. After the consumption of oxygen that penetrated the particle earlier, the particle burns at its periphery until it becomes small. At this size the particle burns and decreases both in size and density. Because of this, the decrease of the particle diameter becomes small. From figures 4.4, 4.5, one

can see that the model has been used to describe process simulations of combustion processes of large particles where the volume of O_2 available is 21 %.

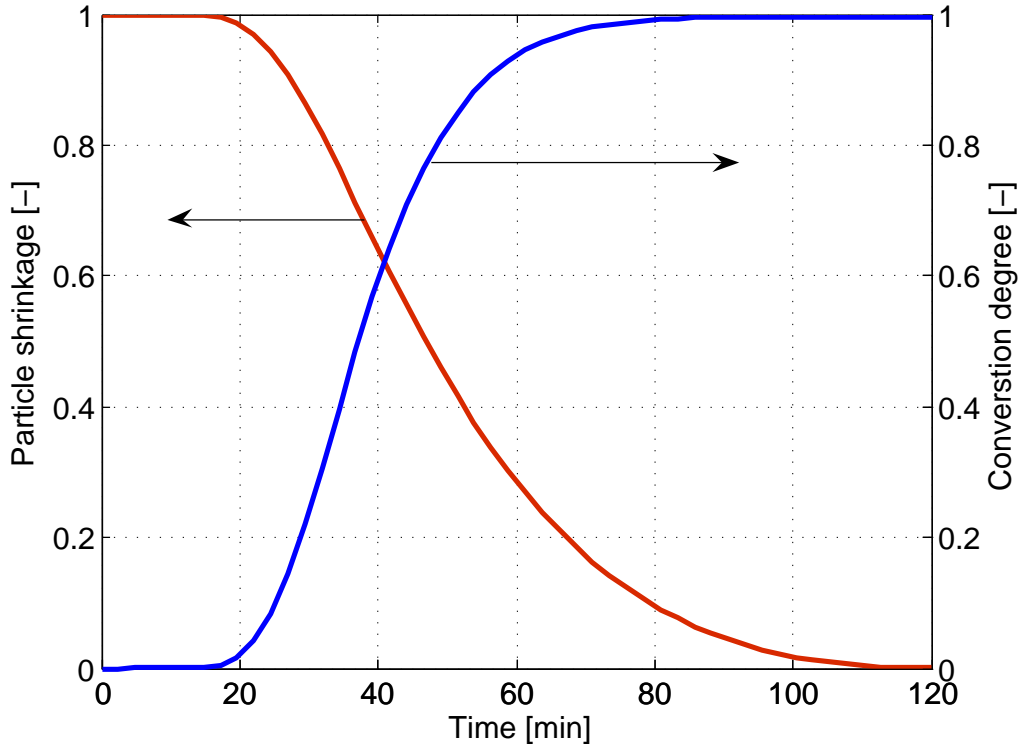The temperature of the particle over the lifetime of a coke particle is shown in Figure

Figure 4.5: Profiles of particle shrinkage and conversion degree during combustion

4.6. The plot indicates that the particle conversion degree is relatively constant under the burning condition $T_p < 650\ °\text{C}$. The particle temperature increases from the heat of a nonreactive particle in a hot gaseous environment to a value that exceeds the gas temperature. As the conversion increases, the particle diameter decreases and the particle temperature increases due to a decrease in radiative heat losses.

Figure 4.7 shows the calculated particle shrinkage profile as a function of conversion during combustion of the particle. Once the oxygen that penetrated the particle earlier is consumed, the burning is confined to the particle periphery. Therefore, the particle shrinkage decreases continually while increasing the conversion of the particle.

Despite the fact that the particle temperature remains approximately constant along the radial distance inside the particle, it has been found that the temperature at the center of the particle is less than the temperature at the surface, figure 4.8. Figure 4.8 shows the temperature profiles along the radial distance inside the particle. It shows
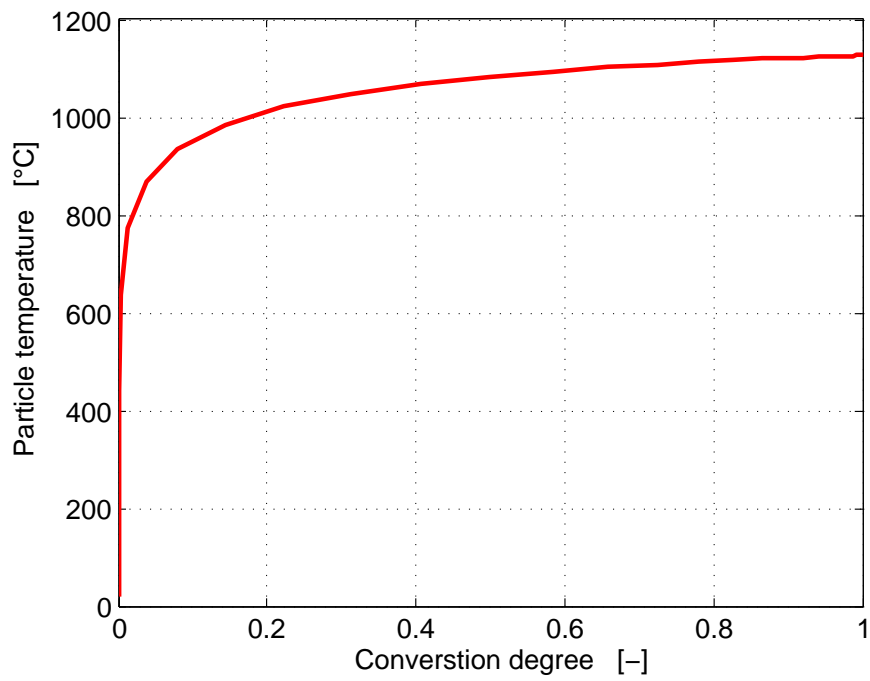
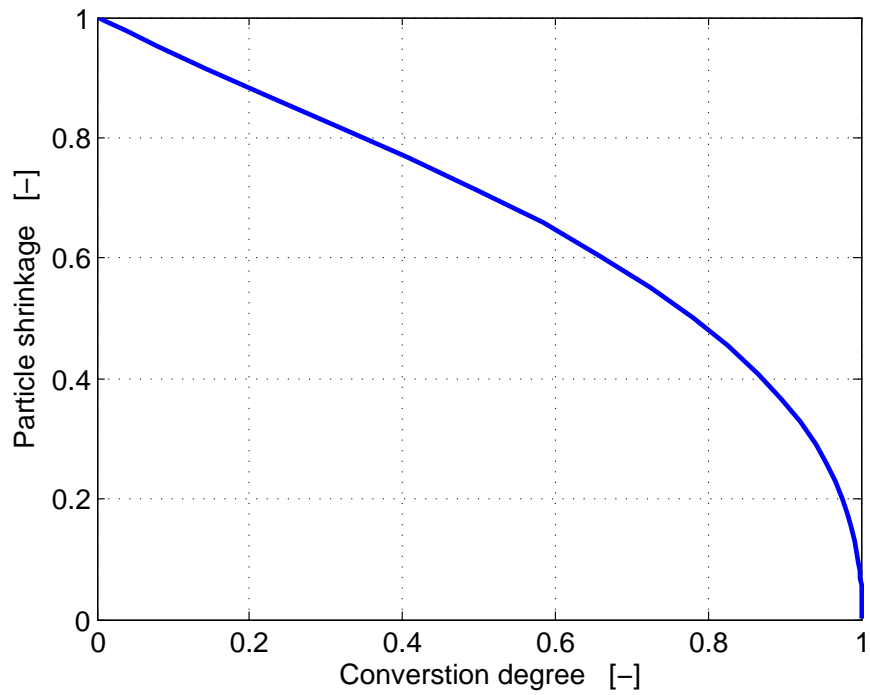Figure 4.6: Particle temperature as a function of conversion

Figure 4.7: Particle shrinkage as a function of conversion

that, at the beginning, the temperature difference between the center and surface of the particle is constant and start changing with time. When preheating, the temperature difference increases until the ignition, after that the temperature difference is reduced to become approximately constant. During combustion, the result agree with the fact of the constant temperature along the radial distance inside the particle
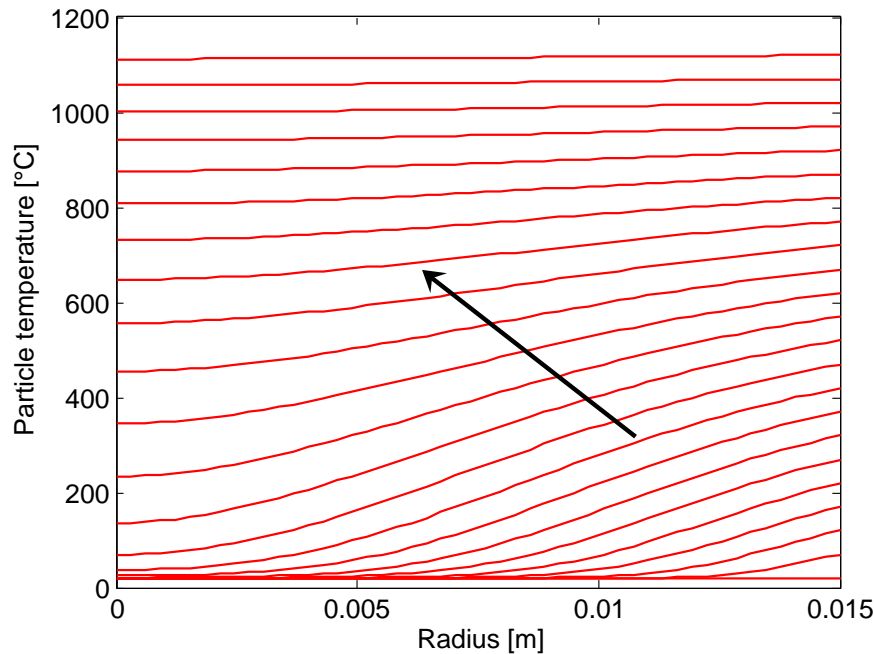
Figure 4.8: Temperature profiles along the radial distance inside the particle of a diameter of 0.03 m

4.4 Concluding remark

The objective of single coke particle modeling is the development of a mixed feed lime kiln model. Simulations of a single particle combustion have been conducted using unsteady state model that include a detailed description of transport phenomenon coupled with chemical reactions. Model takes into account the reaction takeing place inside the entire geometry of the particle. The effective values of diffusivity and thermal conductivity used to solve the mathematical model give a good approximation to the real process. The model predicts the particle temperature, the mass fraction of the particle, the particle shrinkage and the conversion of the particle. The results of simulations are compared with experimental data available in the literature. The information provided by single coke particle model will be used in the modeling of the kiln which is described in the sixth chapter.

Chapter 5

Modeling Limestone Calcination

5.1   Introduction

Limestone ($CaCO_3$) is an important natural raw material for many branches of industry. The greater part of limestone is decomposed to lime (CaO) and carbon dioxide (CO_2) in many different kinds of reactors before final utilization. Therefore, the understanding of limestone decomposition has been the subject of intensive study over the years. However, there are many aspects not well understood about the decomposition process. To achieve better optimization of calcination processes, it is important to know the decomposition behaviour of a single particle of limestone under the operating conditions. The endothermic decomposition behaviour is determined by three processes: heat transfer by convection from the surrounding gas phase to the solid surface and by conduction from the surface to the reaction front through the oxide shell, chemical reaction at the front, mass transfer of the gas CO_2 by diffusion from the reaction front to the surface through the pours oxide layer and the boundary layer of the gas phase [53, 5]. Most of the studies published in the literature focused on the decomposition kinetic, reaction mechanism, heat and mass transfer, diffusion of CO_2 and the parameters, effect on them. [54] presented a mathematical model that described the decomposition of the parent material at the reactant-product interface, the diffusion of CO_2 through the growing CaO layer and the sintering of the CaO layer. [55] developed a model to describe the decomposition reaction and mass transport. The solution of partial differential equations is achieved by orthogonal collocation based upon finite elements. [56] studied the calcination reaction of 10 different limestone samples by using the thermogravimetric analysis (TGA) technique and applied the shrinking core model to experimental results. [57] studied the calcination reaction of limestone with different porous structures and used the particle reaction model to predict their experimental results. [58] studied the decomposition of lumpy limestone based on the shrinking core model and showed that the reaction rate coefficients of limestone of different origin vary from 0.003 to 0.012 m/s with a factor of 4. [59] presented a kinetic model that described the calcination rate of small

particles. [60,61] studied the calcination of pulverized limestone particles, they found that the calcination rate is determined by chemical kinetics. [62] used the numerical model HYTEC (a reaction transport numerical code) to model the change in reactive surface areas during the experiment. [63,64,65,66] studied the properties of limestone from different origins and their effect on the decomposition behaviour.

5.2 Decomposition Model of limestone

The calcination of limestone ($CaCO_3$) is a highly endothermic reaction, requiring 3.16 MJ of heat input to produce 1 kg of lime (CaO). The reaction begins only when the temperature is above the dissociation temperature of limestone. Once the reaction starts the dissociation of limestone proceeds gradually from the surface of the particle towards the core, leaves behind it a layer of lime in which carbon dioxide (CO_2) is produced by the reaction and then diffuses out. The reaction for thermal decomposition of limestone can be expressed as:

$$CaCO_3(s) + Heat \rightarrow CaO(s) + CO_2(g) \tag{5.1}$$
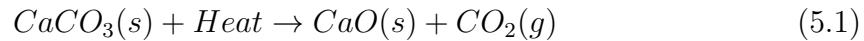
Where ΔH_R is the reaction enthalpy and is $178kJ/mole$ relative to $25C$, and $168kJ/mole$ relative to $900C$ [5].

The decomposition process can be explained using a partially decomposed piece of carbonate, as shown schematically in figure 5.1. The specimen is comprised of a dense limestone core surrounded by a layer of porous oxide. In the calcination reactor at temperature T_g heat is transferred by convection and radiation ($\alpha_e ff$) to the oxide layer surface at temperature T_s. As a consequence of conduction(λ_{CaO}) the heat penetrates the oxide layer to the reaction front, where the temperature is T_f. During the calcination process the reaction enthalpy is greater than the internal energy. Therefore, the further heat flow into the core is very slight and is negligible during the reaction. Once heat is supplied to the core, the chemical reaction(k), takes place, the driving force of which requires a deviation ($P_{eq} - P_f$)from equilibrium of the CO_2 partial pressure. The produced CO_2 from the reaction is released through the porous oxide layer by diffusion(D) to the surface and finally passes by convection(β) to the surrounding in which the CO_2 partial pressure P_g exists.

The four physical transport processes and the chemical kinetics involved are interconnected. Therefore, in order to model the single particle of limestone, it is necessary to know the material properties (chemical and physical) and heat and mass transfer.

5.2.1 Material properties

Limestone exists in large quantities throughout the world in many forms and various limestones differ considerably in their chemical composition and physical structure.
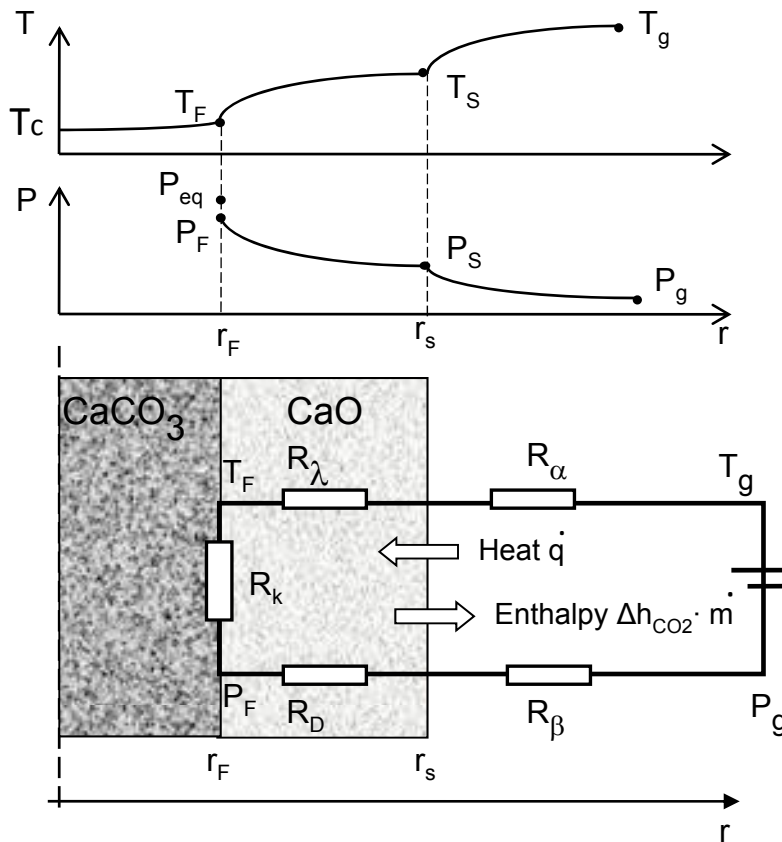
Figure 5.1: Mechanism of limestone decomposition.

Therefore, it is difficult to forecast a specific decomposition behaviour. For this reason, properties of limestone and lime and their influence on the decomposition process have been the object of many studies. In the following sections, the material properties which have a great influence on limestone decomposition, will be described:

5.2.1.1 Heat capacity

The specific heat capacities of limestone and lime depend on the temperature. The variation of specific heat capacity of limestone and lime with temperature has been studied but a few only publications are available. Murray [67] have reported the values of specific heat capacity varied from 802.2 to 1352.4 kJ/kg °C at temperatures from 0 to 800 °C, and from 764.4 to 1289.4 kJ/kg °C at temperatures from 0 to 1200°C for limestone and lime respectively. The specific heat capacities of limestone and lime by Barin and Knacke [68] are shown in figure 5.2. Silva et al. [65] studied the specific heat capacities of limestone and lime. They have reported the specific heat capacity of limestone is only slightly influenced by its origin, while the specific heat capacity of produced lime varies strongly according to its origin.
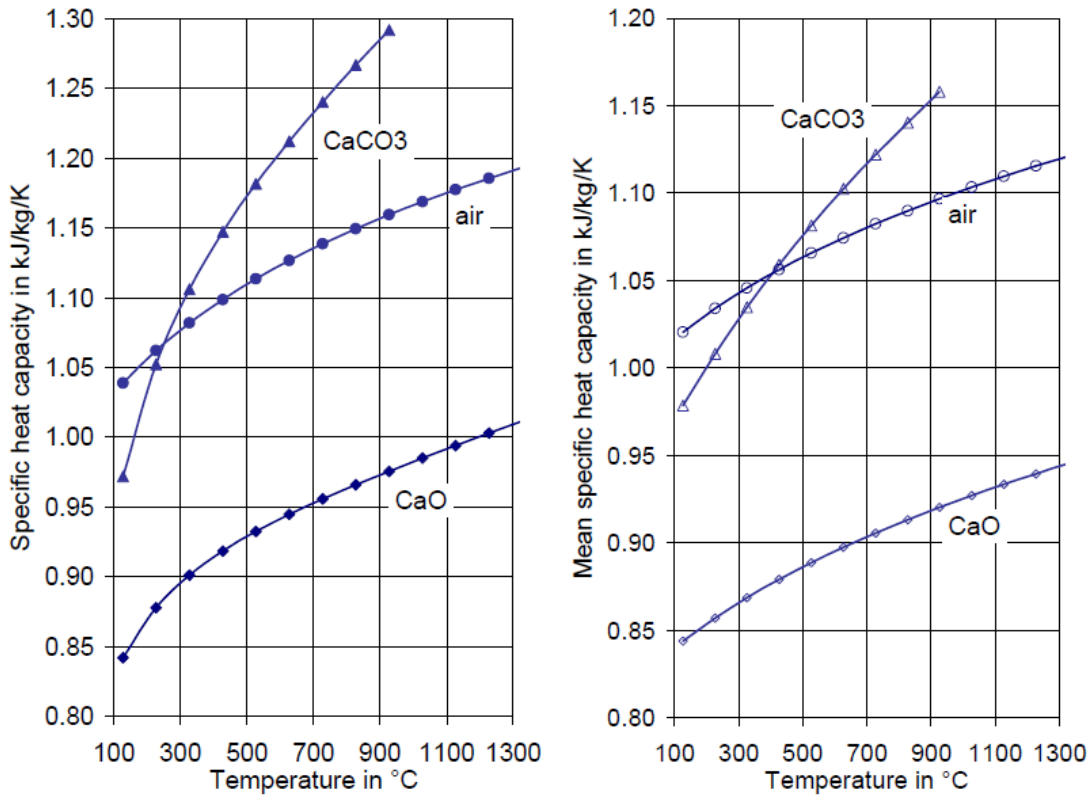
Figure 5.2: The mean values of the specific heat capacity of lime, limestone and air [68].

Some literature gives the values of specific heat capacity as a polynomial function of temperature and others as exponent functions. For the purpose of modeling, exponent functions are used.

The average specific heat capacities of limestone and lime are formulated as exponent functions with a reference temperature of 20 °C.

$$cp_{CaCO_3} = 180T_f^{0.26}$$

where T_f is unreacted limestone core temperature

$$cp_{CaO} = 303T_{av}^{0.16}$$

where T_{av} is the average temperature of porous oxide layer

5.2.1.2 Thermal conductivity

Thermal conductivity depends on the particles porosity and structure. It decreases with increasing temperatures. The values of thermal conductivity have been reported

in a range of 2.5788 to 1.743 W/m K and 0.63 to 0.84 W/m K for limestone and lime respectively by [69]. [63,58] have reported the values of thermal conductivity of lime in a range between 0.55 to 0.85 W/m K. In figure 5.3, some values of thermal conductivity of the lime (CaO) layer from the literature are derived, using special direct measurement methods.

Figure 5.3: Thermal conductivity of calcium oxide.

5.2.1.3 Equilibrium pressure

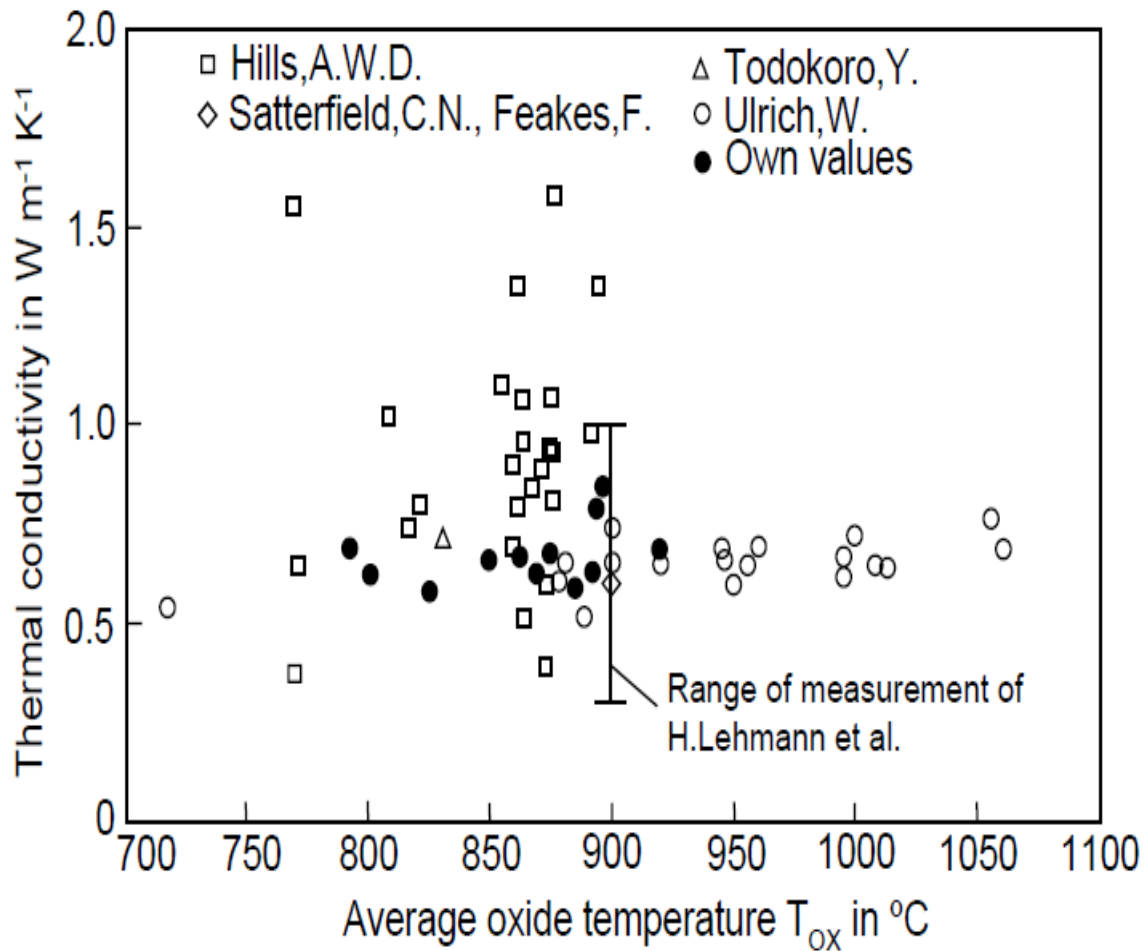Limestone decomposes to solid lime and carbon dioxide in gaseous form. The equilibrium state is thus determined only by the pressure of carbon dioxide. To expel the produced carbon dioxide from decomposition through the outer shell of lime, the pressure at the reaction zone must be greater than that at the surface of the particle.

The CO_2 equilibrium pressure (decomposition pressure) can be approximated by:

$$P_{eq} = P_0 exp(-\frac{\Delta H_R}{RT_f})$$ (5.2)

where ΔH_R is the decomposition enthalpy.
P_0 is the pre-exponential coefficient.
T_f is the decomposition temperature.
R is the universal gas constant.

The CO_2 equilibrium pressure has been measured and some values of P_0 and ΔH_R which were obtained from the literature, have been listed here. The reaction enthalpy ΔH_R of $CaCO_3$ is 167 kJ/mole relative to 900C and P_0 is $4*10^7$ bar according to [70], ΔH_R of $CaCO_3$ is 163.6 kJ/mole and P_0 is $1.886 * 10^7$ bar [71]. [63,64] measured the CO_2 equilibrium pressure for different types of limestone and reported ΔH_R of $CaCO_3$ is 168 kJ/mole and P_0 is $2.15 * 10^7$ bar. Some searchers calculated the CO_2 equilibrium pressure related to gas temperature where the decomposition temperature depends on the CO_2 partial pressure in gas and consequently on gas temperature. The values obtained from equilibrium pressure measurements by other various researchers have been shown in figure 5.4.
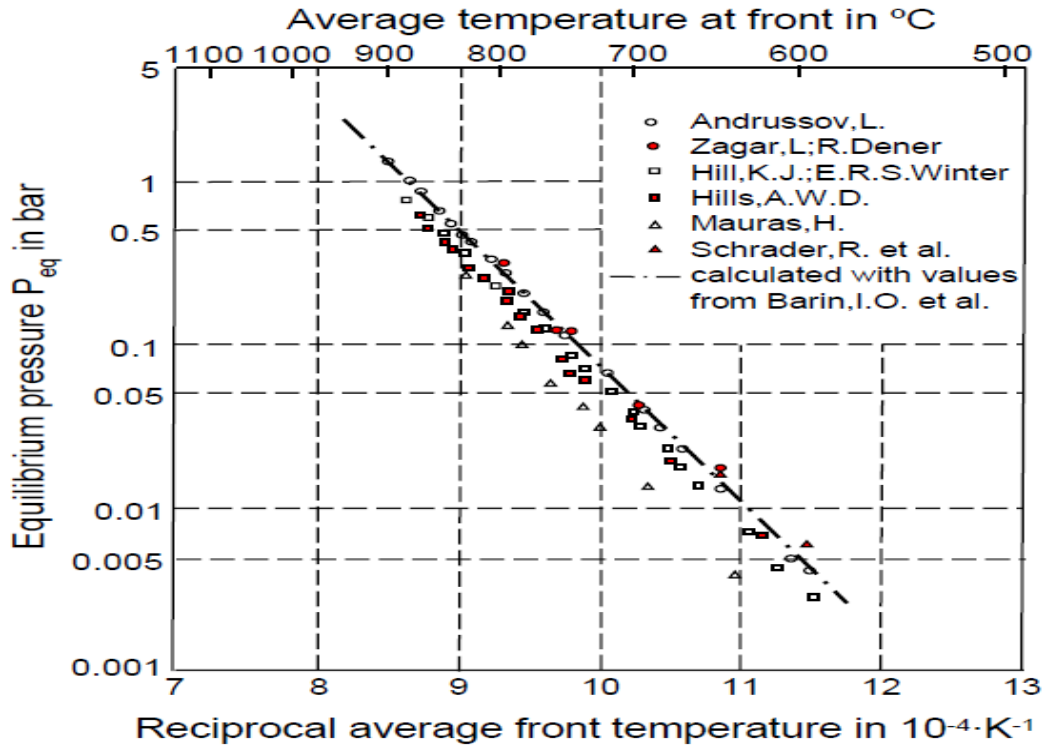
Figure 5.4: Equilibrium pressure of limestone decomposition.

5.2.1.4 Reaction coefficient

The reaction kinetics of limestone decomposition with different particle sizes of limestone, starting from micrometer to centimeter, have been studied by many researchers. The studies of reaction kinetics of different limestones show a large variation due to their differences in crystalline structure and nature of impurities. The values of the Arrhenius parameters, E =110 to 1600 kJ/mol and A = 10^4 to 10^{69} 1/S have been reported under varying experimental conditions [72]. The values obtained from reaction coefficient measurements by various researchers are summarized in figure 5.5.
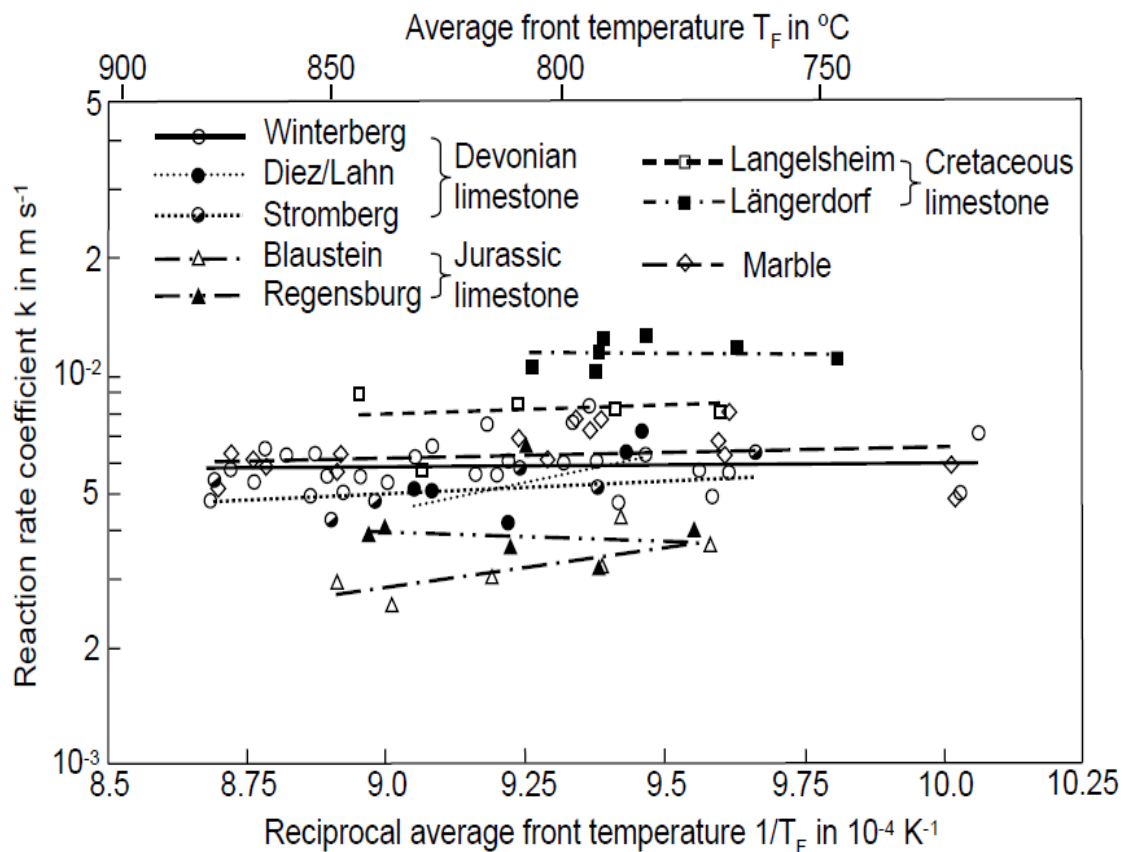
Figure 5.5: Reaction coefficient of limestone decomposition.

5.2.1.5 Diffusion coefficient

The CO_2 produced from decomposition of limestone is drained out by diffusion through the oxide layer which is produced behind the reaction of limestone. The diffusion of gas CO_2 in porous lime depends both on the nature of limestone and on

the temperature. [70] described the effective pore diffusion coefficient of lime by the following equation.

$$D_{eff,l} = 630 exp(-\frac{160000}{RT_{av}})$$ (5.3)

Where T_{av} is the average temperature of porous oxide layer.

The values obtained from the literature for the effective diffusion coefficient have been shown in figure 5.6.
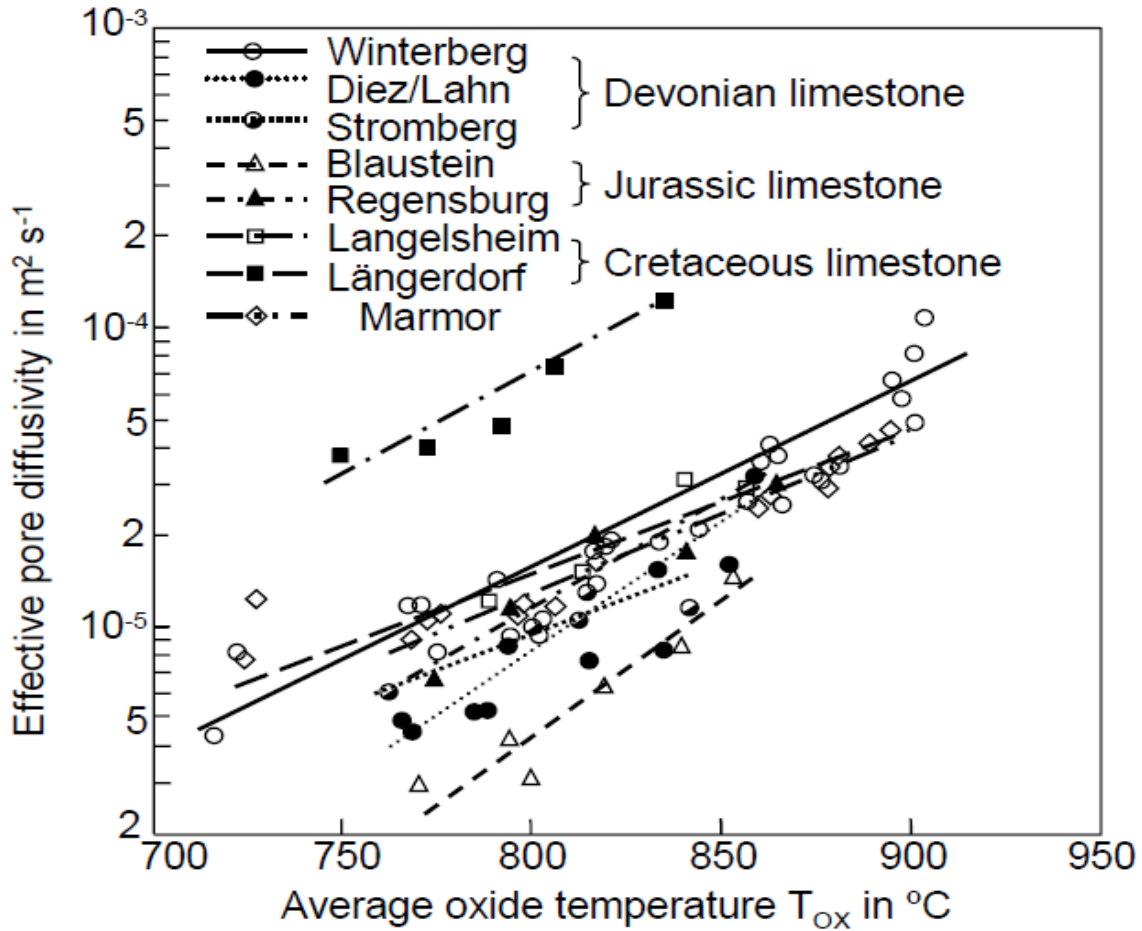
Figure 5.6: Effective pore diffusion coefficient of limestone decomposition [70].

5.2.2 Determination of heat transfer coefficient

The heat transfer coefficient α between fluid and a single solid sphere is calculated by the Nusselt function with laminar and turbulent according to Gnielinski (quoted by [64]).

The Nusselt function for asingle sphere particle in laminar flow is given as:

$$Nu_{lam} = 0.644 Re^{1/2} Pr^{1/3} \tag{5.4}$$

The Nusselt function for a single sphere particle in turbulent flow is given as:

$$Nu_{turb} = \frac{0.037 Re^{0.8} Pr}{1 + 2.443 Re^{-0.1}(Pr^{2/3} - 1)} \tag{5.5}$$

From the two values, the Nusselt function for a single sphere particle can be averaged as:

$$Nu_p = 2 + (Nu_{lam}^2 + Nu_{turb}^2)^{1/2} \tag{5.6}$$

where The Prandtl number of the particle is calculated as:
$Pr = \frac{\mu_g cp_g}{\lambda_g}$
μ_g stands for the dynamic viscosity of the surrounding gas.
λ_g stands for the thermal conductivity of the surrounding gas.
and cp_g stands for the heat capacity of the surrounding gas.
The Reynolds number of the particle is calculated as:
$Re = \frac{\rho_g U_g d_p}{\mu_g}$
ρ_g is the density of the surrounding gas.
U_g is the superficial velocity of the surrounding gas.

Therefore, the heat transfer coefficient, α, is obtained by:

$$\alpha = \frac{Nu_p \lambda_g}{d_p} \tag{5.7}$$

5.2.3 Determination of mass transfer coefficient

The mass transfer coefficient β of produced CO_2 from a single particle surface to the surrounding gas is calculated by the Sherwood function. The Sherwood function for a single sphere particle in a laminar flow is given as:

$$Sh_{lam} = 0.644 Re^{1/2} Sc^{1/3} \tag{5.8}$$

The Sherwood function for a single sphere particle in a turbulent flow is given as:

$$Sh_{turb} = \frac{0.037 Re^{0.8} Sc}{1 + 2.443 Re^{-0.1}(Sc^{2/3} - 1)} \tag{5.9}$$

The Sherwood function for a single sphere particle can be averaged at above two values:

$$Sh_p = 2 + (Sh_{lam}^2 + Sh_{turb}^2)^{1/2} \tag{5.10}$$

Where Schmidt number is defined as:
$Sc = \dfrac{\mu_g}{\rho_g D_{CO_2-g}}$

Where the binary diffusivity of CO_2 in gas, D_{CO_2-g} can be calculated as a function of gas temperature.
$D_{CO_2-g} = 0.135 * 10^{-4} (\dfrac{T_g}{T_0})^{1.71}$
Where T_0 is a reference temperature of 273K.
Then the mass transfer coefficient of CO_2, is calculated from:

$$\beta = \frac{Sh_p D_{CO_2-g}}{d_p} \tag{5.11}$$

5.2.4 The model

Due to low internal porosity of limestone, we have chosen to use the shrinking core model in order to describe the reactive particle [28, 58]. The model is illustrated in figure 5.7. The calcination reaction is assumed to initially take place at the outer surface of the particle where the heat is transferred from the surrounding gas to the surface of the limestone particle by convection and radiation. As the reaction proceeds, the exterior surface of the particle is covered by the porous lime layer, while the unreacted core remains in the interior region of the particle. The carbon dioxide produced from the reaction is drained out by diffusion.
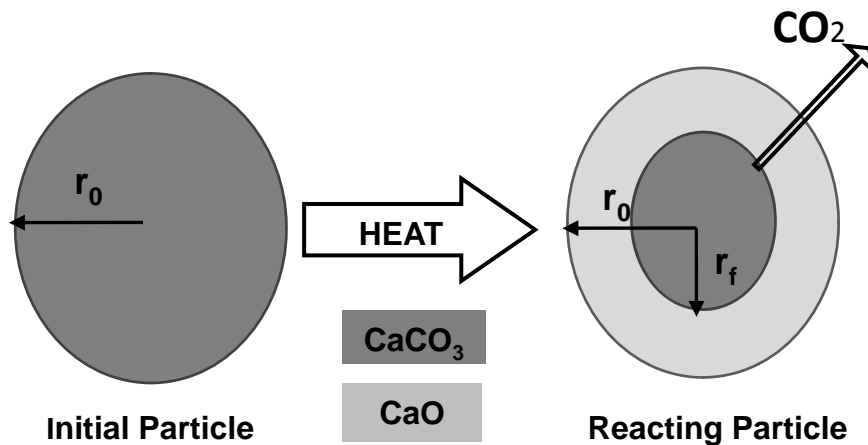

Figure 5.7: Shrinking core model of limestone decomposition

For a mathematical description of the calcination process, 1-D shrinking core model can be used based on the following assumptions:

1. the limestone particle is an ideal geometric shape such as a sphere, cylinder or plate.

2. heat supply is symmetrical.

3. the particle has a homogenous chemical composition and structure.

4. the reaction starts uniformly on the surface, always forming a geometrically smooth decomposition front which advances continuously into the interior of the particle.

Based on the shrinking core model, [73,63] have derived analytical equations to evaluate the calcination of limestone for spherical and cylindrical particles.
For a steady state, constant material properties and spherical geometry, the mathematical expressions describing the calcination process are computed as follows:
The progress of the shrinking core that ensues from the mass balance on the reacting core can be computed as:

$$\frac{dm_{ls}}{dt} = -A_{lsp}k_{ls}M_{ls}\frac{1}{R_{CO_2}T_f}(P_{eq} - P_f) \tag{5.12}$$

Where k_{ls} is the reaction rate coefficient of limestone
$k_{ls} = 0.012\exp(-\frac{-168000}{RT_f})$
and P_{eq} is the equilibrium pressure of CO_2 a computed at the reacting core according to [63,58]:
$P_{eq} = 4.10^7 exp(-\frac{-168000}{RT_f})$
Thus, equation 5.9 can be rewritten as:

$$\frac{dr_{ls}}{dt} = -\frac{M_{ls}}{\rho_{ls}}k_{ls}\frac{1}{R_{CO_2}T_f}(P_{eq} - P_f) \tag{5.13}$$

The computation of mass rate of CO_2 is computed as follows:
The mass rate of CO_2 produced by the decomposition reaction at the reacting core is calculated by:

$$\frac{dm_{co_2,r}}{dt} = -A_{ls}k_{ls}M_{co_2}\frac{1}{R_{CO_2}T_f}(P_{eq} - P_f) \tag{5.14}$$

By using the ideal gas law:

$$C_{CO_2,f} = \frac{P_{CO_2,equ}}{RT_f} \tag{5.15}$$

The mass rate of CO_2, transferred by diffusion inside the lime layer, which is produced by the calcination of limestone, is calculated according to:

$$\frac{dm_{co_2,l}}{dt} = \frac{4\pi r_r r_l M_{co_2} D_{eff,co_2}}{r_l - r_r}(C_{co_2,f} - C_{co_2,s}) \tag{5.16}$$

Where D_{eff,co_2} stands for the effective diffusion coefficient inside lime layer. It is described in the properties of materials.

The mass rate of CO_2, transferred by convection and diffusion inside the gases surrounding the particle, is calculated as:

$$\frac{dm_{co_2,g}}{dt} = A_l\beta(C_{co_2,s} - C_{co_2,g}) \tag{5.17}$$

Where β stands for the overall external mass transfer coefficient to the particle. The mass rate of CO_2 is derived by combining the reaction at front, diffusion of CO_2 inside the lime layer and mass transfer of CO_2 at the particle surface.

$$\frac{dm_{co_2}}{dt} = A_{ls} \frac{k_{ls}}{k_{ls}r_r^2(\frac{1}{D_{eff,co_2}}(\frac{1}{r_r} - \frac{1}{r_l}) + \frac{1}{\beta r_s^2}) + 1}(C_{co_2}^\star - C_{co_2,g}) \tag{5.18}$$

Where $C_{co_2}^\star$ is the equilibrium concentration and is related to the equilibrium pressure. The energy balance over the lime layer and limestone core can be written as:

$$m_l c_{p,l}\frac{dT_s}{dt} = \alpha_p A_p(T_g - T_s) + \sigma e(T_g^4 - T_s^4) - \frac{4\pi\lambda_l r_f r_l}{r_l - r_f}(T_f - T_s) \tag{5.19}$$

$$m_{ls} c_{p,ls}\frac{dT_f}{dt} = \frac{4\pi\lambda_l r_l r_r}{r_l - r_r}(T_s - T_r) + A_{ls}k_{ls}(C_{co_2}^\star - C_{co_2,r})(-\Delta H_R) \tag{5.20}$$

5.3 Concluding remark

A model for the calcination process of limestone in terms of heat transfer, chemical kinetics, mass transfer and limestone properties has been developed. The model was compiled from a number of existing models that described part of the process. It was developed for use in a model of a mixed feed lime kiln which is described in the sixth chapter, where the limestone is preheated and decomposition took place from 20 to about 1100°C.

Chapter 6

Mathematical Model of Mixed Feed Lime Kiln

6.1 Packed bed

The mixed feed lime kiln is basically a packed bed with the upward-flow of hot gases passing countercurrently to the downward flow of solid particles. Packed bed design is based upon mechanisms of heat and mass transfer and the flow and pressure drop of the gas through the bed of solids. These mechanisms are influenced by the void fraction of the bed. For the simulation of the processes occurring in such a kiln, the details of the mechanisms of the bed should be studied.

6.1.1 Void fraction

The void fraction of the particle bed is normally defined as the free volume fraction of the bed, it can be calculated from the voids' volume and the total volume of the bed as:

$$\varepsilon_b = \frac{V_{void}}{V_{total}} = 1 - \frac{V_{solid}}{V_{total}} \tag{6.1}$$

Where V_{void}, V_{solid}, V_{total}, are the void volume, solid volume and total volume of the bed respectively. Void fraction of a packed bed can be influenced by the method of charging (random or regular, loose or dense), particle shape (sphere, cylinder, lumpy, etc.) and particle size distribution. These factors have been the point of many experimental and theoretical investigations.

For random packing with spherical particles:

the mean void fraction can be calculated from the correlation $\varepsilon_b = 0.375 + 0.34\dfrac{d_p}{D_k}$ [74], the value of the void fraction typically falls in the rang of $\varepsilon_b = 0.36 - 0.42$ [75].

For random packing with cylindrical particles:

the minimum void fraction is $\varepsilon_b = 0.25$ [76] and the maximum value is $\varepsilon_b = 0.445$ [77],

For regular packing with spherical particles, the void fraction for three different regular models of packing are given in table 6.1.

Table 6.1: void fraction of geometrical models

	Geometrical model	Void fraction
1	Simple cubic	$1 - \dfrac{\pi}{6}$
2	Face-centered cubic	$1 - \dfrac{\pi}{3\sqrt{2}}$
3	Hexagonal close	$1 - \dfrac{\pi}{3\sqrt{2}}$

For a size distribution in a particle bed, figure 6.1 shows the influence of particle size distribution for bi-dispersed, random packing of spheres.
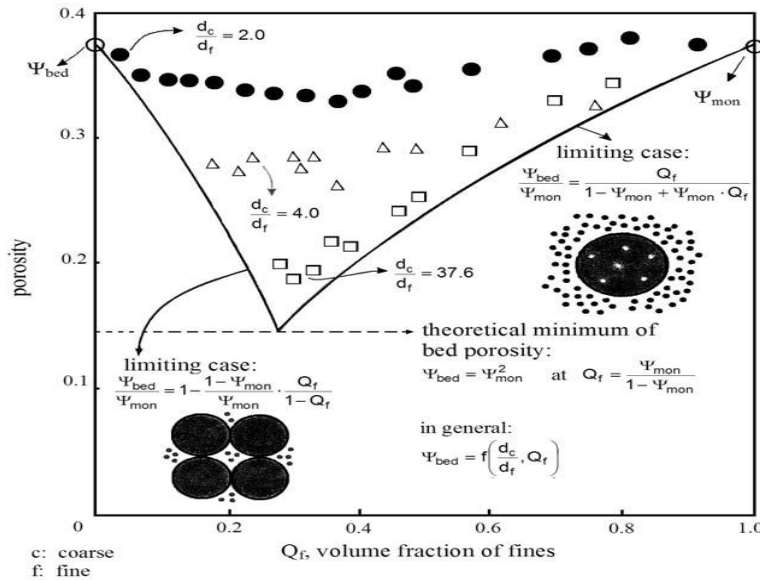

Figure 6.1: Bed porosity of bi-dispersed packing of spheres [78].

Void fraction is one important parameter in the simulation of mixed feed lime kiln. The solid charge to the kiln has two different sizes of solid particles, the limestone

size and coke size, the size of limestone is bigger than the size of coke. So, the void fraction in our simulation is assumed to be dense packing.

6.1.2 Pressure drop

Pressure drop in a packed bed is important for designing the kiln and also to achieve the maximum efficiency in the kiln. Therefore, a number of experimental and theoretical studies have been conducted on the pressure drop in a packed bed. The most widely used correlation is the Ergun equation [79]. The Ergun equation is a combination of both the Kozeny-Carmen and Burke-Plumber equations, which both look at energy losses due to flow through a packed bed. The Kozeny-Carmen equation models laminar flow through a packed bed, taking into account the energy losses due to viscosity. The Burke-Plummer equation examines turbulent flow through a packed bed and accounts for kinetic energy losses. The Ergun equation for pressure drop through the packed bed is as follows:

$$\frac{\Delta P}{\Delta L} = 150 \frac{(1 - \varepsilon_b)^2}{\varepsilon_b^3} \frac{\mu_f U}{(\varphi \overline{d}_p)^2} + 1.75 \frac{1 - \varepsilon_b}{\varepsilon_b^3} \frac{\rho_f U^2}{\varphi \overline{d}_p}. \tag{6.2}$$

From the well known Ergun's Equation, the pressure drop along the length of the packed bed depends on the void fraction, the properties of fluid (viscosity and density), velocity of fluid and particle geometry. The influence of these parameters on the pressure drop in a packed bed will be described here:

The pressure drop is extremely sensitive to changes in the void faction ε_b which has been described above.
The pressure drop through packed beds is the result of frictional losses and inertia characterized by the linear dependence of the superficial fluid velocity and quadratic dependence of the superficial fluid velocity. The superficial fluid velocity (the flow rate as if there was no packing in the bed) can be calculated with the known gas volumetric flow at STP $\dot{V}_0$ and the kiln cross section area A_k. Since the gas's volumetric flow changes with the temperature, the superficial gas velocity is temperature dependent:

$$U = \frac{\dot{V}_0}{A_k}(\frac{T}{T_0}). \tag{6.3}$$

The pressure drop increases with an increasing superficial fluid velocity [80, 26].
Ergun's Equation is based on experimental data for many shapes of particles, but it is more accurate for spherical particles. However, when the particles are irregular and never have a perfect spherical form, sphericity of particles φ and an equivalent particle diameter $\overline{d}_p$ have to be calculated.
Sphericity is a description of overall form of the particle irrespective of angularity of

edges and corners. For most particles, the sphericity can be calculated by the following ratio:

$$\varphi = \frac{\pi^{1/3}(6V_p)^{2/3}}{A_p},$$ (6.4)

where V_p is volume of the particle and A_p is the surface area of the particle. Sphericity of a perfect sphere is one but the sphericity of real particles is always less than one because the real particle with the same volume has the a larger surface area.

In the lime industry, a widely adopted statistical value of sphericity of the limestone particles after crashing is 0.832 [81].

For a packed bed composed of irregular particles, they must be regarded as a sphere with an equivalent particle diameter (mean Sauter diameter). The preferred method of calculation for the mean Sauter diameter is the following:

$$\overline{d}_p = \frac{1}{\sum_{i=1}^{n} \frac{x_i}{d_{pi}}}$$ (6.5)

Where x_i is the mass fraction of particles which is related to size of particles d_{pi}.

For the pressure drop in a packed bed, consisting of spherical particles, another equation obtained by Brauer [82] can be applied, which is similar to the Ergun equation:

$$\frac{\Delta P}{\Delta L} = 160 \frac{(1-\varepsilon_b)^2}{\varepsilon_b^3} \frac{\mu_f U}{(\varphi \overline{d}_p)^2} + 3.1 \frac{1-\varepsilon_b}{\varepsilon_b^3} \frac{\rho_f U^2}{\varphi \overline{d}_p} [\frac{\mu_f(1-\varepsilon_b)}{\rho_f U \varphi \overline{d}_p}]^{0.1}$$ (6.6)

Brauers correlation is based on experimental data and applies to a packed bed, consisting of spherical particles of the same diameter. Therefore, in this case, the Sauter mean diameter is equal to the sphere diameter. For the calculation of a pressure drop for a bed consisting of spherical particles of different size, appropriate correction functions have to be considered.

6.1.3 Determination of heat transfer coefficient

6.1.3.1 Based on a flow over a single particle

The values of the heat transfer coefficient between fluid and solid particles in a packed bed are significantly higher than the values of the heat transfer coefficient between fluid and a single sphere particle. The heat transfer coefficient for a packed bed can be calculated by the Nusselt correlation for single particle and a correction factor for a packed bed according to [83]. The Nusselt number for a single sphere was described in detail in chapter 5.

The Nusselt number in a packed bed:

$$Nu_b = f_{\varepsilon_b} Nu_p$$ (6.7)

Where the form factor f_{ε_b} of a packed bed consisting of spheres of equal size can be calculated by:

$$f_{\varepsilon_b} = 1 + 1.5(1 - \varepsilon_b) \tag{6.8}$$

Where ε_b is the void fraction of a packed bed and equation 6.8 is valid in the range $0.26 < \varepsilon_b < 1$.

For cylinders with a length l to diameter d ratio within the range $0.24 < l/d < 1.2$ $f_{\varepsilon_b} = 1.6$; For a cube $f_{\varepsilon_b} = 1.6$; For the Raschig rings $f_{\varepsilon_b} = 2.1$.

The heat transfer coefficient, α_b, for a packed bed is calculated by:

$$\alpha_b = \frac{Nu_b \lambda_g}{d_p}. \tag{6.9}$$

6.1.3.2 Based on a hydraulic diameter

The heat transfer coefficient in a packed bed based on a hydraulic diameter for particles is given by [84]. If the packing in a packed bed can be described as a bundle of parallel pipes, the Nusselt function can be calculated by the following equation:

$$Nu_b = 2 + \frac{1 - \varepsilon_b}{\varepsilon_b}(1.12 Re_\varepsilon^{1/2} Pr^{1/3} + 0.0056 Re_\varepsilon Pr^{1/3}) \tag{6.10}$$

Where Re_ε is the Reynolds number with hydraulic diameter and is calculated as:

$$Re_\varepsilon = \frac{\rho_g w d_p}{\mu_g} \frac{1}{1 - \varepsilon_b} \tag{6.11}$$

Where w is the velocity of an empty bed.

equation 6.11 is valid in the range $100 < Re_\varepsilon < 4.10^4$ and $0.6 < Pr < 1000$.

[26] has compared the convective heat transfer coefficients obtained from the two approaches. She has showed that, the difference between the results of both approaches is slightly small at low superficial velocity and increases with velocity.

6.1.4 Determination of mass transfer coefficient

6.1.4.1 Based on a flow over a single particle

The mass transfer coefficient in packed bed can be calculated from the Sherwood function. Similarly to heat transfer, the mass transfer coefficient β in the packed bed can be obtained by modification of the mass transfer for a single sphere particle which has been described in detail in chapter 5, with the same factor f_{ε_b} as:

$$Sh_b = f_{\varepsilon_b} Sh_p. \tag{6.12}$$

Then the mass transfer coefficient β is calculated as:

$$\beta = \frac{Sh_b D}{d_p} \tag{6.13}$$

6.1.4.2   Based on a hydraulic diameter

Another approach is to estimate the mass transfer coefficient β in a packed bed, which is given based on hydraulic diameter.

The Sherwood function with hydraulic diameter can be calculated as:

$$Sh_b = 2 + \frac{1 - \varepsilon_b}{\varepsilon_b}(1.12Re_{\varepsilon}^{1/2}Sc^{1/3} + 0.0056Re_{\varepsilon}Sc^{1/3}) \tag{6.14}$$

6.2   The model

The mathematical model of a mixed feed lime kiln was developed here in 1-D, i.e. the properties in any cross section are assumed constant, and the variations are limited to the vertical direction. It includes a number of assumptions, the most important of which are given in this section. Such assumptions are necessary because of the complex chemical and physical nature of solid particles (coke and limestone) which are fed to the kiln. The model focuses on detailed descriptions of the chemistry and mass and heat exchange mechanisms. It has been built on the principle of mass and energy balances in the kiln.

6.2.1   Basic assumptions

The following assumptions are assumed to derive the differential equation in a 1-D approximation,

- steady state operating conditions in the kiln.

- the solid particles (coke and limestone) entering the kiln are spherical.

- the number of coke particles are constant until burnout.

- constant void fraction of particle bed.

- heterogeneous reactions only on the outer surface of coke.

- no disintegration of solid particles.

- the ash in coke leaves the kiln as fly ash and does not react with any phases.

- limestone particles preserve their shape during decomposition into lime and CO_2. They leave the kiln with the same shape and size they had when they entered.

- the heat transfer by radiation is negligible.

6.2.2 Mass balances

In the 1-D mathematical model, the mass balance is calculated for the gas stream and solid streams.

6.2.2.1 Mass balances on gas

The main components of gas stream are nitrogen, carbon dioxide, oxygen and carbon monoxide. The nitrogen does not participate in any chemical reactions (except for some NO_x formation, which is ignored at present). The change of gas flow is due to the reaction between phases. The mole balance equations of the total amount of gas and its components are written as:

$$\frac{d\dot{N}_g}{dz} = \frac{M_{O_2}(-\Re_1) + M_{CO_2}(\Re_1 - \Re_2 + \Re_3) + M_{CO}(2\Re_2)}{M_g} \tag{6.15}$$

$$\frac{d\dot{N}_{O_2}}{dz} = -\Re_1 \tag{6.16}$$

$$\frac{d\dot{N}_{CO_2}}{dz} = \Re_1 - \Re_2 + \Re_3 \tag{6.17}$$

$$\frac{d\dot{N}_{CO}}{dz} = 2\Re_2 \tag{6.18}$$

$$\frac{d\dot{N}_{N_2}}{dz} = 0 \tag{6.19}$$

where $\Re$ is the reaction rate of chemical reactions occurring in the kiln, these are defined in detail in the reaction rates of chemical reactions section.
The inlet boundary conditions for gas species are given as input into the model in terms of air flow rate and composition. The inlet air is typically ordinary atmospheric air.

6.2.2.2 Mass balances on solid

The change of molar flow of solid (coke, limestone and lime) along the axial coordinate is determined by the rate of consumption or production of the reactions. The mole balance equations of the solid can be written as:

$$\frac{d\dot{N}_C}{dz} = \Re_1 + \Re_2 \tag{6.20}$$

$$\frac{d\dot{N}_{ls}}{dz} = \Re_3 \tag{6.21}$$

$$\frac{d\dot{N}_l}{dz} = -\Re_3 \tag{6.22}$$

with the boundary conditions at z=0 (top of the kiln) the mass flow rate of solid is the initial value.

6.2.3 Energy balances

The energy balance of the kiln is calculated for the gas stream and solid streams.

6.2.3.1 Energy balance on gas

The heat balance on gas is given by:

$$\frac{d}{dz}(\dot{m}_g c_{pg} T_g) = \Re_1(-\Delta H_1) + \Re_2(-\Delta H_2) - q_{gc} - q_{gl} - q_{gw} \tag{6.23}$$

The terms in the equation represent the following: the left-hand side term is the rate of enthalpy change of the gas streams along the kiln axis, the first two terms on the right-hand side are the rate of heat released or consumed by chemical reactions and the rest of the terms on the right-hand side is the rate of heat transferred from other phases and the wall of the kiln by convection. The terms of the equation are described in detail in later sections.

The boundary condition is the temperature of air at inlet of the kiln. The air is not preheated, so the temperature is the ambient temperature, depending on the factory and the time of year.

6.2.3.2 Energy balance on solid

The energy balance on coke:

$$\frac{d}{dz}(\dot{m}_c c_{pc} T_c) = \Re_1(-\Delta H_1) + \Re_2(-\Delta H_2) + q_{gc} \tag{6.24}$$

The energy balance on limestone (surface and core):

$$\frac{d}{dz}(\dot{m}_l c_{pl} T_l) = q_{gl} - q_{sr} \tag{6.25}$$

$$\frac{d}{dz}(\dot{m}_{ls} c_{pls} T_{ls}) = q_{sr} + \Re_4(-\Delta H_R) \tag{6.26}$$

The temperature of the solid as it enters the kiln at the top (z=0) is given as input to the model and provides the required boundary condition. The inlet temperature of the solid is the ambient temperature.

6.2.4 Heat transfer

6.2.4.1 Heat transfer by convection

The heat transfer from the gas to the solid particles is dominated by convection in the model. The convective heat transfer is modeled based on established Nusselt correlations for single spherical particles with a laminar and a turbulent contribution as described in detail in heat transfer in a packed bed. The heat transfer coefficient is calculated from the correlation:

$$\alpha = \frac{Nu_b \lambda_g}{d_p} \tag{6.27}$$

Where Nu_b is the Nusselt number for the kiln.
The convective heat transfer from gas phase to coke is calculated using the expression:

$$q_{gc} = \alpha_{gc} a_c (T_g - T_c) \tag{6.28}$$

Where a_c is the surface area of coke per unit volume of the kiln. The calculation of a_c is described in later sections.
The convective heat transfer from gas phase to limestone surface is calculated from:

$$q_{gl} = \alpha_{glsi} a_{lsi} (T_g - T_l) \tag{6.29}$$

Where a_{lsi} is the surface area of limestone per unit volume of the kiln. The calculation of a_{lsi} is described in later sections.
The heat loss through the kiln wall is calculated using the following expression:

$$q_{gw} = \alpha_{gweff} a_w (T_g - T_a) \tag{6.30}$$

The mixed feed lime kiln is considered as a cylinder so, the surface area of the wall per unit volume is $a_w = 4/d_k$. The effective heat transfer coefficient α_{gweff} is a coupling of convective heat transfer coefficients and thermal conductivities of the wall.

6.2.4.2 Heat transfer by conduction

The heat conduction within the limestone particles should account for: (1) heat conduction from the surface of particles to the core through a porous layer of CaO with low thermal conductivity (2) heat conduction from the front of reaction to the center of the particle. In the model, it is assumed that the temperature of the core is uniform and equal to T_{ls}.
The heat conduction inside the lime layer is estimated as:

$$q_{sr} = \frac{4\pi \lambda_l r_s r_r}{r_s - r_r} (T_l - T_r) \tag{6.31}$$

Where λ_l is the thermal conductivity of the lime layer. and r_s, r_r are the lime radius and reaction front radius respectively.
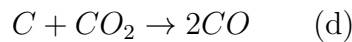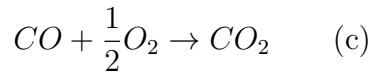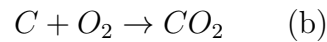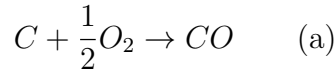
In the model, it is assumed that the coke particles have a uniform temperature. Since the temperature gradient in the coke particle in the combustion zone (the important zone) is at a minimum when the reaction rate is controlled by mass transfer.

6.2.5 Chemical reactions

The chemical reactions considered in mixed feed lime kiln are combustion of coke, gasification of coke (Boudouard reaction) and decomposition of limestone.

### 6.2.5.1 Combustion and gasification of coke

In the combustion zone of mixed feed lime kiln, the possible reaction between coke and oxygen are:

$$C + \frac{1}{2}O_2 \rightarrow CO \qquad \text{(a)}$$

$$C + O_2 \rightarrow CO_2 \qquad \text{(b)}$$

$$CO + \frac{1}{2}O_2 \rightarrow CO_2 \qquad \text{(c)}$$

$$C + CO_2 \rightarrow 2CO \qquad \text{(d)}$$

Coke reacts with oxygen to form CO and CO_2 according to reactions (a)and (b) respectively. CO reacts with oxygen in the gas phase to form CO_2, according to reaction (c), which subsequently is reduced on the coke surface according to reaction (d). A number of investigators modeled the combustion behavior in certain types of furnaces. [85] considered reactions (a),(c) and (d). The reactions (b),(c) and (d)have been considered by [86], whereas [38] considered reaction (b) only. In the present simulation, the reactions (b) and (d) have been considered. The present simulation considered these reactions to simplify the model and also assumed that:
Separation of O_2 to O+O occurred at a very high temperature.
The oxidation of CO (c) is catalyzed by the presence of traces of water vapor in the mixed feed lime kiln, the water vapor is not present in the combustion zone where there is a content of water in limestone and fuel is evaporated in the preheating zone, and the water vapor in the air will exit with the lime. Therefore, the following chemical reactions were considered in the model:

$$C + O_2 \rightarrow CO_2 \qquad \text{(1)}$$

$$C + CO_2 \rightarrow 2CO \qquad \text{(2)}$$
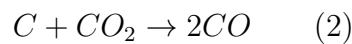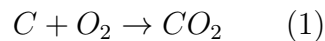
6.2.5.2 Decomposition of limestone

The limestone is decomposed to lime and carbon dioxide in an endothermic reaction according to the following:

$$CaCO_3 + \Delta H_R \rightarrow CaO + CO_2 \qquad (3)$$
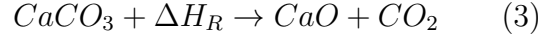
where $\Delta H_R = 168\,kJ/kg$ at 900°C.

6.2.6 Reaction rates of chemical reactions

6.2.6.1 Coke combustion

The reaction between coke and oxygen is important for the lime production process since it generates the heat required for various chemical reactions in lime kiln. In small particles, such as the ones present in pulverized coal, the oxidation takes place on both the particle's surface and inside the pores. The particle diameter and the porosity of the particle is changed through the combustion of char [87, 49]. In mixed feed lime kiln, the size of coke particles lie in the range of several centimeters. The Thiele modulus ϕ for the reaction with O_2 is large. The Thiele modulus is the ratio of the rate reaction to the rate of diffusion inside the burning particle, it is defined as:

$$\phi = \frac{d_p}{2}\sqrt{\frac{k\rho_c a_{in}}{CD_{eff,c}}} \qquad (6.32)$$

Therefore, a large value indicates that the reaction is closed in narrow zone of the particle surface and the transport into the particle is negligible [88, 89]. So in the model takes into account the external reaction rate (the reaction on the outer surface of particle) only.

The reaction rate $\Re_1$ per unit volume of the kiln is expressed as follow:

$$\Re_1 = a_c \frac{1}{\frac{1}{k_{O_2}} + \frac{1}{\beta_{O_2}}} C_{O_2,g} \qquad (6.33)$$

Where k_{O_2} is reactivity of coke with O_2

$k_{O_2} = 1.225 * 10^3 exp(-\dfrac{9.977 * 10^4}{RT_c})$

and $C_{O_2,g}$ is the oxygen concentration in the gas phase.

6.2.6.2 Coke gasification

The reaction between coke and carbon dioxide in lime kiln is the source of energy loss and CO production in flue gases. During the combustion of coke particles, CO_2 reacts with coke to produce CO which diffuses towards the gas to react with O_2.

Therefore, the CO_2 is considered the coke oxidizing agent and CO_2 gasification is, in itself, important to the combustion. The coke gasification is calculated on the outer surface of the particle similar to the reaction rate of coke combustion.

The reaction rate $\Re_2$ per unit volume of the kiln is given by:

$$\Re_2 = a_c \frac{1}{\frac{1}{k_{CO_2}} + \frac{1}{\beta_{CO_2,c}}} C_{CO_2,g} \tag{6.34}$$

where k_{CO_2} is the reactivity of coke with CO_2

$$k_{CO_2} = 7.351 * 10^3 exp(-\frac{1.38 * 10^5}{RT_c})$$

and $C_{CO_2,g}$ is the carbon dioxide concentration in the gas phase.

6.2.6.3 Limestone decomposition

The carbon dioxide produced from the reaction escapes through the outer shell of lime due to the differences in the partial pressure of CO_2. Consequently, the reaction rate is proportional to the difference between the concentration of CO_2 at the reaction front $C_{co_2}^\star$, and outside the boundary layer $C_{co_2,g}$, and the diffusion resistances.

The reaction rate $\Re_3$ per unit volume of the kiln is expressed as follows:

$$\Re_3 = a_{ls} \frac{k_{ls}}{k_{ls}r_{ls}^2(\frac{1}{D_{eff,l}}(\frac{1}{r_{ls}} - \frac{1}{r_l}) + \frac{1}{\beta_{co_2,l}r_l^2}) + 1}(C_{co_2}^\star - C_{co_2,g}) \tag{6.35}$$

where $C_{co_2}^\star$ is equilibrium concentration. It is related to the equilibrium pressure (see chapter 5) by the following relation:

$$C_{co_2}^\star = \frac{P_{eq}}{RT_r}$$

and k_{ls} is reaction rate coefficient of limestone

$$k_{ls} = 0.012 exp(-\frac{168000}{RT_r})$$

The reaction rate at the reaction front is proportional to the area of reaction front and the chemical reaction coefficient.

$$\Re_4 = a_{ls}k_{ls}(C_{co_2}^\star - C_{co_2,r}) \tag{6.36}$$

6.2.7 Gas phase

If the temperature dependence of the material properties cannot be neglected they can be calculated with the following equations according to [70]:

$$\frac{\lambda}{\lambda_0} = (\frac{T}{T_0})^{n_\lambda}$$

$$\frac{\mu}{\mu_0} = (\frac{T}{T_0})^{n_\mu}$$

$$\frac{a}{a_0} = (\frac{T}{T_0})^{n_\mu - n_c + 1}$$

$$\frac{\rho}{\rho_0} = (\frac{T}{T_0})^{-1}$$

$$\frac{C_p}{C_{p0}} = (\frac{T}{T_0})^{n_c}$$

$$\frac{\nu}{\nu_0} = (\frac{T}{T_0})^{n_\mu + 1}$$

where $T_0 = 273K$.

Material properties of gases in temperature $T_0 = 273K$ are gathered in table 6.2.

Table 6.2: Material properties of gases in $T_0 = 273K$ [70].

Gas	$\tilde{M}$	ρ_0	C_{p0}	n_c	λ_0	n_λ	μ_0	n_μ	Pr
unit	$kg/kmol$	kg/m^3	kJ/kgK	-	W/mK	-	mg/ms	-	-
N_2	28	1.26	1.00	0.11	0.024	0.76	16.8	0.67	0.7
CO	28	1.26	1.00	0.12	0.024	0.78	16.8	0.67	0.7
Air	29	1.29	1.00	0.10	0.025	0.76	17.4	0.67	0.7
O_2	32	1.44	0.9	0.15	0.025	0.8	19.7	0.67	0.7
CO_2	44	1.98	0.84	0.3	0.017	1.04	14.4	0.77	0.73
H_2O	18	0.81	1.75	0.2	0.016	1.42	8.7	1.13	0.95

The properties of gas mixtures can be calculated with the following formulas:

$$\rho_M = \sum \rho_i \tilde{x}_i \tag{6.37}$$

$$\lambda_M = \sum \lambda_i \tilde{x}_i \tag{6.38}$$

$$C_{pM} = \sum C_{pi} x_i = \frac{1}{\rho_g} \sum C_{pi} \tilde{x}_i \rho_i \tag{6.39}$$

where $\tilde{x}_i$ is the volume fraction of component i in a gas mixture. and x_i is the mass fraction of component i in a gas mixture.

6.2.8 Coke properties

The chemical and physical properties of coke widely depend on the properties of used coal and the carbonization method. The density of coke is approximately 1000 kg/m^3. The ash in the coke is removed due to the attrition of burden and leave the kiln as fly ash. The heat capacity of coke is one important basic physical property in the analysis of the temperature distribution in the lime kiln, but the heat capacity of metallurgical coke has not been reported so much. [90] studied the variation of specific heat with temperature and the effect of coke composition and obtained the following equation:

$$c_{p,c} = 3 \frac{R}{(\sum_i \frac{x_i}{M_i})^{-1}} e^{(1200/T_c)} \left[\frac{1200/T_c}{e^{(1200/T_c)} - 1} \right]^2 \tag{6.40}$$

The specific surface area of coke particles per unit volume of the kiln is needed for computing the reaction rates of combustion. It is computed as follows:
A constant number of coke particles, N_c at all vertical positions of the kiln can be assumed,

$$\frac{dN_c}{dz} = 0 \tag{6.41}$$

The diameter of coke particles varies with the particles that descend down in the kiln. The expression for coke diameter can be derived as:

$$d_c = d_{ci} \sqrt[3]{\frac{m_c}{m_{ci}}} \tag{6.42}$$

The expression for the surface area of coke per unit volume of the kiln, a_c can be derived from the diameter of coke particle and the numbers of particles. One can express it through the following expression:

$$a_c = A_p N_c \tag{6.43}$$

Where N_c is the number of coke particles

$$N_c = \frac{m_c}{V_p \rho_c A_k v_c} \tag{6.44}$$

Where v_c is the velocity of coke in the kiln.

$$v_c = \frac{1}{(1 - \varepsilon) A_k} \sum_i \frac{m_{si}}{\rho_{si}} \tag{6.45}$$

From the equations 6.44 and 6.45 with equation 6.43, the expression for Specific surface area of coke particles per unit volume of kiln is:

$$a_c = \frac{6(1 - \varepsilon)}{d_c} \frac{\frac{m_c}{\rho_c}}{\sum_i \frac{m_{si}}{\rho_{si}}} \tag{6.46}$$

For more properties of coke see chapter 4.

6.2.9 Limestone properties

The chemical and physical properties of limestone depend on its origin. Apparent density is a function of the porosity, the crystal density and the amount of water in the pores. It varies from 1500 to 2700 kg/m^3 and increases for dense calcium limestone.

The decrease of limestone particle diameter in the kiln can be described in the same way as for the coke particles. The diameter of limestone particles can be evaluated with the following expression:

$$d_{ls} = d_{lsi} \sqrt[3]{\frac{m_{ls}}{m_{lsi}}} \tag{6.47}$$

Where d and m are the diameter and mass flow rate of limestone respectively.
Through the assumption for the size and shape of limestone particles, the expression for lime diameter can be derived as:

$$d_l = d_{lsi} - d_{ls} \tag{6.48}$$

The expression for the surface area of limestone per unit volume of the kiln, a_{ls} can be derived from the ε and the formulas for the surface area and volume of a particle.

$$a_{ls} = \frac{6(1 - \varepsilon)}{d_{ls}} \frac{\dfrac{m_{ls}}{\rho_{ls}}}{\sum_i \dfrac{m_{si}}{\rho_{si}}} \tag{6.49}$$

The properties of limestone which used in the present simulation of kiln have been described in chapter 5.

6.3 Solving the system

The model consists of mass and heat balance, together with the boundary conditions at z=0 and $z = H_f$, the constitutive equations concerning mass and heat transfer, and the rates of reactions. Table 6.3 lists the important computed variables by the model. The model is composed of twelve ordinary differential equations and a number of algebraic equations under described boundary conditions. Since we are dealing with a complex coupling of equations and boundary conditions, the boundary value solver (bvp4c) of matlab-7 is suitable to solve the system.

Table 6.3: Summary of important variables computed by the model

No.	variable	symbol	eq. type
1	temperature of gas	T_g	ODE
2	coke temperature	T_c	ODE
3	lime temperature	T_l	ODE
4	reacting core temperature	T_r	ODE
5	volume fraction of species i in the gas	$\tilde{x}_{ig}$	ODE
6	coke conversion	X_c	ODE
7	limestone conversion	X_{ls}	ODE
8	molar flow of gas	$\dot{N}_g$	ODE
9	molar flow of limestone	$\dot{N}_{ls}$	ODE
10	molar flow of lime	$\dot{N}_l$	ODE
11	molar flow of coke	$\dot{N}_c$	ODE
12	superficial velocity of the gas	U	Alg.
13	pressure drop	ΔP	ODE

6.4 Results of the model and discussion

6.4.1 Geometrical and operating parameters

the mathematical model developed contains a number of parameters, some of which are for the geometry of the kiln and the others for input data, such as the properties of raw materials and their amounts. Table 6.4 describes the geometrical and operating parameters that are used in the model.

6.4.2 Model results

The developed model can predict the gas, coke, lime and limestone temperatures, the conversion of solid materials and mass flow rates of gas phase and solid phase and the gas concentration profiles inside the kiln. The model also predicts the pressure drop and velocity of the gas phase.

Figure 6.2 shows the temperature profiles of the gas, coke, lime and limestone predicted by the model. At the bottom of kiln ($z = H_f$), the air has a temperature of 30 °C, whereas the solid materials enter at the top at ambient temperatures. The solid feed materials are heated by the hot gas leaving the reaction zone in countercurrent flow. At some point, the coke starts to combust, but this is not visible on the temperature profile because the heat of combustion is so low, the beginning of the burning of the coke starts when the coke conversion is at about 2m (see figure 6.3). Here, at this length, the limestone is still heated until it reaches calcination temperature at about 850 °C at 4.5 m. At this point, the limestone starts to decompose, the beginning of calcination zone is determined by the beginning of the limestone conversion (see figure

Table 6.4: Input data for the model

Parameters	Units	value
Height of the bed	m	18
Internal diameter of kiln	m	3.104
Void fraction	-	0.38
Temperature of feed solid materials	°C	20
Temperature of feed air	°C	30
Inlet diameter of fuel	m	0.03
Inlet diameter of limestone	m	0.08
Air input flow	m_N^3/h	3140
Fuel input flow	$t/(d.m^2)$	1.11
Limestone input flow	$t/(d.m^2)$	19.73
mass fraction of CO_2 in limestone	-	0.44
Molecular weight of limestone	$kg/kmol$	100
Molecular weight of lime	$kg/kmol$	56
Density of coke	kg/m^3	1000
Density of anthracite	kg/m^3	1600
Density of limestone	kg/m^3	2700
Density of lime	kg/m^3	1500
Thermal conductivity of limestone	W/mK	2.26
Thermal conductivity of lime	W/mK	0.7
Enthalpy of reaction $(1)\Delta H_1$	kJ/mol	- 396
Enthalpy of reaction $(2)\Delta H_2$	kJ/mol	172.5
Enthalpy of decomposition reaction ΔH_R	kJ/mol	178

6.3). In calcination zone, the coke combustion rate increases and the temperatures of the gas phase and solid phase rise faster to maximum temperatures of 1300, 1200 and 1100 °C for coke, gas and lime respectively at 11 m. At the beginning of the calcination zone, the limestone temperature and the lime temperature are the same but the lime temperature increases faster with the increase of limestone calcination when the heat is transferred to the limestone surface by convection. The temperature of limestone begins to decrease before it leaves the calcination zone, which is partly due to the consumption of energy by the decomposition reaction. At the length approximately of 12 m, the calcination of limestone is stopped and lime starts in cooling by the air entering the kiln from the bottom where the lime gives away the heat to the countercurrent flowing air. Due to the excess air number of 1.14 used in the model, the lime exit with low temperature about 33 °C and the flue gas exits with a high temperature of about 150 °C.

Figures 6.3 and 6.4 show the conversion of the solid phase and mass flow rates of gas and solid phases. It is seen from the figures that the coke combustion and calcination
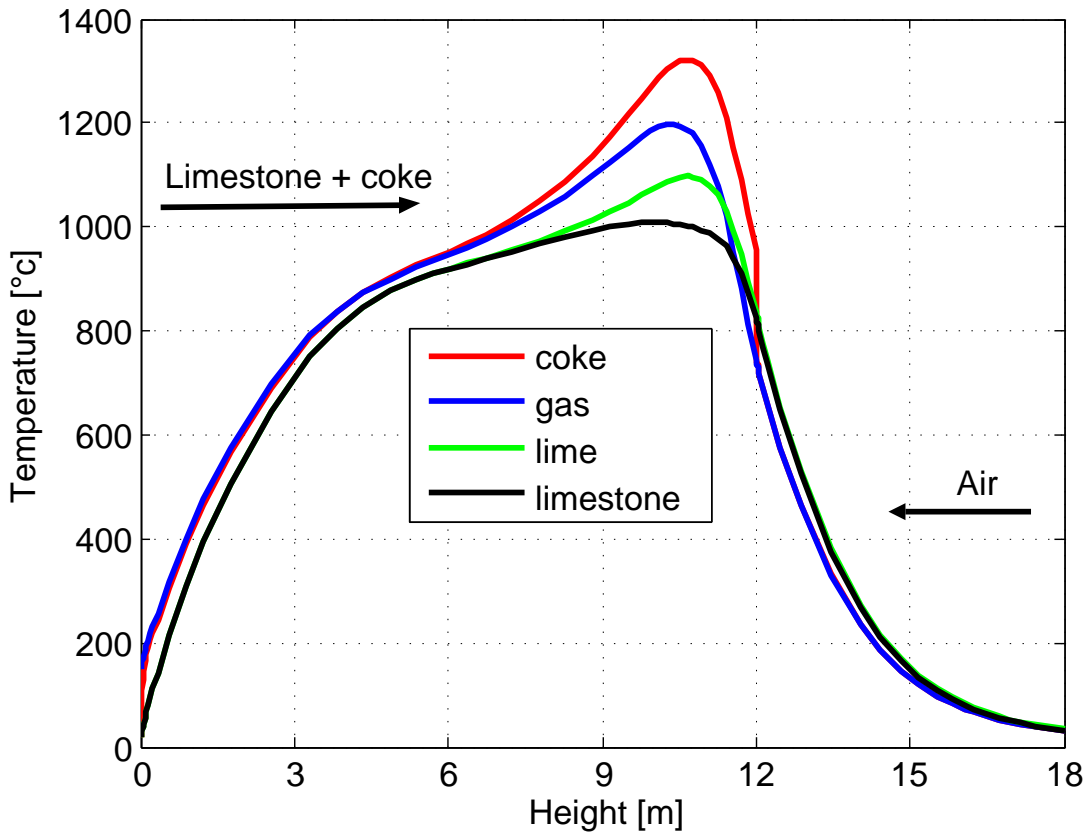
Figure 6.2: Temperature profiles along the kiln.

of limestone mainly occur in the central part of the kiln whose length is approximately 7 m. In the upper and lower regions of the kiln, the conversion of coke and limestone and the mass flow rates stay constant where there are no reactions. As seen from figure 6.3 the coke combustion reached 100 % conversion while, the decomposition of limestone reached 78 %. This means, the complete combustion of coke was achieved while the limestone was still not completely burned. This is due to the fuel ratio of 5.6 % and excess air number of 1.14. From figure 6.4, one can see that the limestone starts to decompose at approximately 4.5 m from the top of the bed, leading to a decreasing limestone mass flow rate and an increasing lime mass flow rate. Mass flow rate of the gas increases continuously from cooling zone to preheating zone due to the products of combustion and released carbon dioxide from limestone calcination.

Figure 6.5 shows the mole fraction of the gas components ($O_2, CO, and CO_2$) predicted by the model. It shows that, the concentration of gas components are constant in the preheating and cooling zones and the change occurs mainly in the reacting zone where there are reactions. The oxygen concentration in gases decreases due to its
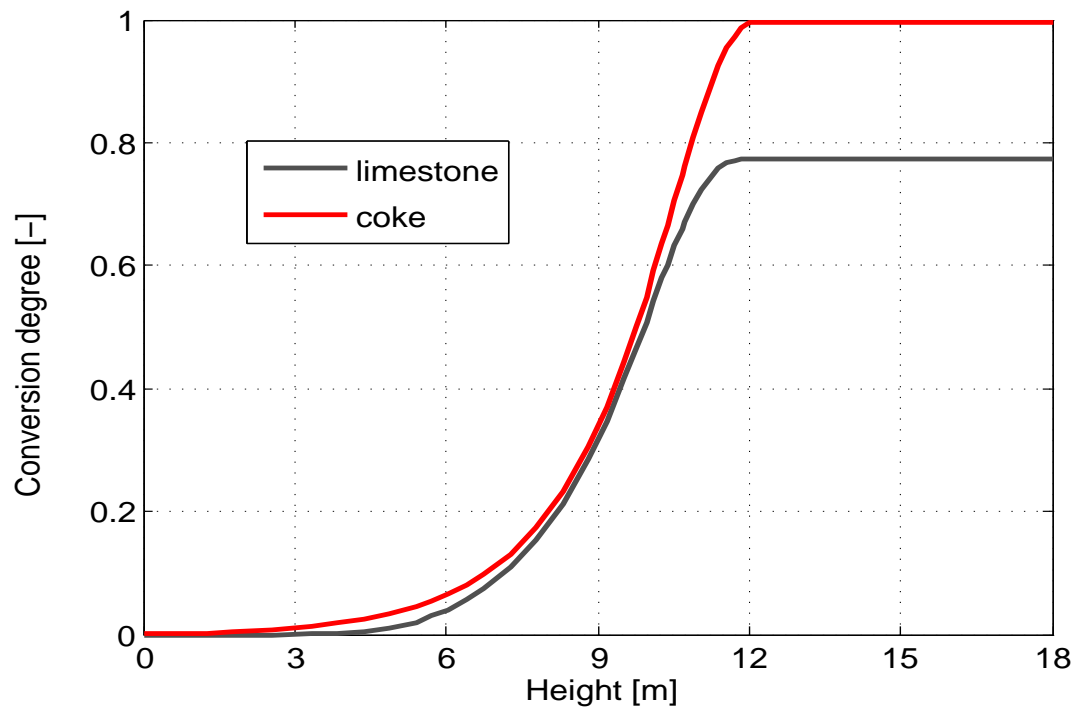
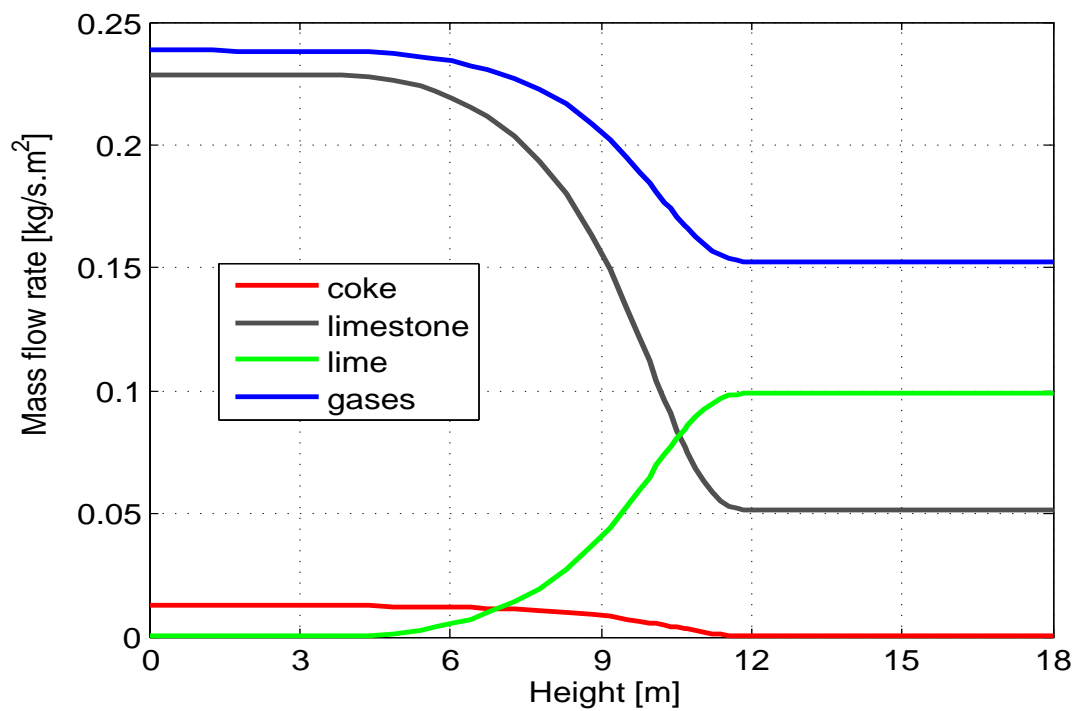Figure 6.3: Profiles of conversion degree along the kiln.

Figure 6.4: Profiles of mass flows along the kiln.

consumption by the combustion reaction. Its reaction with coke forms the net product CO_2 because CO is rapidly oxidized in the gas phase when oxygen is present. Consequently, the concentration of CO_2 increases sharply due to CO_2 production from limestone calcination and coke combustion while the mole fraction of CO stays constant where the oxygen is present because the actual air excess number is higher than the theoretical.
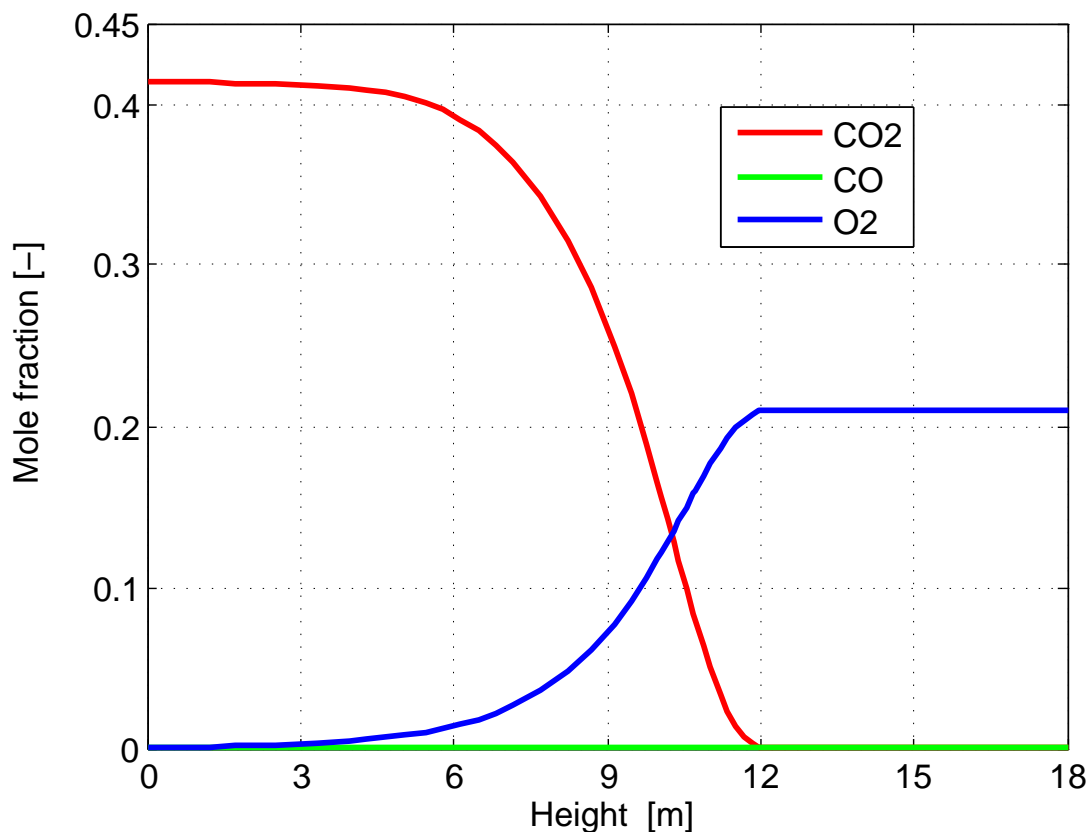

Figure 6.5: Profiles of volumetric concentration of the gas along the kiln.

A strong change in gas velocity profile over the height of the kiln is shown in Figure 6.6. The gas velocity profile is strongly influenced by the gas temperature profile because the density of gas depends on the gas temperature which experiences large changes over the kiln height and also because of the supply of CO_2 gases which are released from the limestone calcination in the calcination zone. It can be seen that the maximum value of gas velocity of 2.3 m/s is encountered with the maximum gas temperature. When increasing the gas velocity, there is an increase of heat and mass transfer between solid and gas phases inside the kiln.
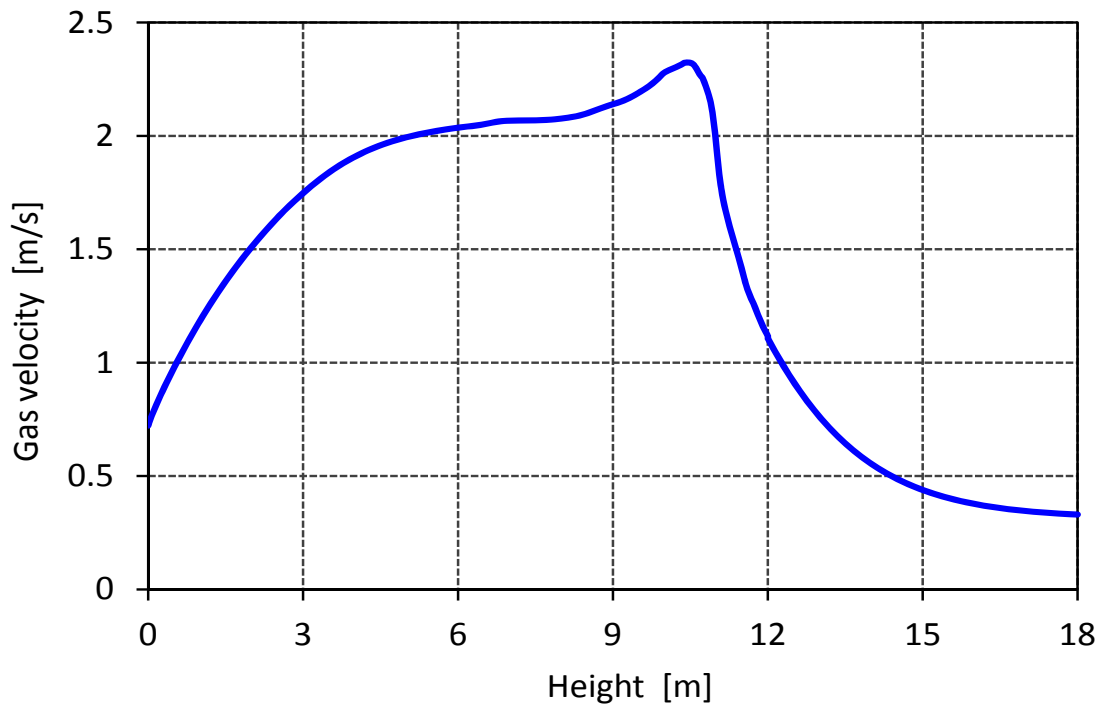
Figure 6.6: Profile of gas velocity a long the kiln.

Figure 6.7 shows the profile of pressure drop along the kiln. The pressure drop depends on the gas velocity, void fraction and the properties of gases according to Ergun's law. In the cooling zone, the pressure drop increases slightly when increasing the air velocity. After that, it increases sharply due to the large increase in gas velocity in the calcination zone.

6.5 Validation

The mathematical model is based on a detailed description of the processes inside the kiln, and in this section, the temperature profiles, concentration profiles and conversions profiles predicted by the model are compared to measurements for validating the model. The data that was obtained through the experiments described in chapter 3 are used for the validation. Figure ?? shows the measured temperature profiles and the predicted profiles of the gas, coke, lime and limestone temperatures. It was assumed for the measured temperature values that these are the temperatures of lime in the kiln so, the temperature profiles measured with the thermometer should be compared to the temperature of the lime. One can see from the figure that the model
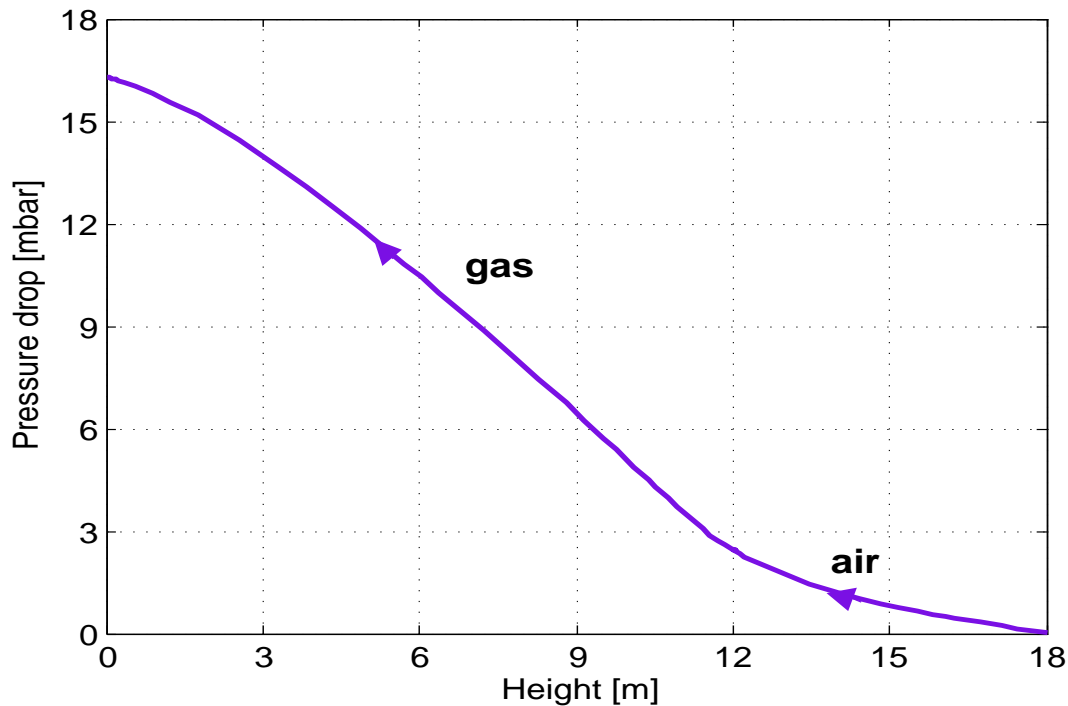
Figure 6.7: Profile of pressure drop of the gas along the kiln.

fits the measured data well at the beginning of the cooling zone and that the maximum temperature predicted and measured is nearly the same. In preheating and calcination zones, the model predicts higher lime temperatures than the measured values. The model is 1-D, and thus, the temperature is an average temperature over the kiln cross section. The simulated results did not agree well with the measured temperature profile where the kiln has problems in operation (see chapter 3) and the measured temperature for one side of the kiln. The measured temperature profile in the cooling zone is linear, this means the amount of air and lime is the same but this is different with the actual where the amount of air is 1.7 times of lime. So the validation was performed for the different outputs of the kiln. Table 6.5 sums up the comparisons between the predicted results by model and outputs from the kiln. The results show very good agreement except in the case of the temperature of outflow gas with a relative error of 25 % because the losses of heat by the kiln walls were about 10 % and this reduced the measured flue gas temperature. In the case of the volumetric concentration of CO_2, the outflow gas had an error of 10 % where the model assumes pure limestone,with the other relative errors being less than 6 %. From the validation, it can be concluded that the model generally performs reasonably well. This indicates that the assumptions made are reasonable for the model to describe the most important phenomena in the kiln.
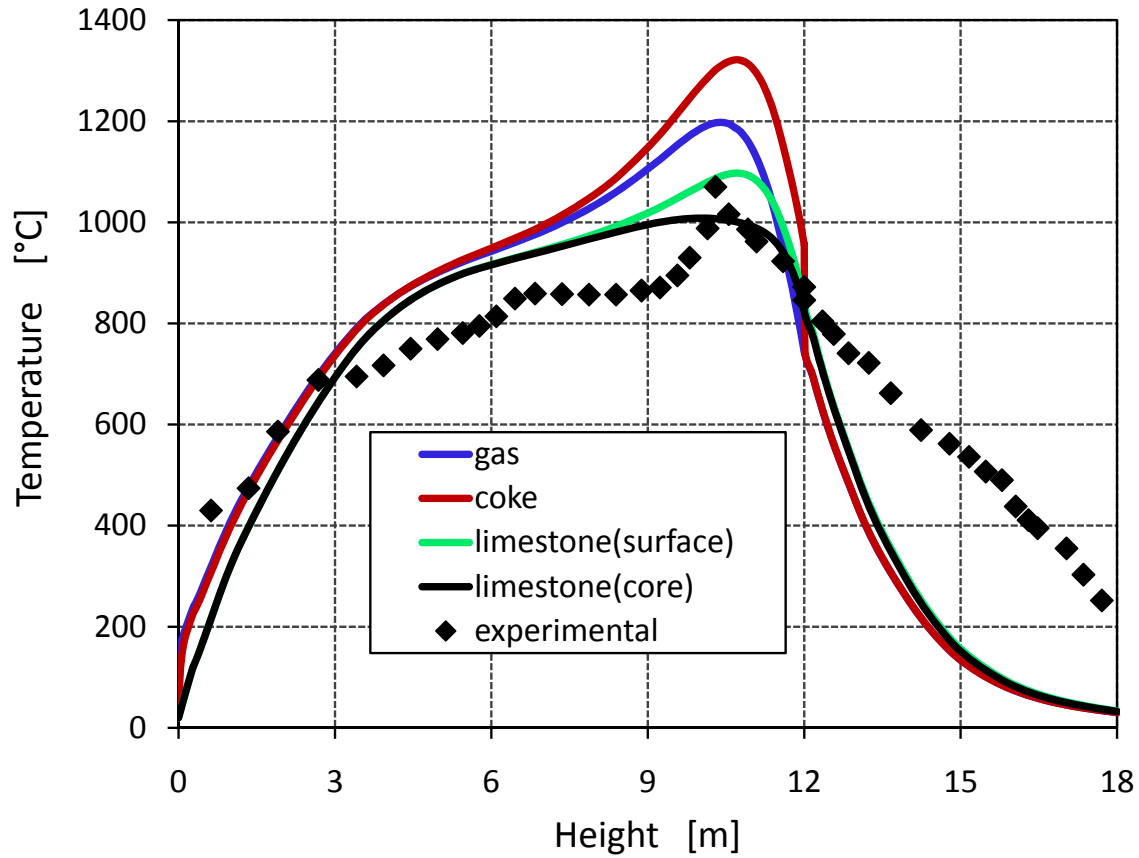
Figure 6.8: Temperature Profiles predicted and measured.

Table 6.5: Comparison between predicted and measured results

	Numerical prediction	Experimental results
Volumetric output flow rate of gas (N_N^3/h)	4310	4385
Temperature of the outflow gas (°C)	150	120
Volumetric fraction of CO_2 (%)	41	37
Residual mass fraction of $CaCO_3$ (%)	20.8	21.6
Temperature of outflow lime (°C)	33	35
Mass flow rate of lime (t/d)	98.07	98
Initial calcination temperature (°C)	850	860
Pressure drop of the kiln (mbar)	16	15.6

6.6   Concluding remark

The developed model of a mixed feed lime kiln is a static 1-D mathematical model. All variations are restricted to the vertical direction of the model. The model built on mass and energy balances for gas and solid phases. The model predicts the gas, coke, lime and limestone temperatures, the conversion of solid materials and mass flow rates of gas and solid phases and the gas concentration profiles inside the kiln. The model also predicts the pressure drop and velocity of the gas phase. The model has been validated against the experimental measurements. The validation showed that the model has captured the essential phenomena in the kiln operation and describes these accurately.

Chapter 7

Application of a Mathematical Model of the Kiln

7.1 Parametric study

The mathematical model of a mixed feed lime kiln has been used to study the effects of important operating parameters on the kiln operation. For production quality lime and carbonation gas, a suitable supply of fuel, limestone and air is needed so, the operating parameters which were studied with the model include the mixing ratio of coke and limestone, the amount of air, and the properties of limestone and the properties of fuel. The effects of these operating variables on the kiln performance will be described in the next sections, the results are constrained by the assumptions on which the model is based.

7.1.1 Fuel ratio

A suitable fuel ratio is required to produce the high quality lime and high CO_2 in flue gases. When the fuel ratio is low, the kiln temperature is lower than normal, producing much unburned lime and low CO_2 in flue gas. When the fuel ratio is high, the kiln temperature exceeds the limits, forming clinkers and causing damage to the refractory bricks of the kiln. In this section, the influence of the fuel ratio on the kiln operation has been investigated through simulations with the mixed feed lime kiln model.

Figure 7.1 shows the temperature profiles of gas and lime from two simulations performed with two values of fuel ratio (5.6, 7.8 %). The other operating conditions used were the same as those listed in table 6.4. The plot shows that, the kiln zones (preheating, calcination and cooling) move with the changing of the fuel ratio. When increasing the fuel ratio, the temperature profiles moved towards the top of the kiln, the length of preheating zone decreased and the length of the cooling zone increased. The high fuel ratio has a higher peak temperature and is narrower than the low fuel

ratio. The temperature of lime leaving the kiln from the bottom (z=H) is slightly lower in the case of a high fuel ratio. Due to the decrease in the length of the pre-heating zone, the temperature of gases leaving the kiln is higher, although the heat transfer coefficient between the gas and the solid increases because the air excess number is constant. It is difficult to show all the results various of fuel ratios of the kiln performance, therefore, the results that various fuel ratios effects have on the maximum temperatures of individual streams, the outlet temperatures, the conversion of limestone and the content of CO_2 in flue gas have been shown.
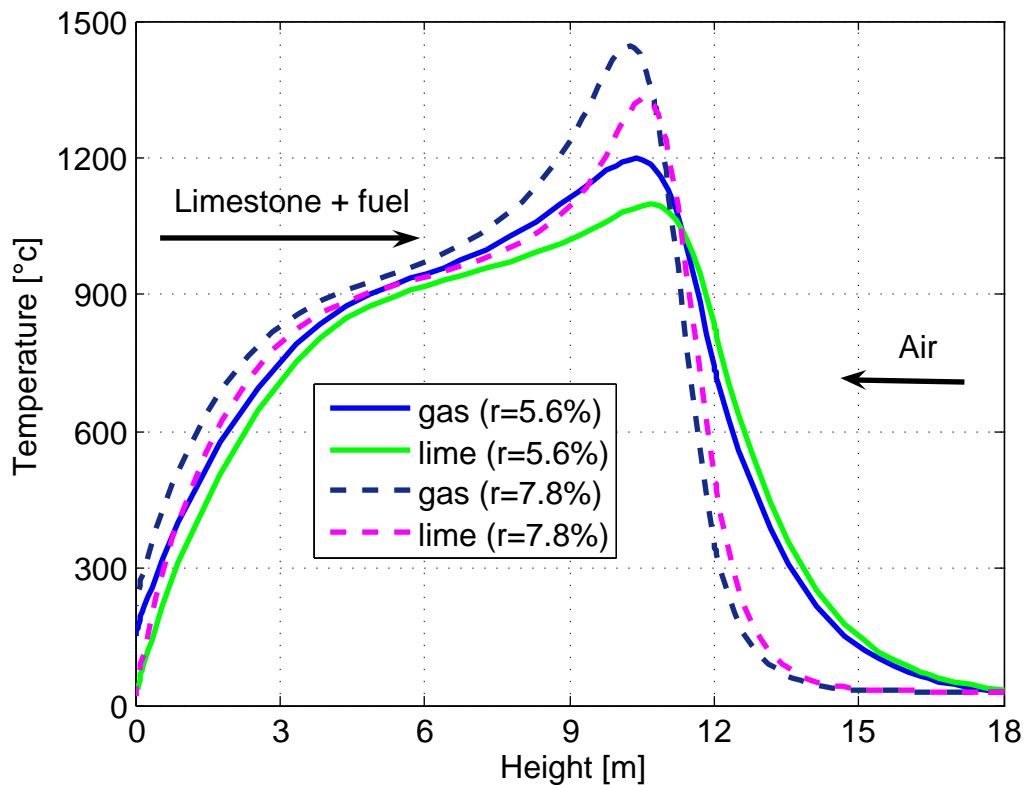

Figure 7.1: Temperature profiles in a mixed feed lime kiln at two fuel ratios and data from table 6.4.

Figure 7.2 shows the effect of fuel ratios on the maximum temperature of coke, gas and lime streams. It is seen that the maximum temperature of all streams increases with the increase of fuel ratio. The maximum temperatures of streams increase strongly at higher fuel ratio. In this case, increasing the fuel ratio above 7.5 % should be done with caution to avoid the formation of slag in the kiln which forms at temperatures above 1300C [40].

The outlet temperatures of gas and lime in dependence on the fuel ratios are shown in figure 7.3. At higher fuel ratio, the outlet lime temperature is slightly reduced.

The outlet gas temperature increases when increasing the fuel ratio because of the preheating zone length becomes shorter and this leads to a large energy loss with exhaust gases.

Figure 7.4 shows the conversion degree of limestone plotted against the fuel ratio. When increasing the fuel ratio, the limestone conversion degree increases until complete conversion at fuel ratio 7.8 %. The heat required for the endothermic decomposition reaction increases, consequently large amounts of limestone convert to lime.

The relation between fuel ratio and CO_2 in flue gas is shown in figure 7.5. As expected, CO_2 in flue gas increases when increasing the fuel ratio. At fuel ratio 7.8 %,, complete conversion of limestone, the concentration of CO_2 in flue gas is the highest.

7.1.2 Air excess number

The injected air in the kiln is for the combustion of fuel so the calculation of combustion air requirements is based on the fuel analysis. In practice, for efficient kiln performance, some excess air over the theoretical amount is used to achieve complete combustion of the fuel. Almost 10 to 20 % excess air over the theoretical amount is needed (depending on the mixing of fuel and air). When the amount of air is not enough, the oxygen required for combustion is not available, causing problems such as unburned lime and formation of CO gas in flue gas. Thus, the kiln efficiency is reduced due to energy loss with incomplete combustion of CO. The dependence of the kiln operation on air excess number is investigated with the mixed feed lime kiln model.

Figure 7.6 shows the temperature profiles of gas and lime with two values of air excess number (1, 1.14). With a decrease of the air excess number, the velocity of air will decrease and the heat and mass transfer will reduce correspondingly. The kiln zones also change; the cooling zone becomes shorter while the preheating zone becomes longer. When the air excess number is decreased, the peak temperature of gas and lime becomes slightly higher.

Figure 7.7 shows a plot of the maximum temperatures of the coke, gas and lime as a function of air excess number which indicates that, while the temperatures of gas and coke decreased with an increase in the air excess number, the maximum temperature of lime remains essentially unaffected by the air excess number. This is the result of higher volume and velocity of air thus causing the higher mass and heat transfer rates.

The outlet temperatures of gas and lime streams as a function of air excess number are shown in figure 7.8. The temperature of flue gas increases with increasing the air excess number. Although the gas/solid heat transfer increases with an increase in the gas volume and velocity, an increase of air excess number reduces the length
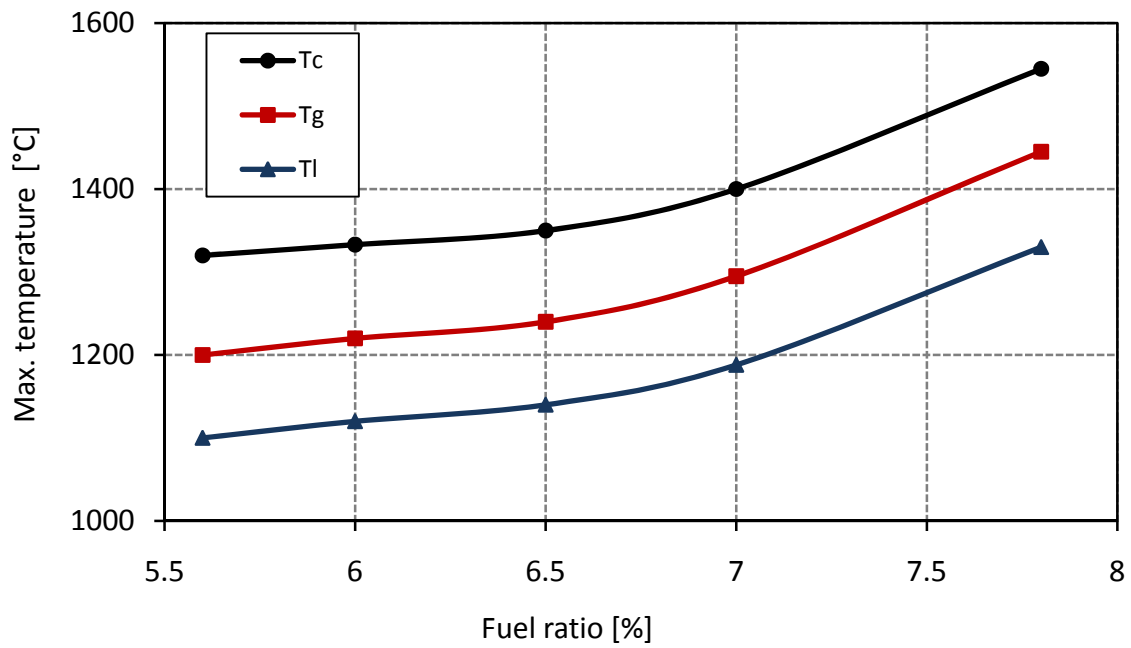
Figure 7.2: Max. temperatures in mixed feed lime kiln at various fuel ratio and data from table 6.4.
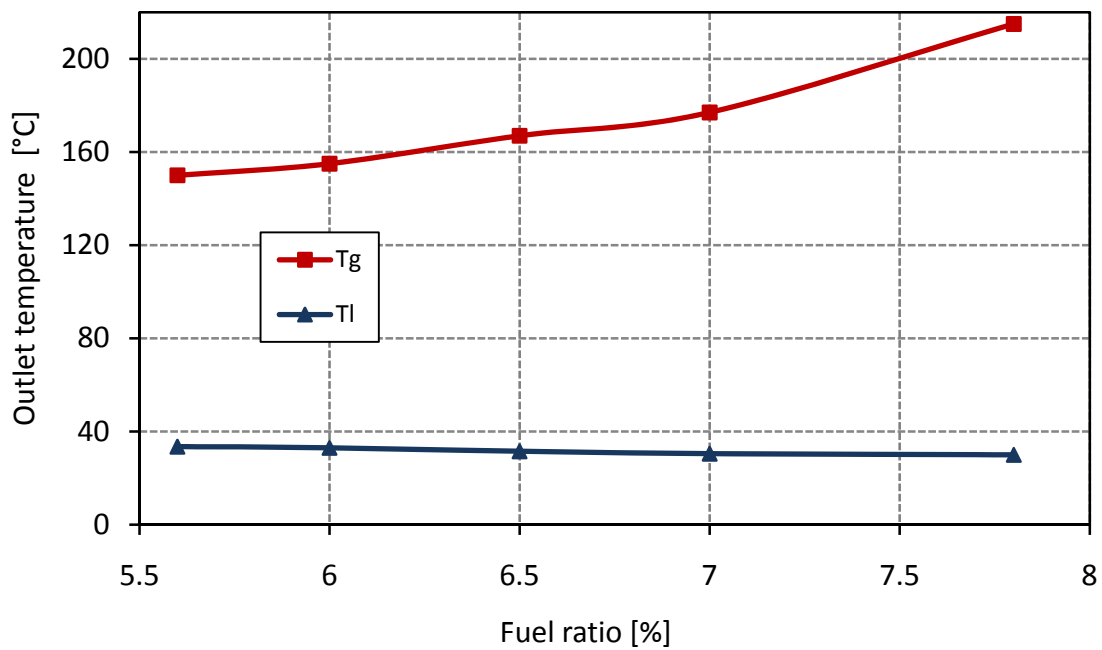

Figure 7.3: Outlet temperatures in mixed feed lime kiln at various fuel ratio and data from table 6.4.
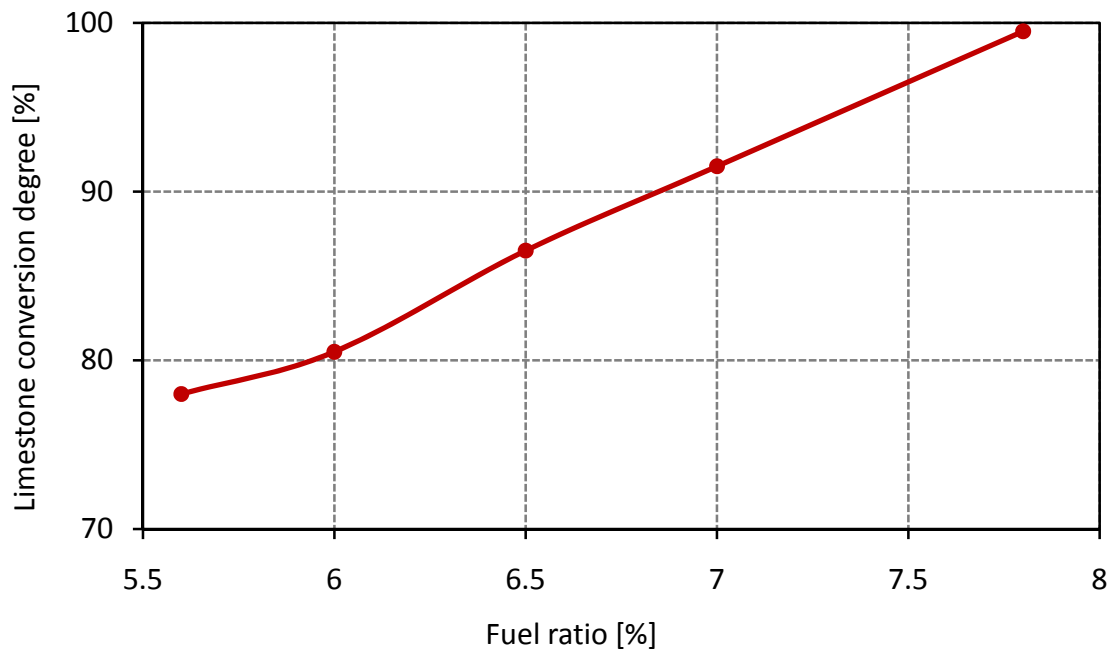
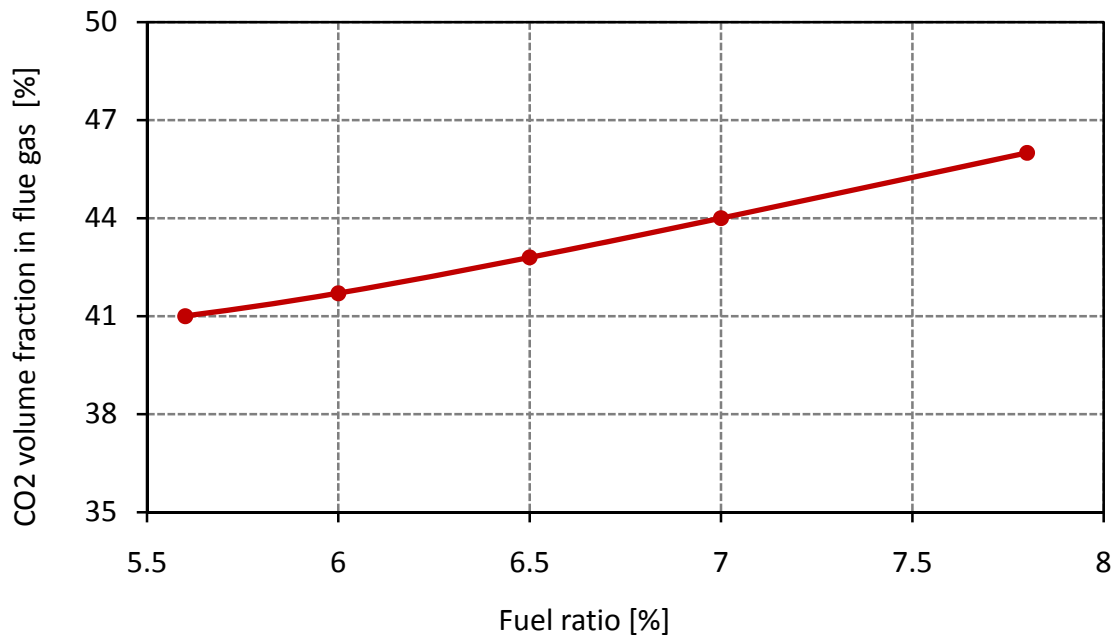Figure 7.4: Conversion degree of limestone for various fuel ratio and data from table 6.4.

Figure 7.5: Volume fraction of CO_2 in flue gas for various fuel ratio and data from table 6.4.
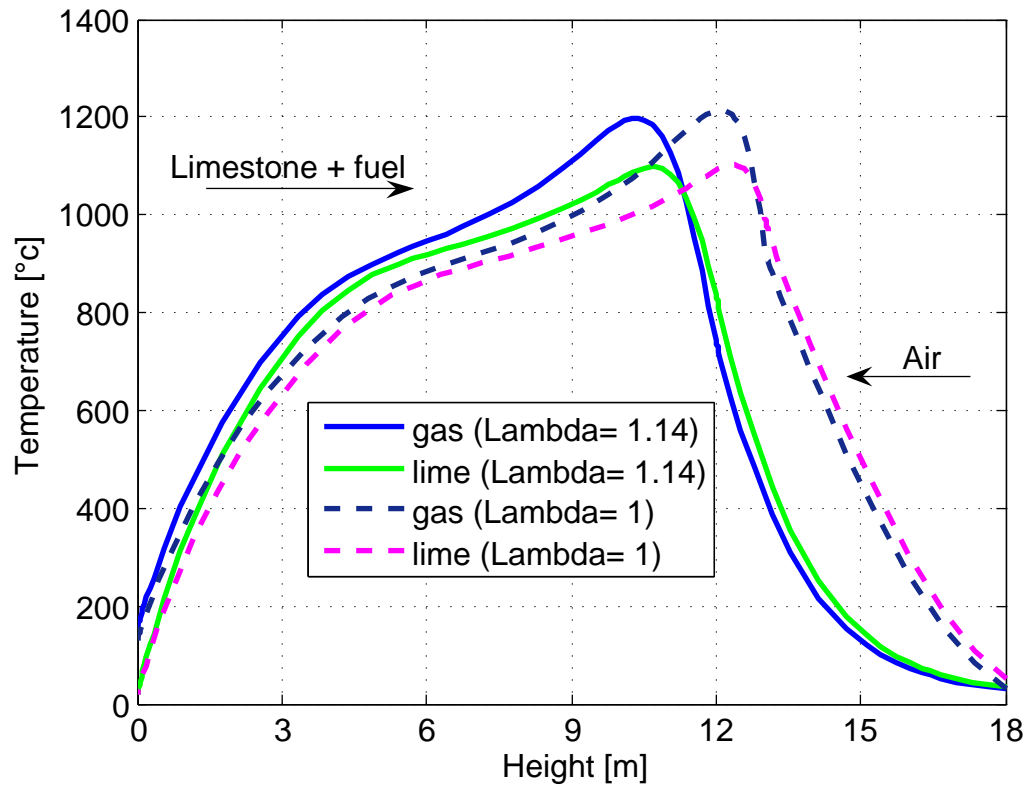
Figure 7.6: Temperature profiles in mixed feed lime kiln at two air excess ratio and data from table 6.4.

of preheating zone reduced due to the movement of the profile towards the top of the kiln. The outlet lime temperature decreased with an increase in the air excess number.

Figure 7.9 shows the conversion degree of limestone as a function of air excess number. With an increase of the air excess number, the limestone conversion degree was reduced because amount of energy required for calcination lost with gases.

Figure 7.10 shows the concentration of CO_2 in the flue gas plotted against the air excess number. The CO_2 in flue gas reduced with an increase of air excess number. It is seen that the plot is similar to the conversion degree of limestone when there is a the complete combustion of fuel. Therefore, the concentration of CO_2 in flue gas depends on the calcination of limestone.

7.1.3 Lime throughput

In a previous section, the effects of changing air excess number on mixed feed lime kiln'performance is investigated. This is one way to increase the load on the mixed
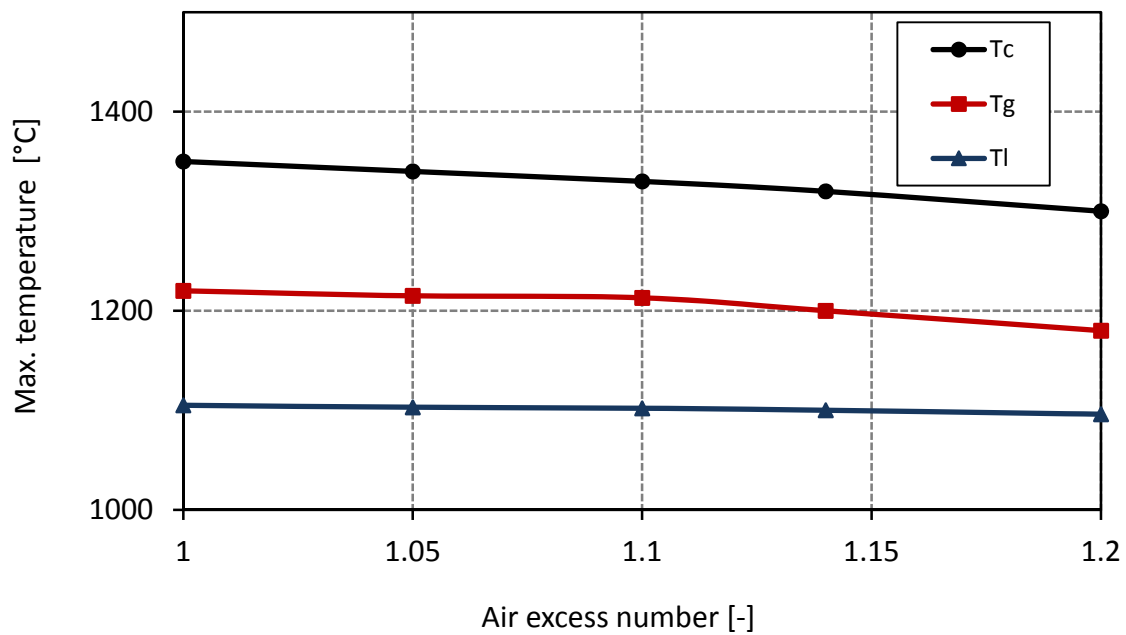
Figure 7.7: Max. temperatures in mixed feed lime kiln at various air excess ratios and data from table 6.4.
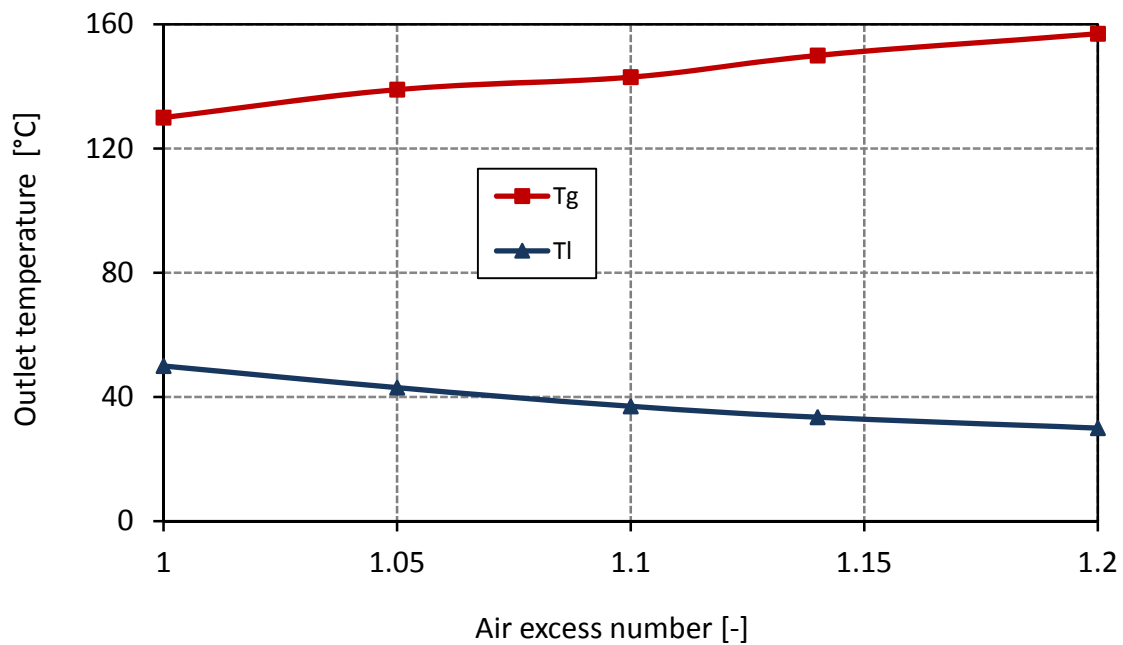

Figure 7.8: Outlet temperatures in mixed feed lime kiln at various air excess ratio and data from table 6.4.
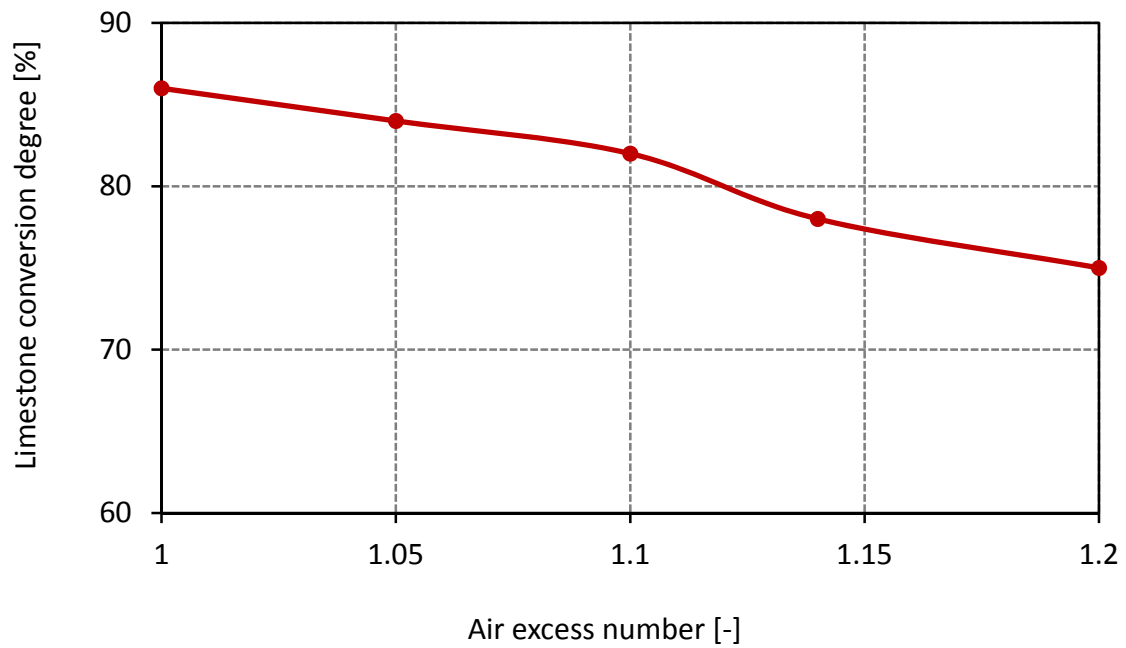
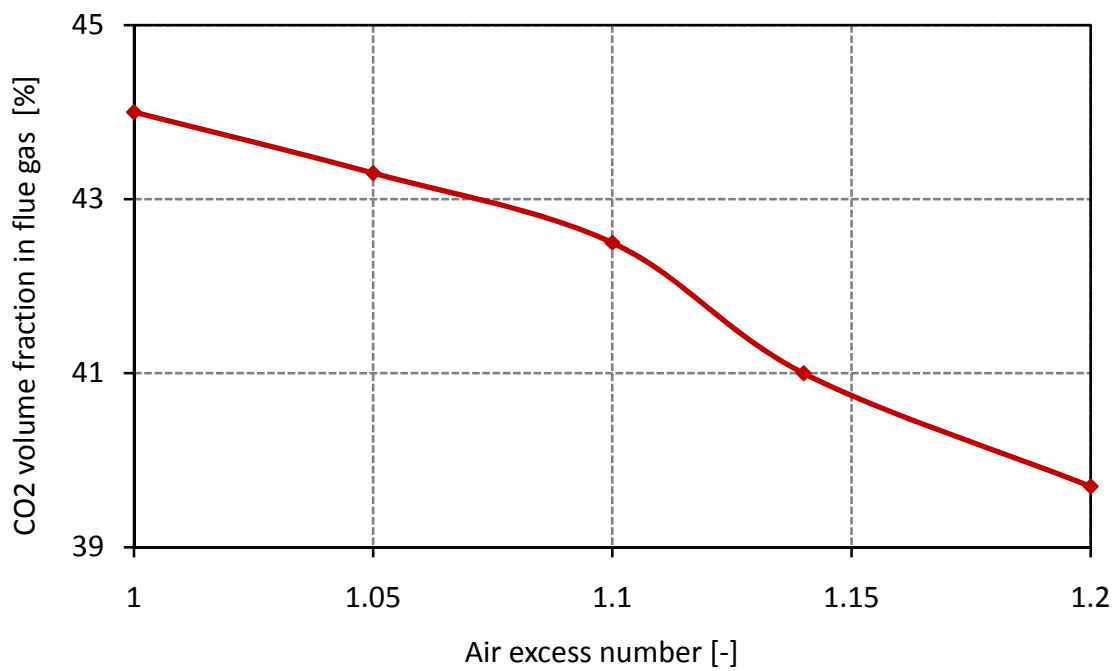Figure 7.9: Conversion degree of limestone for various air excess ratio and data from table 6.4.

Figure 7.10: Volume fraction of CO_2 in flue gas for various air excess ratio and data from table 6.4.

feed lime kiln. Another way is an increase of limestone rate. The influence of lime throughput on the mixed feed lime kiln operation is investigated here by changing the limestone rate while keeping the other input data the same in table 6.4.

Figure 7.11 shows the temperature profiles of lime at three different values of lime throughput. The plot shows that the lime temperature decreases with an increase of the limestone rate because the increase of lime throughput requires more energy to be generated to decompose the limestone. The rate of fuel and air supply is constant as the input is kept constant. The increase of limestone rate affects the length of zones along the whole kiln. With the increase of lime throughput, the discharge lime temperature increases because an amount of heat, which isn't transferred to air out with lime discharge.
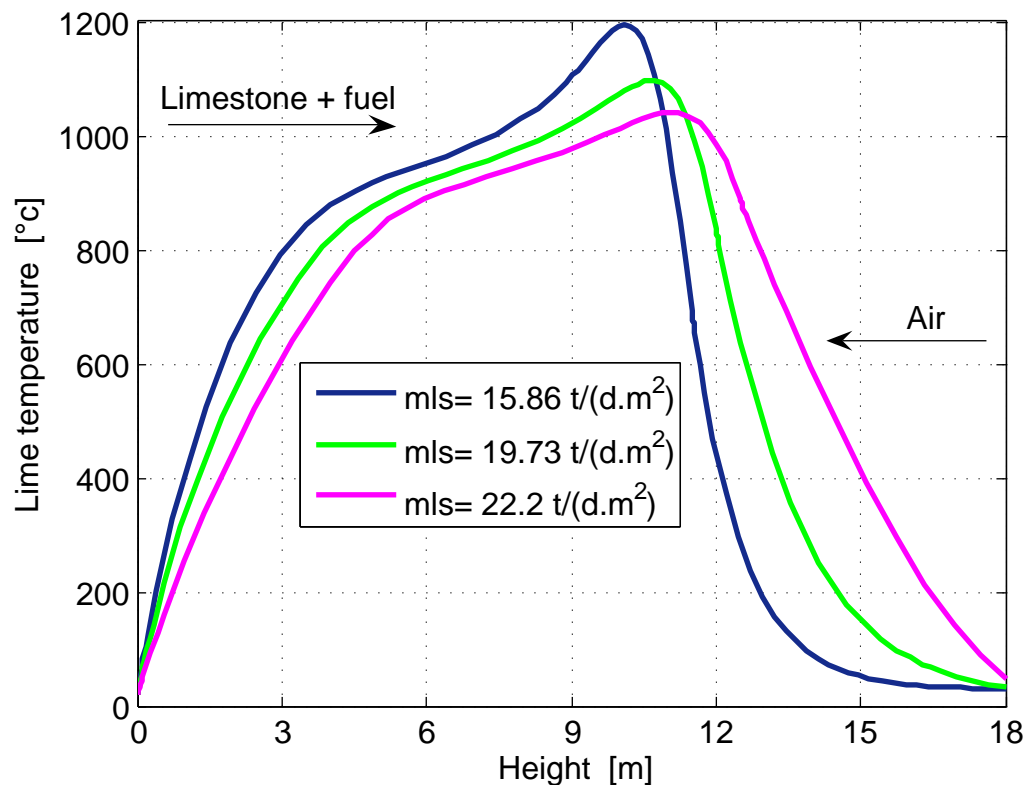
Figure 7.11: Temperature profiles in mixed feed lime kiln at various lime throughput and data from table 6.4.

Figure 7.12 shows the dependence of limestone conversion degree on the lime throughput. It can be seen from the figure that the limestone conversion degree decreases with an increase of the lime throughput. At low limestone throughput, the decomposition of limestone starts early. With the increase of lime throughput, the decomposition of limestone is delayed.
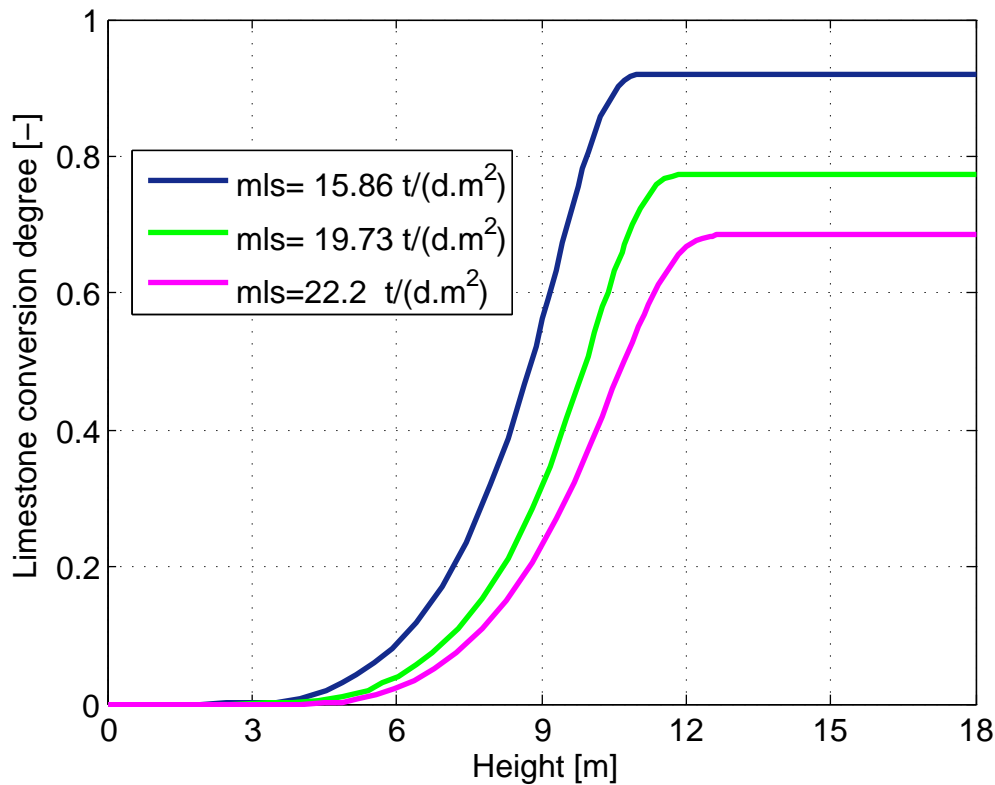
Figure 7.12: Conversion degree of limestone for various lime throughput and data from table 6.4.

7.1.4 Limestone diameter

The size of limestone particles plays an important role in the kiln operation. A suitable limestone particle diameter should be used in the lime kiln. Small pieces of limestone increase the resistance to gas flow in the kiln and might plug the kiln and reduce the production rate. Large pieces of limestone require a longer burning time. The shape of limestone particles charged to the kiln is highly irregular and nonspherical, which is different than the assumption in the model of the kiln, so the results of the simulations should be interpreted with caution. Also, the limestone diameter affects the void fraction of the kiln. This effect is not include in the kiln model which assumes a constant void fraction.

The influence of limestone particle diameter on the kiln operation has been investigated. Figure 7.13 shows the temperature profiles of lime dependent on the diameter of limestone particles. The peak temperature of lime decreases when increasing the size of limestone, while the outlet temperature of lime increases. This is explained by the large size of limestone having a smaller surface area and hence, less effective heat transfer between gas and lime.
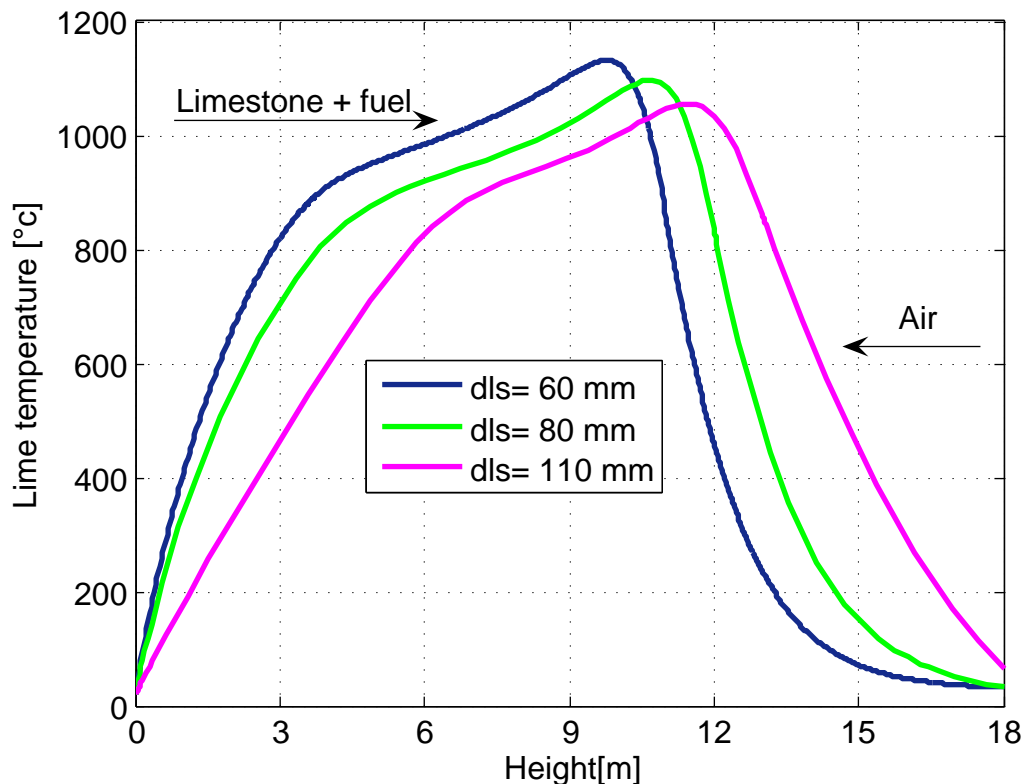
Figure 7.13: Temperature profiles in mixed feed lime kiln at different limestone diameter and data from table 6.4.

The effect of limestone size on the conversion degree of limestone is shown in figure 7.14. The conversion degree of limestone reduces with an increase of the size of the limestone. The larger the particles are, the more delayed the calcination zone is and, hence, more unburned lime leaves the kiln.

Figure 7.15 shows the pressure drop as a function of diameter of limestone. The pressure drop in the kiln decreases with the increase of limestone size. When increasing the limestone size, the gas amount reduced due to more unburned lime and consequently velocity of the gas reduces.

7.1.5   Limestone reactivity

The reactivity of limestone is strongly dependent on its physical and structural properties. In lime industry, limestone particles the size of a centimeter are usually used but nearly all studies on reaction rate coefficient of limestone have been carried out on fine limestone particles or powder to exclude the influence of other parameters. For limestone powder, the decomposition can be considered as a pure chemical kinetic process. For large particles, chemical kinetics is no longer important. The main
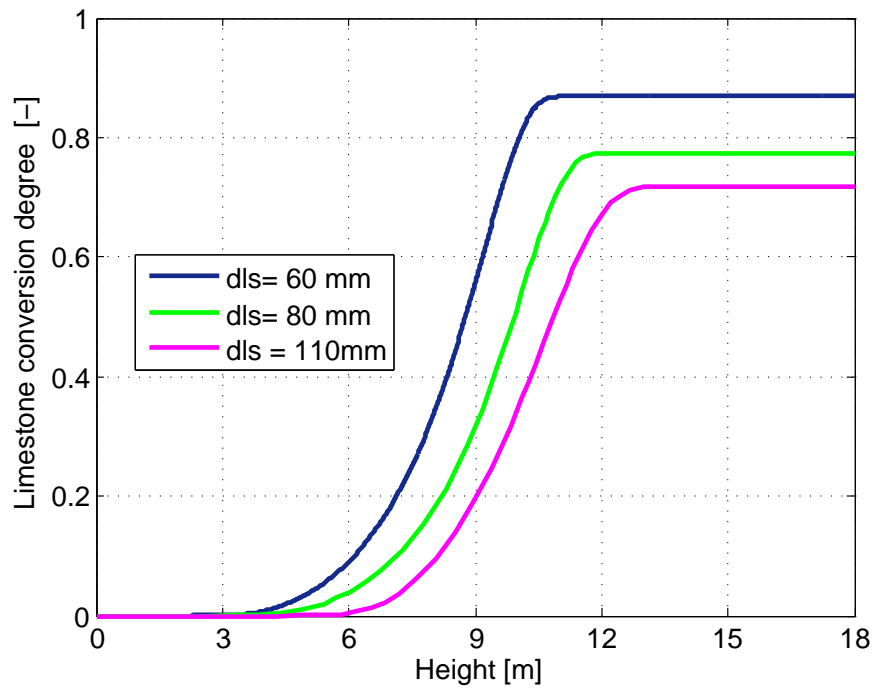
Figure 7.14: Conversion degree of limestone for various limestone diameters and data from table 6.4.
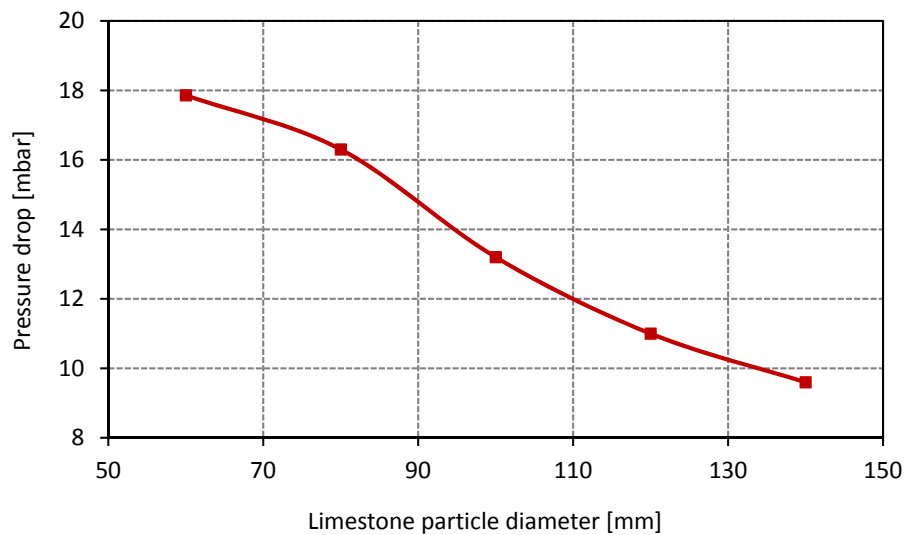
Figure 7.15: Pressure drop at different values of limestone diameter and data from table 6.4.

control steps become mass transfer, rising gas temperature, heat transfer and conduction. In this section, the influence of limestone reactivity on the kiln operation has been investigated.

Figure 7.16 shows the temperature profiles of gas and lime from two simulations performed with limestone of varying reactivity. As noted, the temperature profiles of gas and lime in the preheating and cooling zones remain essentially unaffected by the reactivity of limestone where there is no chemical reaction, while the temperature profiles slightly change in the burning zone. At high limestone reactivity, the temperature of lime decreases where the endothermic calcination reaction is fast.
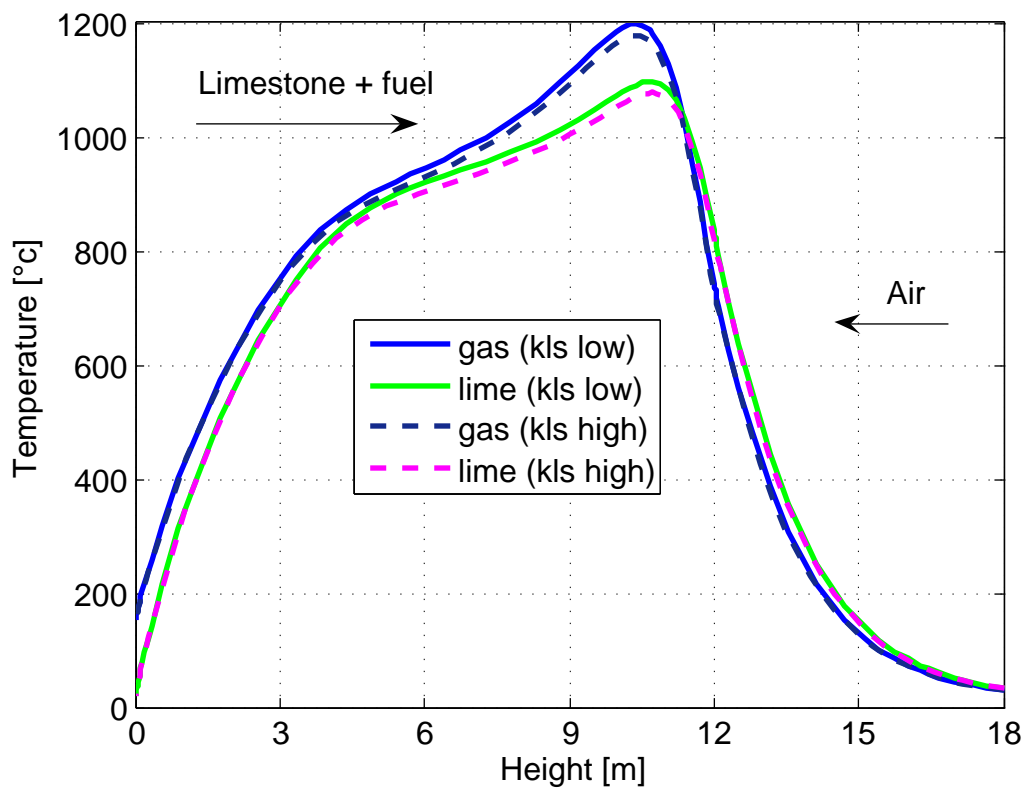
Figure 7.16: Temperature profiles in mixed feed lime kiln at two limestone reactivities and data from table 6.4.

7.1.6   Kind of fuel

Several parameters effect on the choice of fuel for firing mixed feed lime kiln, prices, availability and etc.. Due to recent developments on the market become the price is the main influence on the decision of which fuel is used. In this section, simulations with kind of the fuel are described.

Figure 7.17 shows the temperature profiles of gas and lime with two kinds of fuel; coke
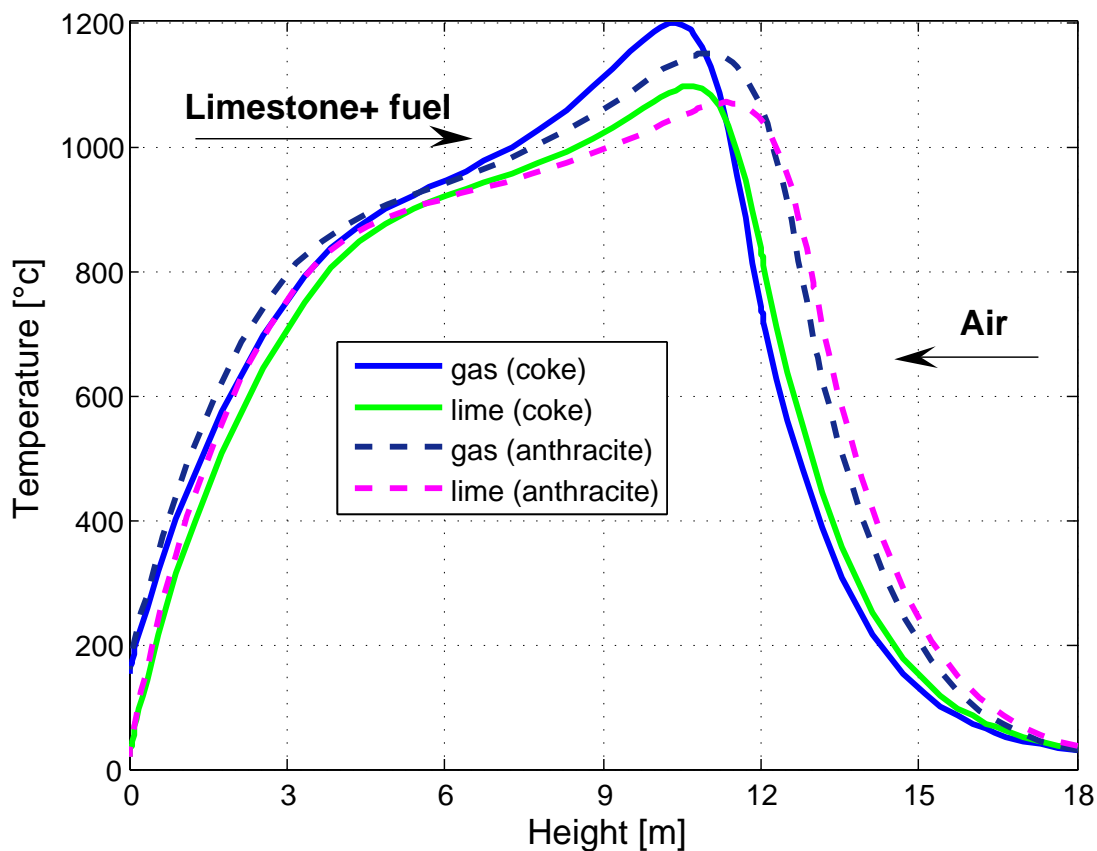
Figure 7.17: Temperature profiles in a mixed feed lime kiln with different kind of fuels and data from table 6.4.

and anthracite. The temperature profiles with anthracite moved towards the bottom of the kiln. The peak temperatures with coke is higher than with anthracite. The temperature of the flue gas and the temperature of discharged lime with anthracite are higher than with coke. The calcination zone starts later with coke where the anthracite has the higher reactivity. The difference in temperature profiles between two fuels in this figure is due to the properties of the fuels. The other operating conditions were the same as those listed in table 6.4.

The influence of fuel type on the conversion degree of limestone is shown in figure 7.18. The conversion degree of limestone reduces with anthracite although, the calcination of limestone starts early with anthracite. The rate of combustion of anthracite is lower than the coke.

7.1.7 Coke size

The size of coke particles play an important role in affecting the kiln operation. Small particles burn fast and energy is lost with flue gases. Large particles required
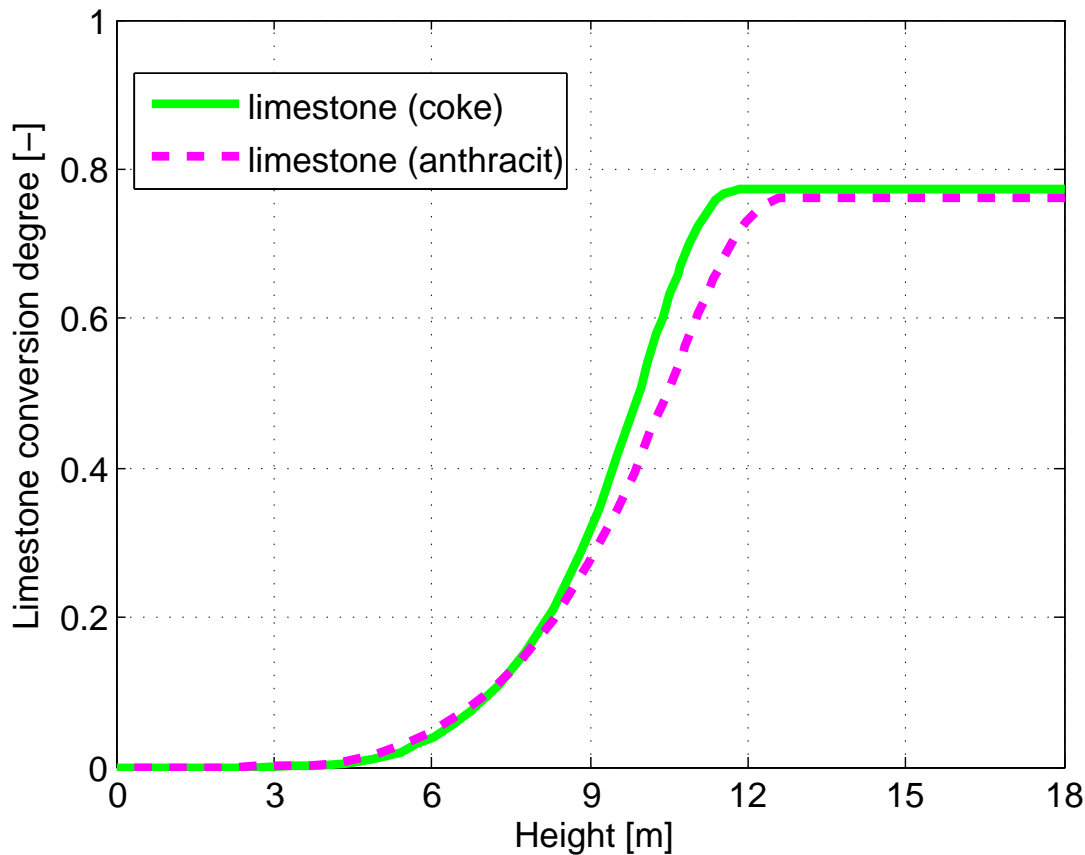
Figure 7.18: Conversion degree of limestone for kinds of fuel and data from table 6.4.

a longer time for burning and energy is lost with discharged lime. In this section, the dependence of kiln operation on the size of coke is investigated using the model of the kiln.

Figure 7.19 shows the temperature profiles of gas and lime dependent on coke size. The temperature profiles moved towards the bottom of the kiln with the increase of coke size. The peak temperature increases with an increase of the size of coke. Because the large coke particles have a smaller surface area per unit mass. The rate of coke gasification decreases and more heat is produced in burning zone. The temperature of the flue gas decreases with an increase of the size of coke while the outlet temperature of lime increases.

7.1.8   Coke reactivity

To mention the market and prices of coke again, several types of coke are used and every type is different in its reactivity. The reactivity of coke influences the kiln operation in several zones. The reactivity of coke towards CO_2 influences the Boudouard
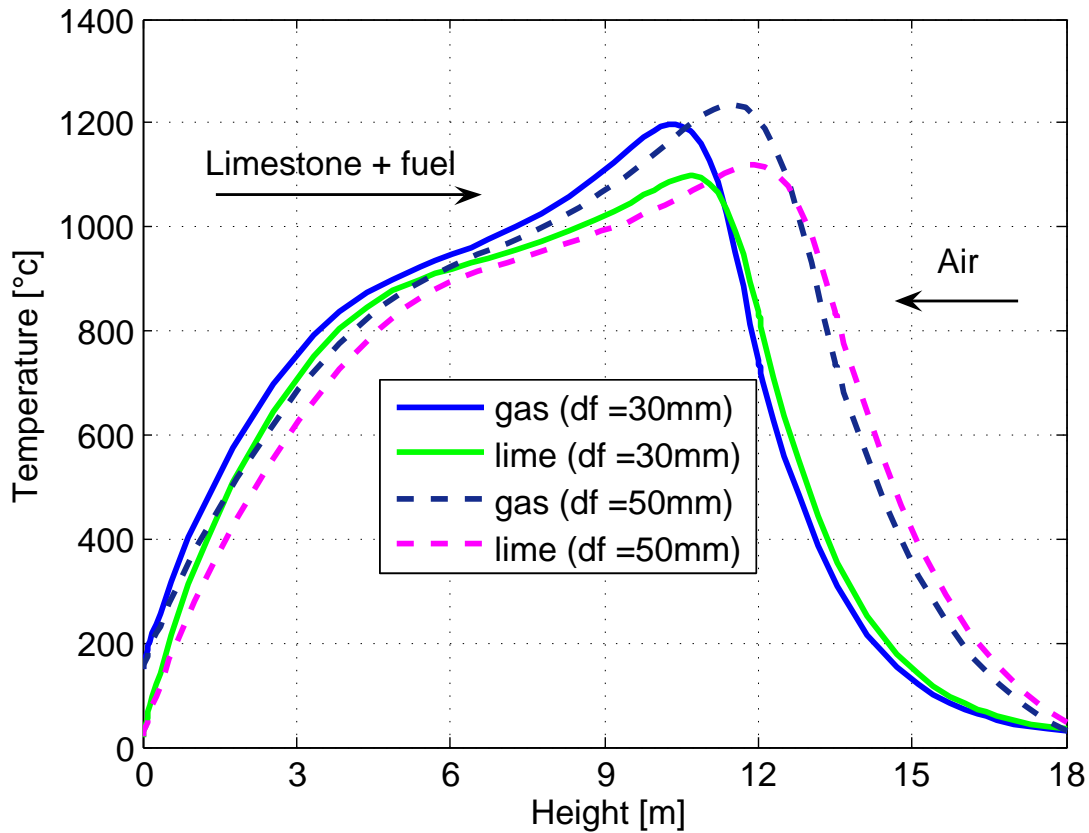
Figure 7.19: Temperature profiles in a mixed feed lime kiln with different coke sizes and data from table 6.4.

reaction (this reaction occurs when there is little or no oxygen and the temperature is high) and combustion zone while the reactivity of coke towards O_2 effects only the combustion zone. In the combustion zone, Coke reacts with CO_2 to form CO which react quickly with O_2 to form CO_2 so the CO_2 is considered the oxidizing agent in the combustion. In a mixed feed lime kiln, the low reactivity of coke towards CO_2 is desired to minimize the energy loss and formation of CO. The influence of coke reactivity on kiln performance has been investigated using the kiln model.

Figure 7.20 shows the temperature profiles of gas and lime at different coke reactivities. The lime peak temperature is slightly lower with low coke reactivity. It can be seen that the temperature profiles of gas and lime have slightly change by decreasing the reactivity of coke.
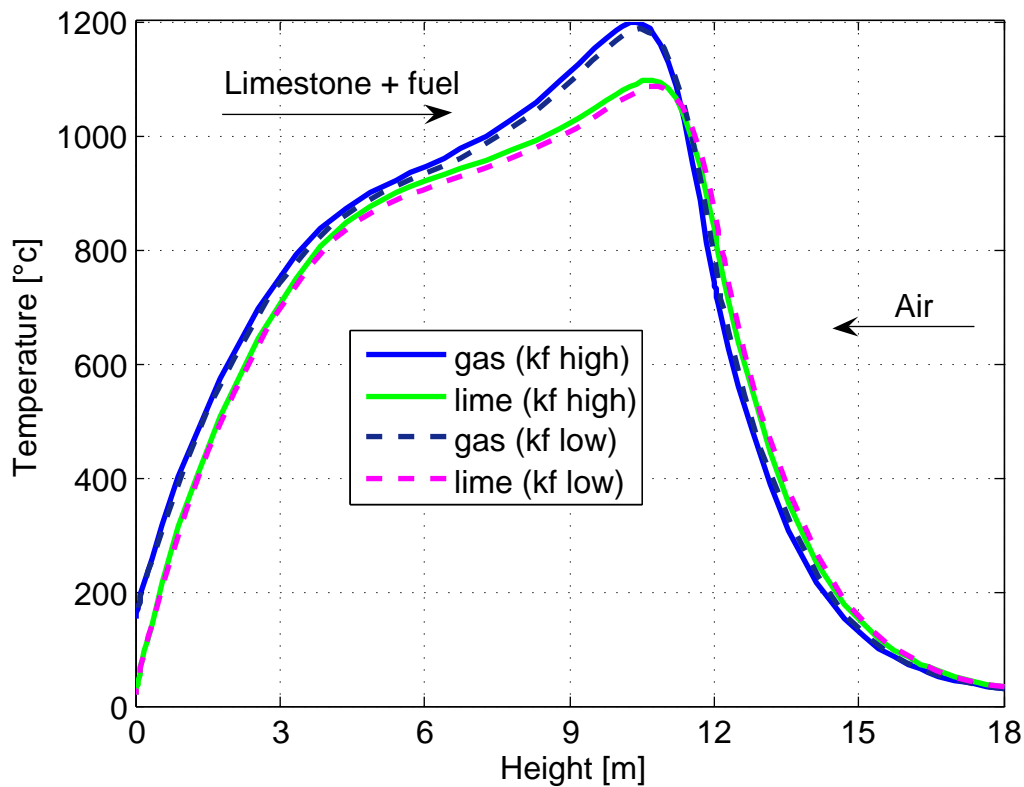
Figure 7.20: Temperature profiles in a mixed feed lime kiln with two coke reactivities and data from table 6.4.

7.2   Concluding remark

The developed mathematical model of a mixed feed lime kiln has been used to predict the effects of the operating conditions of the performance of the kiln. The simulations with the model further showed that the fuel ratio has strong effect on kiln performance and that the fuel ratio should not be increased more than 7.5 % to avoid the formation of clinkers. The influence of air excess number is opposite to the fuel ratio where the increase of air excess number reduced the maximum temperatures, conversion of limestone and concentration of CO_2 in flue gas. Limestone size and coke size have the opposite effect conversion of limestone and concentration of CO_2 in flue gas when they were reduced with increasing Limestone size and increased with increasing coke size . The influence of limestone reactivity and coke reactivity is weak on the performance of the kiln. The simulation explains why operators of mixed feed lime kilns have observed different effects of changes under different operating conditions.

Chapter 8

Conclusions and Outlook

8.1 Conclusions

This work aimed at improving operation of mixed feed lime kiln. To achieve this goal, the mathematical model of the kiln has been developed and supported by both full scale measurements and models of a single particle. The experimental measurements were made to validate the model as well as supply information valuable in it self. The models of single particle were made to determine supply input information to the model.

The energy balance of the whole mixed feed lime kiln is analyzed. The energy consumption, fuel ratio and concentration of carbon dioxide in flue gas of the kiln are calculated. The results showed that the best value of fuel ratio to the kiln is about 7 % for high quality of lime and low concentration of CO in flue gas. The maximum concentration of carbon dioxide in flue gas is achieved at complete calcination of limestone with theoretical excess air.

The experimental measurements of the vertical temperature profile and kiln gas composition have been carried out. The location of the beginning of the calcination has been determined. Measurements of input and output streams from the kiln are also described. The measurements show that the temperature profiles for two positions of the kiln are very different, each zone occupies about one- third of the kiln height and the initial calcination temperature is about 860 °C. The measurement of gas concentration indicates that there is a nonuniform distribution of gas and solid where the flue gas includes CO and O_2 together. The input and output data will be used in the modeling of the kiln and the measurements provide a good basis for validating the kiln model.

A numerical model for describing the combustion behavior of a single coke particle is developed. The mathematical formulation of the model is described in detail.

The model takes into account the fact that the reaction takes place inside the entire geometry of the particle. The model predicts the particle temperature, the mass fraction of particle, the particle shrinkage and the conversion of the particle. The results of the model have a good agreement with the experimental data available in literature.

A model for the calcination process of limestone in terms of heat transfer, chemical kinetics, mass transfer and limestone properties was been developed. The model was compiled from a number of existing models that each described part of the process.

A static 1-D mathematical model of a mixed feed lime kiln was been developed. The model describes chemical reactions, heat and mass transfer between gas and solid phases. The model predicts the temperatures of gas, coke and limestone (surface and core), gas phase composition, mass flow rate of each phase and wall temperature as a function of vertical position all as functions of properties of solid materials and the intensity of air. Also the pressure drop and velocity of gas are predicted by the model. The model was validated against the data obtained from experimental measurements. The validation showed that the model describes the conditions inside the kiln well, indicating that the relevant phenomena are included in the model and described in sufficient detail.

The developed mathematical model of a mixed feed lime kiln has been used to predict the influence of different operating conditions (fuel ratio, air excess number, lime throughput, limestone size and reactivity, fuel kind, and coke size and reactivity) on the performance of the kiln. The simulations with the model further showed that the influence of fuel ratio, air excess number, limestone size and coke size is strong on kiln performance while the influence of limestone reactivity and coke reactivity is weak. The simulation explains why operators of mixed feed lime kilns have observed different effects of changes under different operating conditions.

8.2   Outlook

The mathematical model has been presented to describe the complex phenomena in a mixed feed lime kiln. This is the first time that such a comprehensive formulation has been presented within the context of the mixed feed lime kiln so some simplification is used. The mathematical model given is a simulation and, hence, poses a potential base for further development of a more the complex model. It could be further developed in several ways. The most beneficial improvements are listed below:

- Introduce heat transfer by radiation

- Introduce a particle size distribution for solid materials (limestone and coke).

- Introduce bulk porosity as a function of particle size distribution.

- Better description of the chemical reactions by:

  - Takeing into account the reactions inside coke particles.
  - Use more detailed expressions for the reactions in stead of the lumped expressions that are currently used.

- Extend to multi- dimensional and transient behavior to obtain a model that can be used for the kiln design issues.

Appendices

Appendix A

The BVP Solver

The function bvp4c solves two-point boundary value problems for ordinary differential equations (ODEs). It integrates a system of first-order ordinary differential equations,

$$\acute{y} = f(x, y)$$

on the interval $[a, b]$, subject to general two-point boundary conditions,

$$bc(y(a), y(b)) = 0$$

It can also accommodate other types of boundary value problems, such as those that have any of the following:

- Unknown parameters.

- Singularities in the solutions.

- Multipoint conditions.

In this case, the number of boundary conditions must be sufficient to determine the solution and the unknown parameters.

bvp4c produces a solution that is continuous on $[a, b]$ and has a continuous first derivative there.

bvp4c is a finite difference code that implements the 3-stage Lobatto IIIa formula. This is a collocation formula and the collocation polynomial provides a C^1-continuous solution that is fourth-order accurate uniformly in the interval of integration. Mesh selection and error control are based on the residual of the continuous solution.

The collocation technique uses a mesh of points to divide the interval of integration into subintervals. The solver determines a numerical solution by solving a global system of algebraic equations resulting from the boundary conditions, and the collocation conditions imposed on all the subintervals. The solver then estimates the error of the numerical solution on each subinterval. If the solution does not satisfy the tolerance criteria, the solver adapts the mesh and repeats the process. The user must provide the points of the initial mesh as well as an initial approximation of the solution at the mesh points.

Appendix B

The PDE Solver

The MATLAB PDE solver, pdepe, solves initial-boundary value problems for systems of parabolic and elliptic PDEs in the one space variable x and time t, of the form

$$c(x, t, u, \frac{\partial u}{\partial x})\frac{\partial u}{\partial t} = x^{-m}\frac{\partial}{\partial x}(x^m f(x, t, u, \frac{\partial u}{\partial x})) + s(x, t, u, \frac{\partial u}{\partial x}) \qquad \text{(B.1)}$$

The PDEs hold for $t_0 \leq t \leq t_f$ and $a \leq x \leq b$. The interval $[a, b]$ must be finite. m can be 0, 1, or 2, corresponding to slab, cylindrical, or spherical symmetry, respectively. In Equation B.1, $f(x, t, u, \frac{\partial u}{\partial x})$ is a flux term and $s(x, t, u, \frac{\partial u}{\partial x})$ is a source term. The flux term must depend on $\frac{\partial u}{\partial x}$. The coupling of the partial derivatives with respect to time is restricted to multiplication by a diagonal matrix $c(x, t, u, \frac{\partial u}{\partial x})$. The diagonal elements of this matrix are either identically zero or positive. An element that is identically zero corresponds to an elliptic equation and otherwise to a parabolic equation.

At the initial time $t = t_0$, for all the solution components satisfy initial conditions of the form

$$u(x, t_0) = u_0(x) \qquad \text{(B.2)}$$

At the boundary $x = a$ or $x = b$, for all t the solution components satisfy a boundary condition of the form

$$p(x, t, u) + q(x, t)f(x, t, u, \frac{\partial u}{\partial x}) = 0 \qquad \text{(B.3)}$$

q(x,t)is a diagonal matrix with elements that are either identically zero or never zero. Note that the boundary conditions are expressed in terms of the f rather than partial derivative of u with respect to $x\frac{\partial u}{\partial x}$. Also, of the two coefficients, only p can depend on u.

The pdepe solver converts the PDEs to ODEs using a second-order accurate spatial

discretization based on a fixed set of nodes specified by the user. The time integration is done with ode15s. The pdepe solver exploits the capabilities of ode15s for solving the differential-algebraic equations that arise when Equation B.1 contains elliptic equations, and for handling Jacobians with a specified sparsity pattern. ode15s changes both the time step and the formula dynamically.

After discretization, elliptic equations give rise to algebraic equations. If the elements of the initial conditions vector that correspond to elliptic equations are not "consistent" with the discretization, pdepe tries to adjust them before beginning the time integration. For this reason, the solution returned for the initial time may have a discretization error comparable to that at any other time. If the mesh is sufficiently fine, pdepe can find consistent initial conditions close to the given ones. If pdepe displays a message that it has difficulty finding consistent initial conditions, try refining the mesh. No adjustment is necessary for elements of the initial conditions vector that correspond to parabolic equations

Bibliography

[1] C.Thieme, "Sodium carbonate." *Wiley-VCH Verlag GmbH and Co. KGaA, Weinheim*, 2005.

[2] K. M. Wagialla, I. S. Al-Mutaz, and M. E. El-Dahshan, "The manufacture of soda ash in the arabian gulf." *International Journal of Production Economics*, vol. 21, pp. 145–153, 1992.

[3] D. M. Kiefer, "Soda ash, solvay style." *Today's Chemist at Work*, vol. 11, No. 2, pp. 87–90, 2002.

[4] D. S. Kostick, "Soda ash." *Minerals Yearbook, US Geological Survey*, 2006.

[5] J. Oates, *Lime and Limestone Chemistry and Technology,Production and Uses.* WILEY-VCH Verlag GmbH, 1998.

[6] K. Koike and S. Matsuda, "Characterizing content distributions of impurities in a limestone mine using a feedforward neural network." *Natural Resources Research*, vol. 12, No. 3, 2003.

[7] A. B. Leslie and J. J. Hughes, "High-temperature slag formation in historic scottish mortars: evidence for production dynamics in 18th19th century lime production from charlestown." *Materials Characterization*, vol. 53, pp. 181–186, 2004.

[8] A. I. Gamej, A. Perlevskij, O. Kurchenko, Z. Bol'shakova, and E. Malikova, "Improvement in quality of preparation of limestone charged into the firing units." *Stal*, vol. 12, pp. 9–11, 2004.

[9] H. N. Tran, S. Vollick, M. Gauthier, and C. McNeil, "Correlation between nodule size and residual carbonate content in lime kiln." *Proceedings of Tappi Environmental Pulping and Engineering Conference, Philadelphia*, 2005.

[10] G. Lienbacher and E. D. Cristea, "Investing." *World Cement*, vol. 37, pp. 17–22, 2006.

[11] K. Gehan, F. K. Ngian, and J. W. Grunden, "Solids distribution in vertical shaft mixed feed lime kilns." *Eleventh Australian Chemical Engineering Conference on Chemical Engineering Today, Coping With Uncertaint Brisbane, Aust.*

[12] A. Senegacnik, J. Oman, and B. S. irok, "Annular shaft kiln for lime burning with kiln gas recirculation." *Applied Thermal Engineering*, vol. 28, pp. 785–792, 2008.

[13] V. T. Ryazanov, V. V. Madison, A. S. Dorokhin, and S. S. Shulgin, "Improving the heating system and structure of shaft furnaces for roasting limestone." *Steel in Translation*, vol. 40,No.3, pp. 298–304, 2010.

[14] P. Accinelli, "New life for old lime kilns." *World Cement*, vol. 37, 2006.

[15] D. Terruzzi, E. Barberis, and F. Marangoni, "The latest process know-how for single lime kilns." *ZKG International*, vol. 54, pp. 506–513, 2001.

[16] A. F. Reshetnyak, V. Konev, A. Mamaev, and N. Seryakov, "Improvement of shaft furnace construction for roasting limestone." *Refractories and Industrial Ceramics*, vol. 49,no. 3, pp. 25–27, 2008.

[17] V. I. Matyukhin, Y. G. Yaroshenko, and O. V. Matyukhin, "Improvement of thermal modes of shaft furnaces of nonferrous metallurgy." *Non-Ferrous Metals*, vol. 51,No.3, pp. 255–262, 2010.

[18] P. Zeisel, "Annular shaft kilns with the treivo system." *ZKG International*, vol. 49, pp. 530–539, 1996.

[19] W. Arnold, "Annular shaft kilns with injector air preheating." *ZKG International*, vol. 50, pp. 86–94, 1997.

[20] H. Piringer, "Fuel gases with low calorific value for firing pfr lime shaft kilns." *ZKG International*, vol. 56, NO.6, pp. 66–72, 2003.

[21] E. D. Cristea, D. Maffioli, and T. Christiansen, "Operational performance of twin shaft vertical kilns fired with two fuels and with lean gas." *ZKG International*, vol. 54, pp. 232–242, 2001.

[22] L. Ernstbrunner and S. Lechner, "The use of secondary fuels in the european lime industry." *ZKG International*, vol. 55, pp. 54–63, 2002.

[23] H. Piringer and W. Werner, "Conversion of large-diameter single shaft kilns to lignite dust firing successfully concluded." *ZKG International*, vol. 61, pp. 46–52, 2008.

[24] D. Lewerenz, "Conversion of a conventional shaft kiln to pulverized lignite firing." *Zement-Kalk-Gips, Edition B.*, vol. 38(2), pp. 84–86, 1985.

[25] D. Terruzzi, "Lime shaft kilns using the 'two way pressure system' - a new generation of vertical lime kilns." *ZKG International, Edition B*, vol. 47, pp. 322–326, 1994.

[26] A. Bes, "Dynamic process simulation of limestone calcination in normal shaft kilns." Ph.D. dissertation, Institute of Fluid Dynamics and Thermodynamics, Otto von Guericke University, Magdeburg, 2006.

[27] D. HaiDo and E. Specht, "Numerical simulation of heat and mass transfer of limestone decomposition in normal shaft kiln." *ASME/JSME 2011 8th Thermal Engineering Joint Conference (AJTEC2011) March 1317, 2011, Honolulu, Hawaii, USA.*

[28] F. Marias and B. Bruyres, "Modelling of a biomass fired furnace for production of lime." *Chemical Engineering Science*, vol. 64, pp. 3417–3426, 2009.

[29] Y. Gordon, V. Shvidkiy, and Y. Yaroshenko, "Optimization of the design and operating paramaters of shaft furnaces." *3rd International Conference Science and Technology of Ironmaking, June 1620, 2003, Dusseldorf.*, pp. 311–316.

[30] A. Senegacnik, J. Oman, and B. Sirok, "Analysis of calcination parameters and the temperature profile in an annular shaft kiln. part1:theoretical survey." *Applied Thermal Engineering*, vol. 27, pp. 1467–1472, 2007.

[31] ——, "Analysis of calcination parameters and the temperature profile in an annular shaft kiln. part2: Results of tests." *Applied Thermal Engineering*, vol. 27, pp. 1473–1482, 2007.

[32] X. Zhiguo, "Reduced model for flow simulation in the burner region of lime shaft kilns." Ph.D. dissertation, Institute of Fluid Dynamics and Thermodynamics, Otto von Guericke University, Magdeburg, 2010.

[33] T. Bluhm-Drenhaus, E. Simsek, S. Wirtz, and V. Scherer, "A coupled fluid dynamic-discrete element simulation of heat and mass transfer in a lime shaft kiln." *Chemical Engineering Science*, vol. 65, pp. 2821–2834, 2010.

[34] C. L. Virma, N. G. Dave, and S. K. Saraf, "Performance estimation vis-a-vis design of mixed-feed lime shaft kilns." *Zement Kalk Gips*, vol. 9, pp. 471–477, 1988.

[35] C. L. Virma, "Simulation of lime shaft kilns using mathematical modelling." *Zement Kalk Gips*, vol. 12, pp. 576–582, 1990.

[36] Z. Yi, J. Zhou, and H. Chen, "Numerical simulation of thermal process and energy saving of lime furnace." *Journal of Central South University of Technology.*, vol. 12,no. 3, pp. 295–299, 2005.

[37] V. S. Shagapov, M. V. Burkin, A. V. Voronin, and A. A. Shatov, "Calculation of limestone burning in a coke-fired kiln." *Theoretical Foundations of Chemical Engineering*, vol. 38, pp. 440–447, 2004.

[38] V. S. Shagapov and M. V. Burkin, "Theoretical modeling of simultaneous processes of coke burning and limestone decompostion in a furnace." *combustion, Explosion, and Shock waves*, vol. 44, no. 1, pp. 55–63, 2008.

[39] A. Bes, E. Specht, and G. Kehse, "Influence of the type of fuel on the energy consumption in lime burning." *ZKG International*, vol. 60,no. 9, 2007.

[40] M. Asadi, *Beet-Sugar Handbook.* WILEY-INTERSCIENCE, A JOHN WILEY and SONS, INC., PUBLICATION, 2007, ch. Sugarbeet processing, pp. 195–212.

[41] I. Glassman and R. A. Yetter, *Combustion.* Elsevier, 2008.

[42] M. S. Ulzama, "A theoretical analysis of single coal particle behavior during spontaneous devolatilization and combustion." Ph.D. dissertation, Institute of Fluid Dynamics and Thermodynamics, Otto von Guericke University of Magdeburg, 2007.

[43] S. Wang, H. Lu, Y. Zhao, R. Mostofi, H. Y. Kim, and L. Yin, "Numerical study of coal particle cluster combustion under quiescent conditions." *Chemical Engineering Science*, vol. 62, pp. 4336–4347, 2007.

[44] V. Manovic, M. Komatina, and S. Oka, "Modeling the temperature in coal char particle during fluidized bed combustion." *Fuel*, vol. 87, pp. 905–914, 2008.

[45] R. He, T. Suda, T. Fujimori, and J. Sato, "Effects of particle sizes on transport phenomena in single char combution." *Heat and Mass Transfer*, vol. 46, pp. 3619–3627, 2003.

[46] B. Remiarov, J. Markos, R. Zajdlik, and L. Jelemensky, "Identification of the mechanism of coal char particle combustion by porous structure characterization." *Fuel Processing Technology*, vol. 85, pp. 303–321, 2004.

[47] A. K. Sadhukhan, P. Gupta, and R. K. Saha, "Modelling of combustion characteristics of high ash coal char particles at high pressure: Shrinking reactive core model." *Fuel*, vol. 89, pp. 162–169, 2010.

[48] C. Chen and T. Kojima, "Single char particle combustion at moderate temperature: effects of ash." *Fuel Processing Technology*, vol. 47, pp. 215–232, 1996.

[49] R. E. Mitchell, L. Ma, and B. Kim, "On the burning behavior of pulverized coal chars." *Combustion and Flame*, vol. 151, pp. 426–436, 2007.

[50] A. Kasai, T. Murayama, and Y. Ono, "Measurement of effective thermal conductivity of coke." *ISIJ International*, vol. 33, No.6, pp. 697–702, 1993.

[51] Y. Zhao, H. Y. Kim, and S. S. Yoon, "Transient group combustion of the pulverized coal particles in spherical cloud." *Fuel*, vol. 86, pp. 1102–1111, 2007.

[52] B. Hallak, "Ermittlung der zuendbedingungen fester fossiler brennstoffe gleicher geometrie bei verschiedenen umgebungszuständen." Master's thesis, Institute of Fluid Dynamics and Thermodynamics, Otto von Guericke University, Magdeburg, 2009.

[53] C. H. Satterfield and F. Feakes, "Kinetics of the thermal decomposition of calcium carbonate." *A.I.Ch.E. J.*, vol. 5, pp. 115–122, 1959.

[54] G. D. Silcox, J. C. Kramlich, and D. W. Pershing, "A mathematical model for the flash calcination of dispersed *caco*3 and *ca(oh)*2 particles." *Ind. Eng. Chem. Res.*, vol. 28, pp. 155–160, 1989.

[55] J. Khinast, G. F. Krammer, C. Brunner, and G. Staudinger, "Decomposition of limestone: The influence of co_2 and particle size on the reaction rate." *Chemical Engineering Science*, vol. 51, No.4, pp. 623–634, 1996.

[56] I. Ar and G. Dogu, "Calcination kinetics of high purity limestones." *Chemical Engineering Science*, vol. 83, pp. 131–137, 2001.

[57] F. Garcia-Labiano, A. Abad, L. F. deDiego, P. Gayan, and J. Adanez, "Calcination of calcium-based sorbents at pressure in a broad range of co_2 concentrations." *Chemical Engineering Science*, vol. 57, pp. 2381–2393, 2002.

[58] C. Cheng and E. Specht, "Reaction rate coefficients in decompostion of lumpy limestone of different origin." *Thermochimica Acta*, vol. 449, pp. 8–15, 2006.

[59] R. H. BORGWARDT, "Calcination kinetics and surface area of dispersed limestone particles." *AlChE Journal*, vol. 31, No. 1, 1985.

[60] H. Naiyi and A. W. Scaroni, "Calcination of pulverized limestone particles under furnace injection conditions." *Fuel*, vol. 75, No.2, pp. 177–186, 1996.

[61] J. Stark and B. Wicht, *Zement und Kalk, Birkhäuser, Basel*, 2000.

[62] C. Noiriel, L. Luquot, B. Made, and J. L. L. Raimbault, P. Gouze, "Changes in reactive surface area during limestone dissolution: An experimental and modelling study." *Chemical Geology*, vol. 265, pp. 160–170, 2009.

[63] H. Kainer, E. Specht, and R. Jeschar, "Pore diffusion, reaction and thermal conduction coefficients of various limestones and their influence on decomposition time." *Zement-Kalk-Gips.*, vol. 7, pp. 259–268, 1986.

[64] C. Cheng, E. Specht, and G. Kehse, "Influences of the origin and material properties of limestone on its decomposition behaviour in shaft kilns." *ZKG International*, vol. 60, no. 1, 2007.

[65] M. Silva, E. Specht, and J. Schmit, "Thermphysical properties of limestone as a function of origin (part 1): specific heat capacities." *ZKG International*, vol. 2, 2010.

[66] ——, "Thermphysical properties of limestone as a function of origin (part 2): Calcination enthalpy and equilibrium temperature." *ZKG International*, vol. 6, 2010.

[67] J. Murray, "Specific heat data for evaluation of lime kiln performance." *Rock Prod.*, p. 148, 1947.

[68] I. Barin and O. Knacke, "Thermochemical properties of inorganic substances." *Springer-Verlag, Berlin*, 1973.

[69] R. S. Boynton, *Chemistry and technology of lime and limestone.* John Wiley and Sons, 1980.

[70] E. Specht, "Kinetik der abbaureaktionen." *Cuvillier Verlag, Göttingen*, 1993.

[71] E. H. Baker, "The calcium oxide-carbon dioxide system in the pressure rang 1-300 atmospheres." *J. Chem. Soc.*, pp. 464–470, 1962.

[72] J. Zsako and H. E. Arz, "Kinetic analysis of thermogravimetric data. vii. thermal decomposition of calcium carbonate." *J.Therm. Anal.*, vol. 6, pp. 651–656, 1974.

[73] J. Szekely, J. W. Evans, and H. Y. Sohn, "Gas- solid- reactions." *Academic Press, New York.*, 1976.

[74] R. Jeschar, "Druckverlust in mehrkornsch-uttungen aus kugeln." *Archiv für das Eisenhuettenwesen*, vol. 35, pp. 91–108, 1964.

[75] F. A. L. Dullien, *Porous Media. Fluid Transport and Pore Structure.* Academic Press Inc., 1992.

[76] L. Roblee, R. Baird, and J. Tierney, "Radial porosity variations in packed beds." *A.I.Ch.E.*, vol. 4, pp. 460–464, 1958.

[77] D. Coelho, J.-F. Thovert, and P. Adler, "Geometrical and transport properties of random packings of spheres and aspherical particles." *Physical Review E.*, vol. 55(2), pp. 1959–1978, 1997.

[78] E. Tsotsas, "Product quality in process and chemical engineering handout for master of quality, safety, environment program." *Otto von Guericke University, Magdeburg.*

[79] S. Ergun, "Fluid flow through packed columns." *Chem. Engng. Prog.*, vol. 48(2), pp. 89–94, 1952.

[80] M. Mayerhofer, J. Govaerts, N. Parmentier, H. Jeanmart, and L. Helsen, "Experimental investigation of pressure drop in packed beds of irregular shaped wood particles." *Powder Technology*, vol. 205, pp. 30–35, 2011.

[81] C. Cheng, "Thermal process simulation of reactive particles on moving grates." Ph.D. dissertation, Institute of Fluid Dynamics and Thermodynamics, Otto von Guericke University, Magdeburg, 2007.

[82] M. Brauer, "Grundlagen der einphasen- und mehrphasenstromungen." *Sauerlaender Verlag, Aarau u. Frankfurt*, 1971.

[83] Gnielinski, "Wärme-und stoffübertragung in festbetten." *Chem. Eng. Technol.*, vol. 52, pp. 228–236, 1980.

[84] R. Jeschar, "Heat transfer in pelletizing with mixed feed." *Archiv fr das Eisenhuttenwesen*, vol. 35, 1964.

[85] R. Leth-Miller, A. D. Jensen, P. Glarborg, L. M. Jensen, P. Hansen, and S. B. Jorgensen, "Investigation of a mineral melating cupola furnace. part2 mathematical modeling." *Ind. Eng. Chem. Res.*, vol. 42, pp. 6880–6892, 2003.

[86] N. N. Viswanathan, M. N. Srinivasan, and A. K. Lahiri, "Process simulation of cupola." *ISIJ International*, vol. 38, pp. 1062–1068, 1998.

[87] L. D. Smoot and P. J. Smith, *Coal combustion and gasification.* Plenum Press, New York, 1985.

[88] R. Chakraborty and J. Howard, "Combustion of char in shallow fluidized bed combustors-influence of some design and operating parameters." *Inst Energy*, pp. 48–54, 1981.

[89] H. S. Fogler, *Elements of Chemical Reaction Engineering., 4th ed.* Prentice Hall PRT, 2005.

[90] D. Merrick, "Mathematical models of the thermal decomposition of coal." *Fuel*, vol. 62, pp. 540–546, 1983.

Curriculum Vitae

Name:	Magda K. M. El-Fakharany
Date of Birth:	July 06, 1975; in Kafr Elsheikh, Egypt.
Nationality:	Egyptian
Status:	Married, three Children
E-mail:	Magdaelfakharany@yahoo.com

Education:

1993 - 1998	B.Sc. in Mechanical Engineering. Faculty of Engineering, Tanta University, Egypt.
1998 - 1999	Postgraduate courses for M.Sc. Faculty of Engineering, Tanta University, Egypt.
1999 - 2003	M.Sc. in Mechanical Power Engineering. Faculty of Engineering, Tanta University, Egypt.
2008 - Now	Works towards Ph.D. degree at ISUT, Otto von Guericke University Magdeburg, Germany.

Work Experience:

1998 - 2003	Demonstrator in Dept. of Mechanical power Engineering, Faculty of Engineering, Tanta University, Egypt.
2003 - 2007	Assistant lecturer in Dept. of Mechanical power Engineering, Faculty of Engineering, Tanta University, Egypt.

Magdeburg,09, 01, 2012

Magda El-Fakharany